AD-A116 738 AIR FORCE INST OF TECH WRIGHT-PATTERSON AFB OH F/G 8/7
GEOPHYSICAL INVESTIGATION OF THE RATON BASIN.(U)
MAY 82 R S CHENEY
UNCLASSIFIED AFIT/NR-82-6T NL

END
DATE
FILMED
8 82
DTIC

UNCLASS

SECURITY CLASSIFICATION OF THIS PAGE (When Data Entered)

AD A116738

REPORT DOCUMENTATION PAGE		READ INSTRUCTIONS BEFORE COMPLETING FORM
1. REPORT NUMBER AFIT/NR/82-6T	2. GOVT ACCESSION NO. AD-A116738	3. RECIPIENT'S CATALOG NUMBER
4. TITLE (and Subtitle) Geophysical Investigation of the Raton Basin		5. TYPE OF REPORT & PERIOD COVERED THESIS/~~DISSERTATION~~
		6. PERFORMING ORG. REPORT NUMBER
7. AUTHOR(s) Richard Stephen Cheney		8. CONTRACT OR GRANT NUMBER(s)
9. PERFORMING ORGANIZATION NAME AND ADDRESS AFIT STUDENT AT: Texas Tech University		10. PROGRAM ELEMENT, PROJECT, TASK AREA & WORK UNIT NUMBERS
11. CONTROLLING OFFICE NAME AND ADDRESS AFIT/NR WPAFB OH 45433		12. REPORT DATE May 1982
		13. NUMBER OF PAGES 78
14. MONITORING AGENCY NAME & ADDRESS (if different from Controlling Office)		15. SECURITY CLASS. (of this report) UNCLASS
		15a. DECLASSIFICATION/DOWNGRADING SCHEDULE

16. DISTRIBUTION STATEMENT (of this Report)

APPROVED FOR PUBLIC RELEASE; DISTRIBUTION UNLIMITED

17. DISTRIBUTION STATEMENT (of the abstract entered in Block 20, if different from Report)

LYNN E. WOLAVER
Dean for Research and
Professional Development

18. SUPPLEMENTARY NOTES

APPROVED FOR PUBLIC RELEASE: IAW AFR 190-17

Lynn Wolaver

AIR FORCE INSTITUTE OF TECHNOLOGY (ATC)
WRIGHT-PATTERSON AFB, OH 45433

22 JUN 1982

19. KEY WORDS (Continue on reverse side if necessary and identify by block number)

20. ABSTRACT (Continue on reverse side if necessary and identify by block number)

ATTACHED

DTIC ELECTE JUL 0 9 1982 S E

82 07 07 058

DTIC FILE COPY

DD FORM 1 JAN 73 1473 EDITION OF 1 NOV 65 IS OBSOLETE

UNCLASS

SECURITY CLASSIFICATION OF THIS PAGE (When Data Entered)

"Original contains color plates: All DTIC reproductions will be in black and white"

THESIS ABSTRACT

Name: Richard S. Cheney

Title: Geophysical Investigation of the Raton Basin

Rank: Captain, USAF, 1982

Degree: Master of Science in Geosciences, Texas Tech University

This thesis correlates gravity, magnetic, and seismic data for the Raton Basin of Colorado and New Mexico. The gravity data suggest that the study area, and the region around it, is in isostatic equilibrium. The free air anomaly in the southern portion of the study area suggests lack of local compensation due to Quaternary volcanic rock. The volcanic rock thickness, calculated from the free air gravity data, is 180 m. The gravity data indicated a crustal thickness of about 45 km, and the crust thinned from west to east.

A basement relief map was constructed from the Bouguer gravity data. Computer techniques were developed to calculate the depth to the basement surface and to plot a contour map of that surface. The Raton Basin magnetic map defined the same surface found on the basement relief map since the overlying sedimentary rocks have no magnetism; therefore, any magnetism present is caused by the basement rock.

A seismic survey near Capulin Mountain detected a high level of microseismicity that may be caused by adjustment along faults or dormant volcanic activity.

82-6T

GEOPHYSICAL INVESTIGATION OF THE RATON BASIN

by

RICHARD STEPHEN CHENEY, A.B., M.A.

A THESIS

IN

GEOSCIENCE

Submitted to the Graduate Faculty
of Texas Tech University in
Partial Fulfillment of
the Requirements for
the Degree of

MASTER OF SCIENCE

Approved

D H Shurbet

Chairman of the Committee

S E Cebull

Accepted

Dean of the Graduate School

May, 1982

ACKNOWLEDGEMENTS

The author recognizes the criticisms and advice of Professors S.E. Cebull, J.R. Giardino, and D.H. Shurbet in the preparation of this thesis. Technical advice in computer techniques and graphics was offered by J.R. Giardino and C.W. Baugh of Texas Tech University. The color reproduction of cartographic plates was arranged by Doctors L. Decker, and R. Ballew of the Defense Mapping Agency, St. Louis Air Force Station, Missouri. Mr. R. Wolfe of Teledyne Geotech Corporation, Garland, Texas, provided technical support in the operation of seismic equipment provided by his company under Air Force contract F08606-80-C-0014. Mrs. J.J. Wolff and Doctors D. Cash and K. Olsen of the Los Alamos Laboratory, New Mexico, supported, encouraged and helped evaluate the seismic data of this thesis. Finally, the author extends his sincere appreciation to his wife, Linda, whose moral support and inspiration made this thesis possible.

Partial funding for the preparation of this thesis was provided by the United States Air Force Institute of Technology under the following agreements: ESA - F33600-75-A; TA - 330 (4 MAR 81), and TD - 37 (6 JUL 81).

CONTENTS

LIST OF TABLES

LIST OF ILLUSTRATIONS

Figure		Page

Plate

CHAPTER I

INTRODUCTION

General Statement

The Raton Basin of New Mexico and Colorado (35^{o}-38^{o}N; 104^{o}-105.5^{o}W) is a structural depression which is defined by the Sangre de Cristo Uplift on the West, the Wet Mountains Uplift to the north, the Apishipa Arch on the northeast, and the Sierra Grande Arch on the southeast (figure 1). Today the Raton Basin is outlined by topographic relief caused by the caprock "effect" of the Trinidad Sandstone. The importance of the outlining "effect" of the Trinidad Sandstone is illustrated by both Baltz (1965) and Brill (1952) who draw the eastern boundary of the Raton Basin at the outcrop of Trinidad Sandstone, rather than along the axes of the Apishipa and Sierra Grande Arches.

Extending 175 miles long and a maximum of 65 miles wide, the Raton Basin is divided by the Cimarron Arch into the northern Raton Basin and the Las Vegas Basin on the south. The deepest depression within the Basin is located near the Sangre de Cristo Uplift. Rocks on the west limb of the Basin dip vertically, whereas rocks on the east limb dip one to five degrees (Wanek, 1963). In this thesis, the entire Raton Basin will be referred to as the Basin, while the northern portion will be called the Raton Basin, and the southern portion referred to as the Las Vegas Basin.

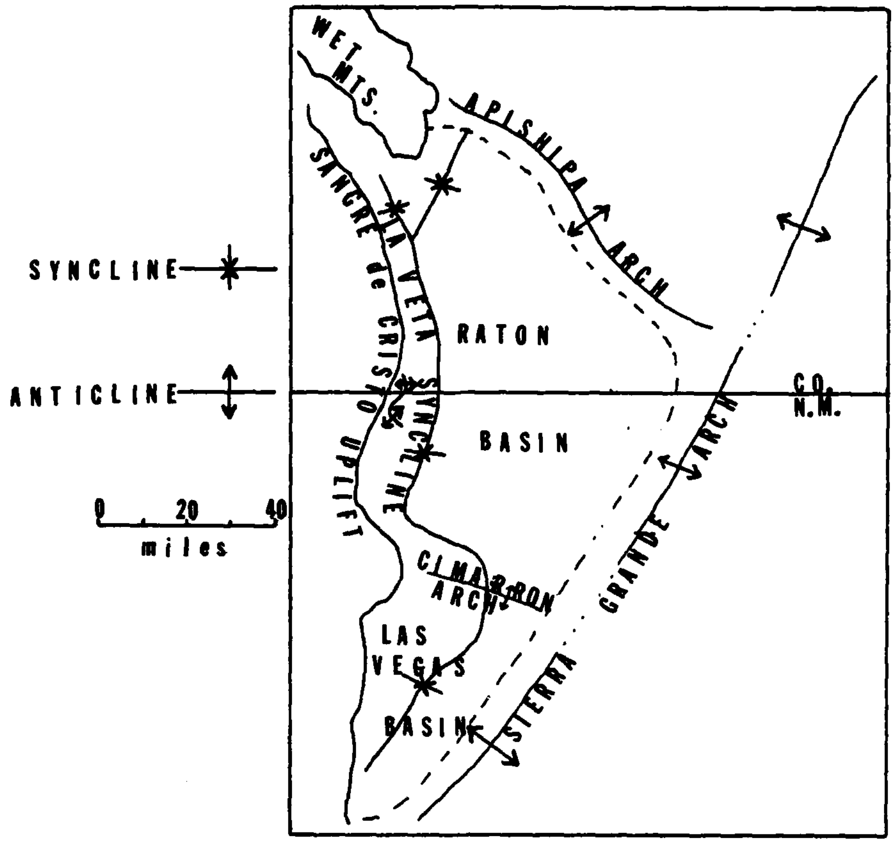

Figure 1. Geologic structures defining the Raton Basin of New Mexico and Colorado.

Purpose of the Investigation

Knowledge of the Basin is incomplete, and correlation of geophysical and geologic data has not been previously published. Therefore, in order to fill this void in the literature this thesis will undertake the following objectives: 1) Obtain and interpret both Free Air and Bouguer Gravity maps; 2) Obtain and interpret a vertical component magnetic map; 3) Obtain vertical, short-period seismic records for the Capulin area in an effort to determine the natural seismic activity; 4) Compare

geophysical data with the geologic structure, and 5) Determine whether economic potential in the Basin can be inferred from geophysical data. The study being reported here includes gravity, magnetic, and seismic surveys of portions of the Basin, including the Sierra Grande Arch and adjacent High Plains (figure 2).

General Geology of the Basin

The first of the two orogenies that have affected the Basin occurred during Pennsylvanian and Permian time (Baltz, 1965), and was responsible for detritus filling the Central Colorado Basin (located in the northern portion of the Raton Basin). The detrital material was derived from both west (San Luis Uplift) and east (the ancestral Wet Mountains Uplift) of the Basin. Contemporaneously, the Rowe-Mora Basin, which was in the general vicinity of the present Las Vegas Basin, also formed. This Basin was defined by the San Luis Uplift to the west, the Sierra Grande Uplift to the east, the Cimarron Arch on the north, and was linked by a low saddle to the Tucumcari Basin to the south. The Colorado and Rowe-Mora Basins filled with sediments which were derived from the ancestral Rockies and deposited in a marine transgressive environment of Pennsylvanian age. The resulting strata show a laterally complex composition reflecting the mixed terrestial-marine origin. These strata are thickest in the regime of the Sangre de Cristo Mountains. Large accumulations of sandstone and limestone occur in the southern portion of the Rowe-Mora Basin, but shale deposits, which are dominated by thick grey to black strata, predominate to the north. In fact, this shale which

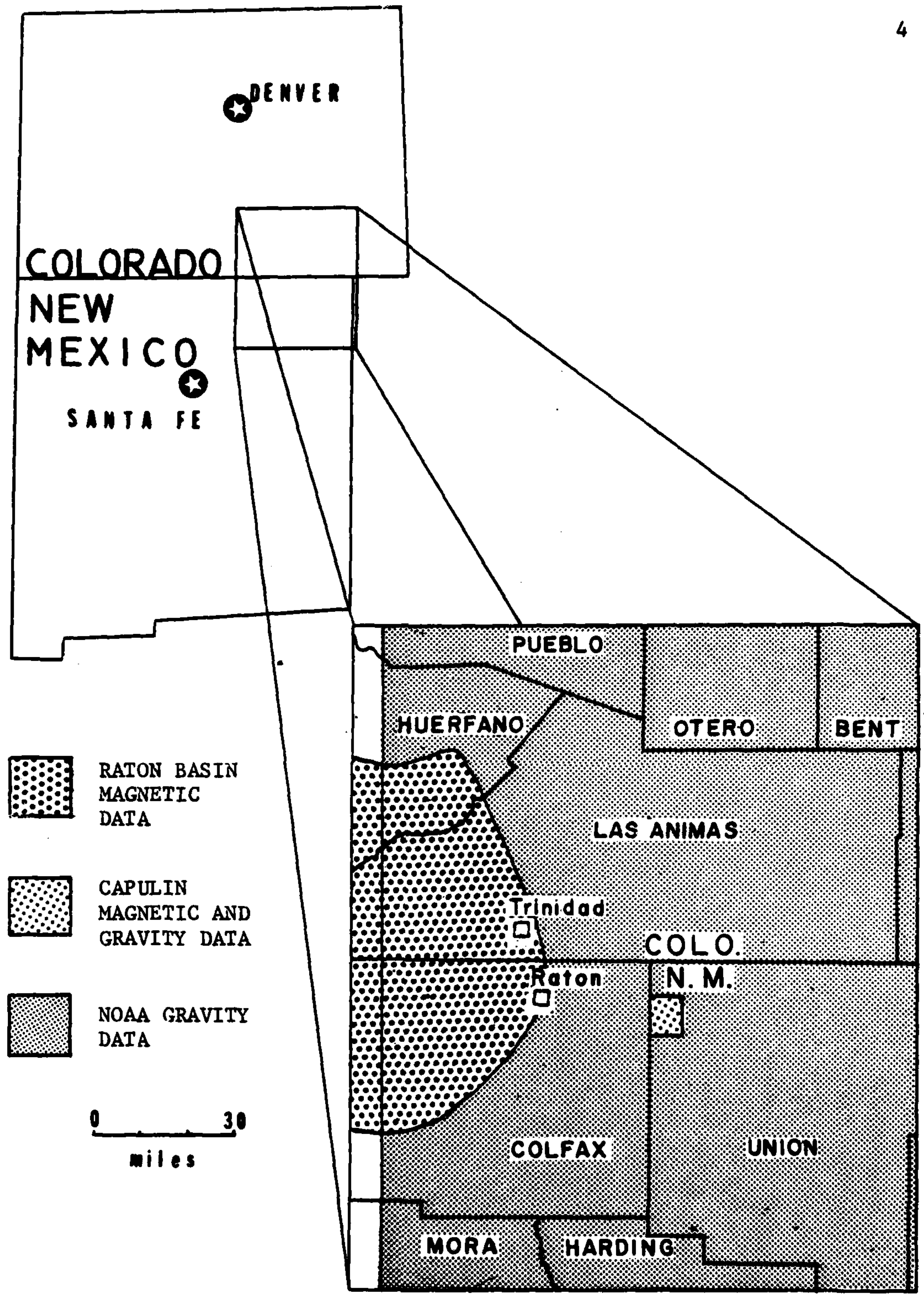

Figure 2. Location of the study area and limits to each survey in this report.

characterizes the northern part of the ancient Central Colorado Basin is a minimum of 9,500 feet thick (Brill, 1952). On the margins of the ancient basins, shale deposits thin towards the San Luis, Sierra Grande, and Wet Mountains Uplifts.

The depositional history of the strata in the Basin is complex as is the correlation between contemporaneous formations in the Las Vegas and Raton Basins (figure 3). Strata which were deposited in the Permian era are dominated by marine shales and clastic rocks. Triassic strata are composed primarily of terrestial clastic rocks but are, however, sparsely represented in the area. Today the Las Vegas Basin area is covered partially by Quaternary volcanic rocks. Discussion of the depositional and orogenic history is limited to the area of the present Basin and is based on rock outcrops and the known geologic structure (plate 1).

The oldest rocks identified in the Basin are marine sandstones and limestones of the Devonian Espiritu Santo Formation (Baltz, 1965) in the Las Vegas Basin and the Devonian Chaffee Formation (Johnson, 1969) in the Raton Basin. Limestone breccia of the Mississippian Tererro Formation rests unconformably on the Espiritu Santo Formation in the Las Vegas Basin. The Tererro Formation is missing in the Raton Basin.

The Pennsylvanian Magdalena Group is composed of sandstone and grey shale of the Sandia Formation and limestone of the overlying Madera Formation. The Sandia Formation in the Las Vegas Basin, which consists of over 1,000 feet of sedimentary rock, is correlative with the Deer Creek Formation and the lower part of the Minturn Formation of the Raton Basin.

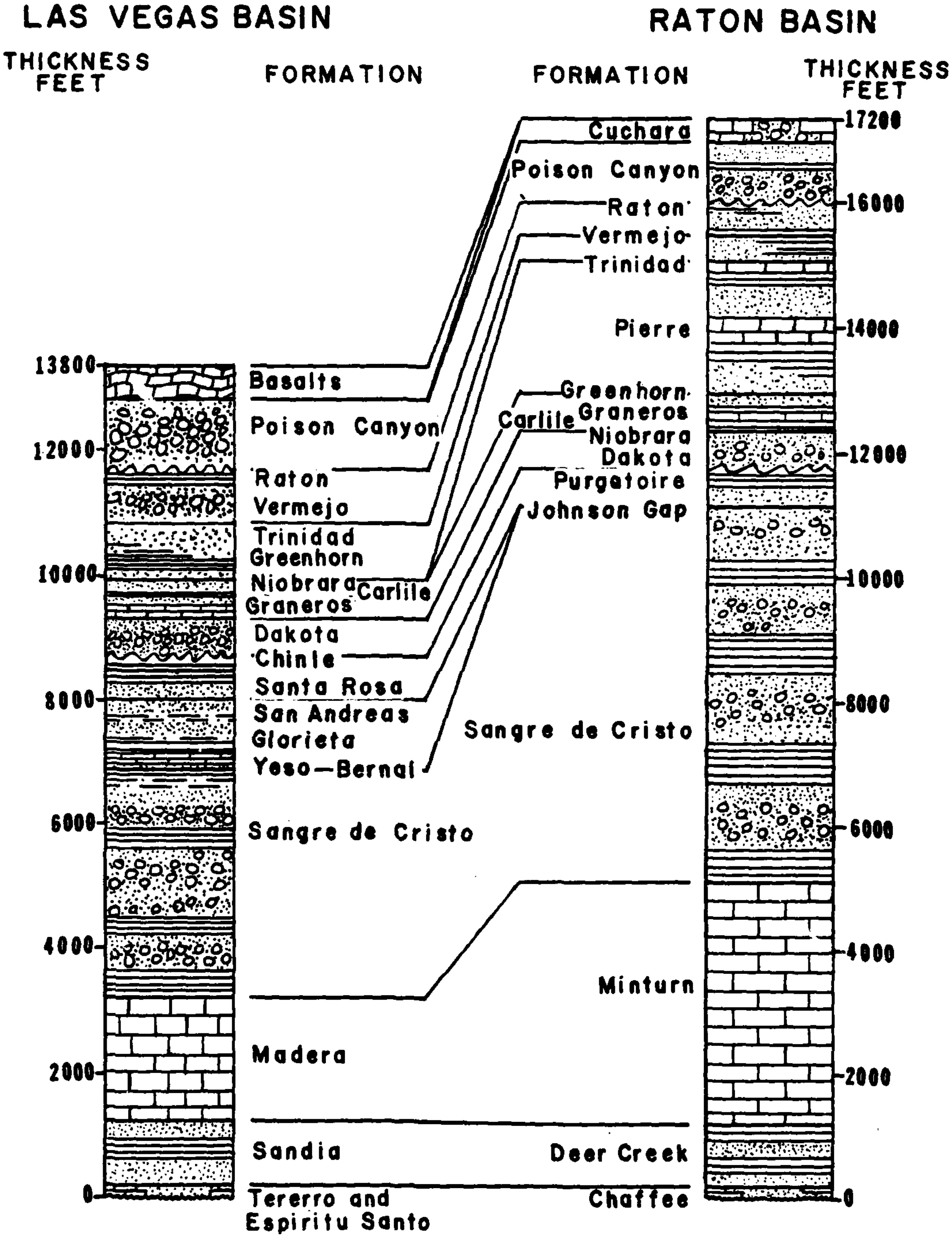

Figure 3. Columnar section of the Las Vegas and Raton Basins. Formation thicknesses are from Baltz (1962); symbols used in the columns are from Compton (1962).

The Madera limestone ranges from 1,000 to 3,000 feet in thickness in the Las Vegas Basin; it grades laterally northward into the Minturn Formation, which has a thickness of 5,500 feet. These units thin to the west and east of the Basin in the general direction of the San Luis and Sierra Grande Uplifts.

The Upper Pennsylvanian/Permian Sangre de Cristo Formation is approximately 3,500 feet thick in the Las Vegas Basin and greater than 9,500 feet thick in the Raton Basin (figure 3).

At the end of the Permian time a sea filled the Rowe-Mora Basin, and deposition of siltstone and shale of the Yeso Formation began. Located above the Yeso Formation is the Glorieta Sandstone and San Andreas Limestone, respectively. Overlying the San Andreas Limestone is the Bernal Formation which is composed of limestone, siltstone, shale, and sandstone. These three formations have a combined, maximum thickness of 1,075 feet (figure 3).

The Late Triassic Dockum Group lies conformably on Permian strata. In the Las Vegas Basin the Group is composed of both the Santa Rosa Sandstone and the overlying Chinle Formation shales. North of the Cimarron Arch the Dockum Group is correlative to the Johnson Gap Formation, which is composed of limestone conglomerate, limestone, siltstone, shale, and sandstone (Baltz, 1965). The Dockum Group is approximately 1,100 feet thick in the Las Vegas Basin and less than 700 feet thick in the Raton Basin.

By Early Cretaceous time the region was part of the Rocky Mountain geosyncline. The Laramide Orogeny, the second orogeny to affect the

area, continued from Cretaceous time through Oligocene time and produced the present Las Vegas and Raton Basins and other associated structures. At the beginning of the orogeny, the San Luis Uplift was still a positive area. By Eocene time the present Raton Basin was defined by the marked uplift of the Sangre de Cristo region and the gentle uplift of the Apishipa-Sierra Grande Arches. The Sangre de Cristo Uplift merged with the San Luis Uplift prior to the formation of the Rio Grande rift. When the Rio Grande rift formed in Miocene/Pliocene time, the San Luis positive area was downfaulted into the rift graben.

The Early Cretaceous Purgatoire Formation is composed of both conglomeratic sandstone and sandstone. The Dakota Sandstone overlies the Purgatoire Formation and is composed of interbedded, buff sandstone and shale. Together, these two formations are up to 650 feet thick, and today they form the primary groundwater aquifer in the Basin. Estimates place the volume of water stored in the Dakota Sandstone at 55 million acre-feet in New Mexico (Griggs, 1948); twice the above volume is estimated for the Basin.

The Graneros Shale, Greenhorn Limestone, and Carlile Shale are Late Cretaceous in age and vary in thickness from 385 feet to 700 feet (Baltz, 1965). The Upper Cretaceous Niobrara Formation is composed of less than 100 feet of shale and sandstone and rests conformably on the Carlile Shale.

Located on top of the Niobrara Formation is the Upper Cretaceous Pierre Shale, which is up to 2,300 feet thick in the Raton Basin but is absent in the Las Vegas Basin. The formation is composed of shale,

thin beds of limestone, and sandstone. Above the Pierre Shale are the Upper Cretaceous Trinidad Sandstone and Vermejo Formation, which are undifferentiated on some geological maps (Bachman and Dane, 1962). The Trinidad Sandstone is composed of arkosic sandstone with thin interbedded shale; it intertongues with the shale, coal, and arkosic sandstone of the Vermejo Formation. The thickness of the two formations varies from 250 feet to 850 feet. The Vermejo Formation is the main source of coal in the Basin, producing high volatile C bituminous coal of coking quality (Wanek, 1963). In the areas of extensive intrusive rocks, much of the coal was destroyed by contact metamorphism (Jurie and Gerhard, 1969).

The Raton Formation is Late Cretaceous to Early Tertiary in age and overlies the Vermejo Formation. It has a maximum thickness of 1,700 feet and is composed of arkosic sandstone, shale, and coal. The Poison Canyon Formation of Paleocene age lies unconformably on the Raton Formation. It consists of as much as 2,500 feet of arkosic sandstone, conglomerate, and thin shale. The youngest significant formation in the Basin is the Cuchara Formation, which is exposed around Spanish Peaks. It is Eocene in age and is composed of conglomeratic sandstone and interbedded shale.

During the latter stages of the Laramide Orogeny numerous intrusive rocks penetrated the sedimentary rocks. Dike swarms, sills, stocks and laccoliths dating from Eocene/Oligocene time are found throughout the Basin. However, the greatest concentration is found in the Spanish Peaks intrusive area. Many small anticlines are attributed to the intrusive

upwelling. Emplacement of many of the dikes, which are silicic to ultra basic in composition, appears to have been fault controlled (Wanek, 1963).

Volcanic activity was concentrated near the Sierra Grande Arch. Baldwin and Muehlberger (1959) identified three sequences of volcanic flows, dating from Miocene to Recent, that they called Raton, Clayton, and Capulin, respectively. Both the Raton and Capulin sequences are composed of basalts, and the Clayton sequence has a varied composition which ranges from extremely alkalic to subsilicic. Geochemical analysis of the volcanic rock suggests the magma originated in the upper mantle (Jones _et al_., 1976). Stormer (1972) suggests eastward migration of the vulcanism across the Rio Grande rift, from the San Juan volcanic field to the Sierra Grande volcanic field, occurred. Sanford _et al_., (1981) also suggest that the Sierra Grande vulcanism might be an eastern extension of the Jemez Lineation of western New Mexico. Further, Hamilton and Pakiser (1965) indicate that the Rio Grande rift is limited to the upper crust. Thus, the mantle may be the magma source in vulcanism on both sides of the rift.

It has been suggested (Edwards _et al_., 1978) that anomalously high heat flows may be caused by igneous activity within the Basin. Typical heat flow values for the Great Plains average 1.5 HFU (1 HFU = 1μcal/cm^2 sec), but values as high as 4.7 HFU are found in the Basin. Suppe _et al_., (1975) proposed a hot spot trace from eastern Arizona to a location near Raton, New Mexico. Reiter _et al_., (1979) theorized that a thermal anomaly formerly existed east of the Southern Rocky Mountains and is now

centered near the Sierra Grande Arch. They noted that radioactivity of the sedimentary rocks within the Basin can account for only ten percent of the observed increased heat flow; the remainder is unexplained.

In summary, the total thickness of sedimentary fill in the Basin is about 17,000 feet. The Basin sediments date from Middle Paleozoic time and have been affected by two orogenies. These sedimentary rocks have economic importance, and mining activities in the Raton Basin have produced coal and graphite in commercial quantities. Cretaceous rocks are also known to have both oil and gas in small quantities. Currently, there is one commercial oil well in Huerfano County, Colorado, at the northern end of the Basin, and a gas field near the Basin in eastern Las Animas County, Colorado. A basement structure map will be developed in Chapter III using the densities of the sediments described above, and the gravity data that will be introduced in Chapter II.

CHAPTER II

DATA COLLECTION AND REDUCTION

General Statement

A portion of the gravity data used in this study were obtained from the National Oceanic and Atmospheric Administration (NOAA), Washington, D.C. The gravity and magnetic measurements in the vicinity of Capulin National Monument, New Mexico and the magnetic measurements in the Raton Basin were made by the author during 1981. Each gravity station in the vicinity of Capulin National Monument was also a magnetic station. In order to provide a detailed analysis of the Basin, additional magnetic stations were spaced midway between the gravity stations. NOAA station density is 0.06341 station per square mile; Capulin gravity station density is 1.333 stations per square mile; and Raton Basin magnetic station density is 0.0650 station per square mile.

Elevation Control

U.S. Geological Survey fifteen minute quadrangle maps were used to determine elevations for stations near Capulin. Such elevation data were supplemented with a preliminary Bureau of Land Management map of Capulin National Monument. Spot elevations on the maps at road intersections and benchmarks were used wherever possible. Elevation accuracy is within five feet, corresponding to ± 0.35 mgal accuracy in gravity measurement. Elevation effects were insignificant in the reduction of

the magnetic data.

Magnetic Data Measurement and Reduction

The Capulin magnetic data were collected using an E.J. Sharpe PMF-3 flux gate magnetometer (50 and 100 gammas per division). Station number one (figure 14) was arbitrarily chosen by the author as the datum for the survey. Station reoccupation resulted in a minimum of three datum measurements each day and a minimum of two cross correlations on stations occupied on previous days. Diurnal correction graphs were computed daily, and were used to adjust all measurements.

The Raton Basin magnetic data were collected using an Askania vertical Torsion magnetometer (2.433 gammas/degree-scale division). Field procedures for the Raton magnetic survey were the same as those employed in the Capulin magnetic survey. Normal field corrections were computed from 36°30'N, 105°15'W using the Regional Vertical Intensity Map 1965. Latitude correction was 909.09 gammas per degree latitude (12.98 gammas per mile); longitude correction was 434.80 gammas per degree longitude (7.9 gammas per mile).

Gravity Data Measurement and Reduction

Datum for gravity data acquired from NOAA is sea level. The density used in Bouguer anomaly calculations was 2.67 g/cc. Gravity data acquired near Capulin National Monument were collected using a North American gravimeter (0.107 mgal per division). Station number one was

selected to coincide with a NOAA station in the survey area and was used as the datum for the Capulin survey. This procedure allowed comparison of the Capulin data to the NOAA data. Latitude corrections were made from $36^{\circ}48'18''$N at a rate of 1.25 mgal per mile.

Seismic Data

A short period vertical Geotech 18300 seismometer with a free period of one second was buried approximately two feet in depth at the Visitor's Center, Capulin National Monument, from 16 July 1981, to 23 September 1981. During this period, 51 daily seismograms containing 1,122 hours of data were recorded by a Sprengnether VR-50 recorder-amplifier. Damping was increased after 14 August 1981 from normal internal resistance to 2,200 ohms resistance across the input terminals of the amplifier. Filters were not used.

Each seismogram contains twenty-four hours of data with the minute marks spaced sixty millimeters apart. The ink trace was approximately 1.0 mm thick and makes it impossible to resolve frequencies higher than one Hertz. Estimated amplification from artificial inputs is between 25,000 to 50,000.

Computer Processing Techniques

Modified computer programs from Davis (1973) and new programs written by the author for this study were employed to process both magnetic and gravity data on an IBM 360 computer housed at Texas Tech University. The machine processing helped to verify manual calculations and also to derive mathematical models that would have been impossible to obtain by

other means.

All data were systematically processed in the same manner. First, the corrected data were filtered by a uniform matrix of either 1,600 or 2,400 elements. The matrix value of each element was obtained by calculating the algebraic average of the six nearest data values. Development of the matrix by interpolation over six data values for each element results in the minimum and the maximum values in the completed matrix to be less than the minimum and the maximum values in the input data. Less than six data values in the interpolation increased the minimum-maximum range in the matrix; however, the areal extent of the maximum and the minimum features would have appeared exaggerated in the final map. This causes mountain peaks to appear as elevated buttes or mesas. The use of more than s x data values in interpolation resulted in excessively reducing the minimum-maximum range in the matrix.

Statistical Analysis System's SAS/GRAPH (Reinhardt, 1981) was used to produce the computer maps from the interpolated matrix. These maps were contoured on a strict mathematical ratio by the computer; therefore, the technique can be used advantageously to compare different data sets (gravity and magnetic) produced at the same scale and in the same geographic area. In order to compare the different mapping techniques, both computer plotted and hand drawn maps using the same data sets have been included in this report.

The computer also was used to compare the computer contoured map of the data contained in matrix form to a surface defined by a polynomial of order n. A polynomial of order 0 represents a dipping plane, and polynomials of very high order very accurately represent the data in

matrix form. A second order polynomial was found to accurately represent the steep gravity dip under the Sangre de Cristo Mountains and the shallow gravity dip of the Great Plains. The residual gravity (Smith, 1970; Dobrin, 1976), or difference, of the second order polynomial from the matrix gravity data was used to construct the basement structure map described in Chapter III.

CHAPTER III

PRESENTATION AND INTERPRETATION OF THE GRAVITY, MAGNETIC, AND SEISMIC DATA

Free Air Gravity Data

The NOAA free air gravity data have been tabulated and included in Appendix A. The gravity data acquired in the Capulin area as part of this study, which will be discussed as an addition to the NOAA data, have been tabulated and included in Appendix B.

The NOAA free air gravity anomaly data are shown, for comparison, in hand drawn (figure 4) and computer plotted (figure 5) formats. The algebraic averages for the station elevation, free air anomaly, and Bouguer anomaly in each one degree block in the study area are shown in figure 6. The free air anomalies for the northern two blocks of the study area are nearly zero and suggest isostatic equilibrium for this area. However, the free air anomalies are significantly positive in the southern two blocks of the study area and could indicate lack of local isostatic adjustment in these areas. The question of regional isostatic equilibrium is, therefore, raised.

Perfect isostatic adjustment assumes that any near surface positive mass has an equal amount of negative mass below the compensation level within the Earth, and in the simple case, such a mass distribution would cause near zero free air gravity anomalies. However, in elevated terrain, as in the study area, the gravitational effect upon a surface

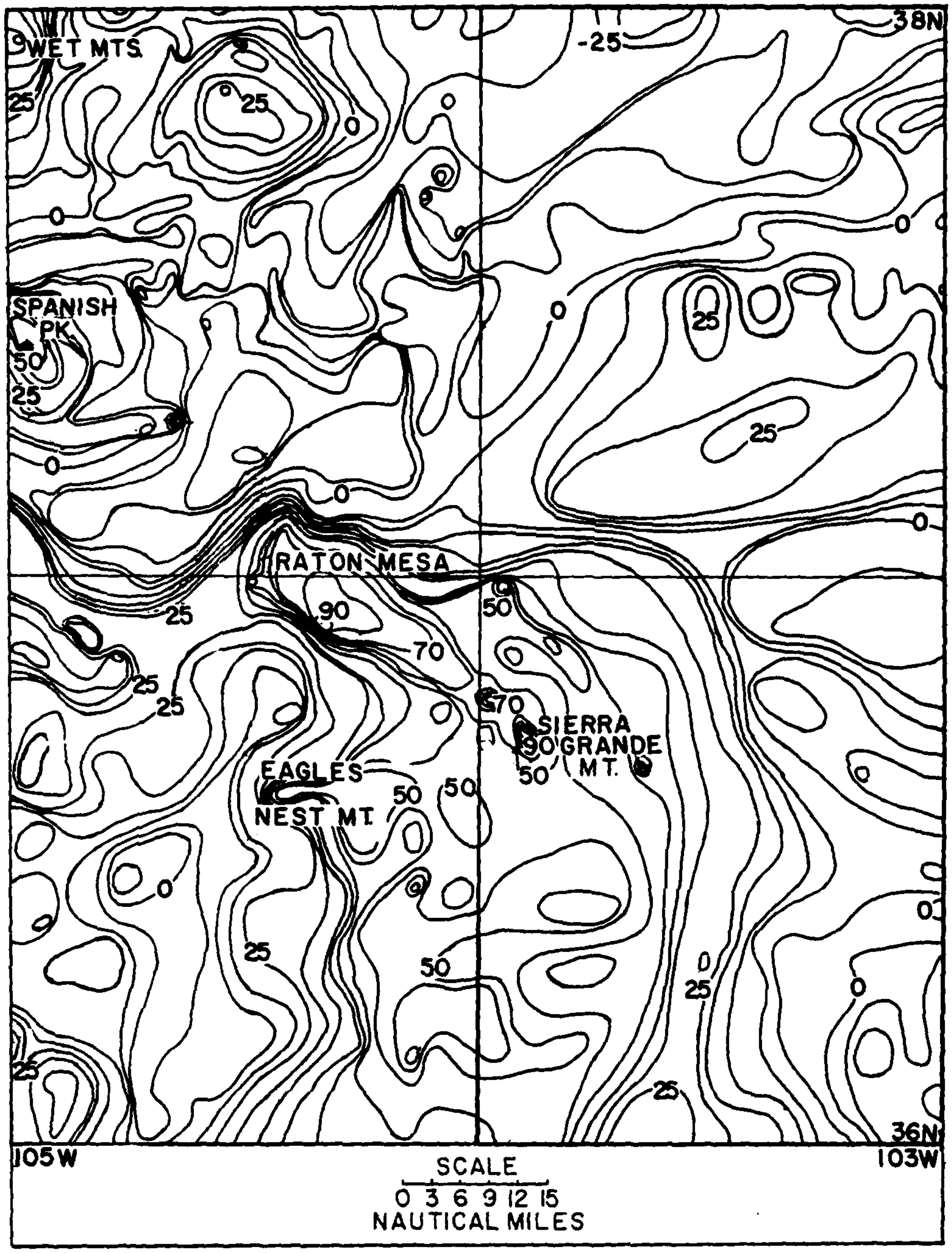

Figure 4. Regional free air gravity map using NOAA gravity data. Datum is sea level and gravity stations are shown in Figure 10. Contoured by hand.

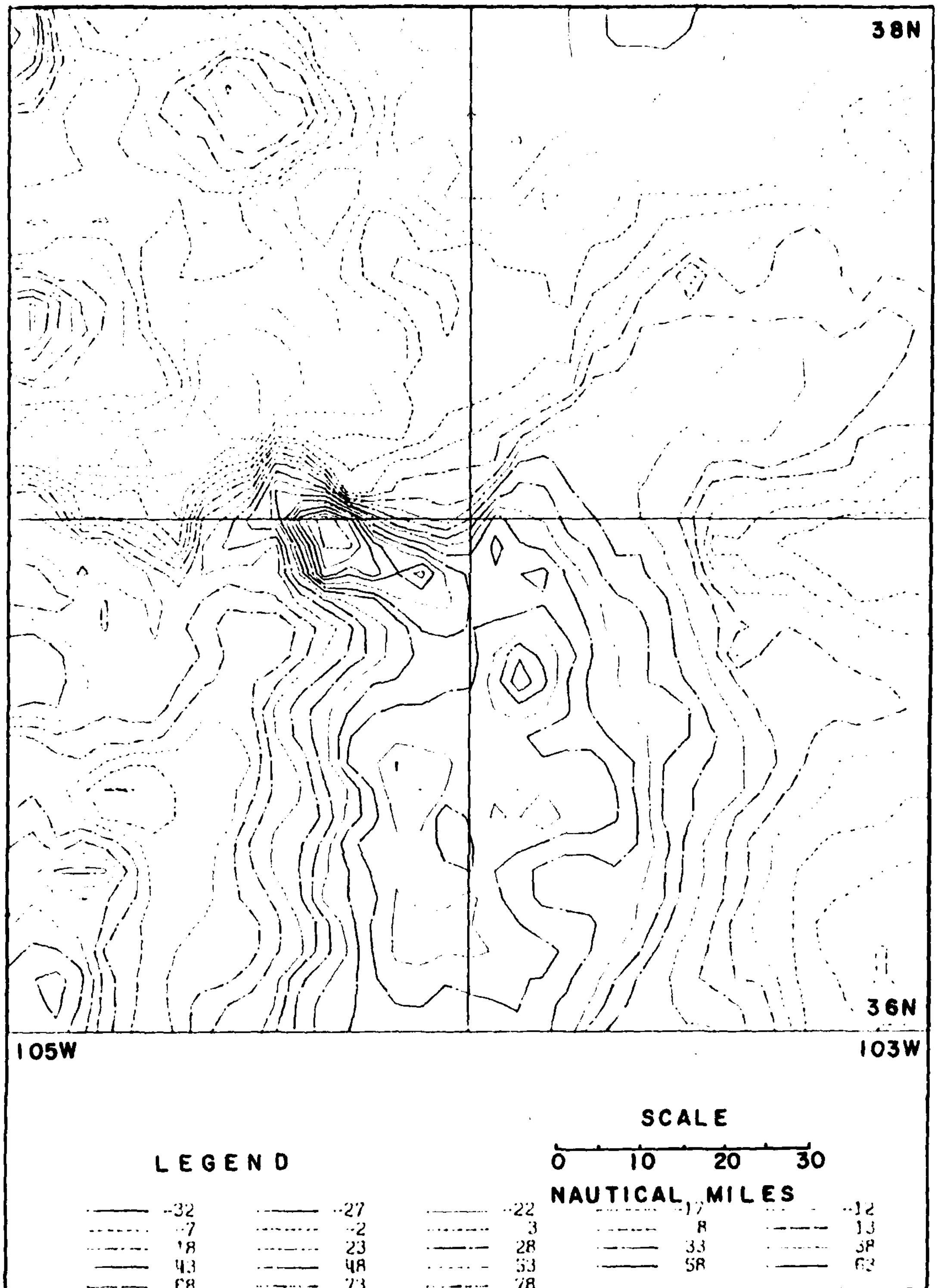

Figure 5. Regional Free Air anomaly map of the study area. Gravity stations are the same as in figure 10. Contour interval is 5 mgal, datum is sea level.

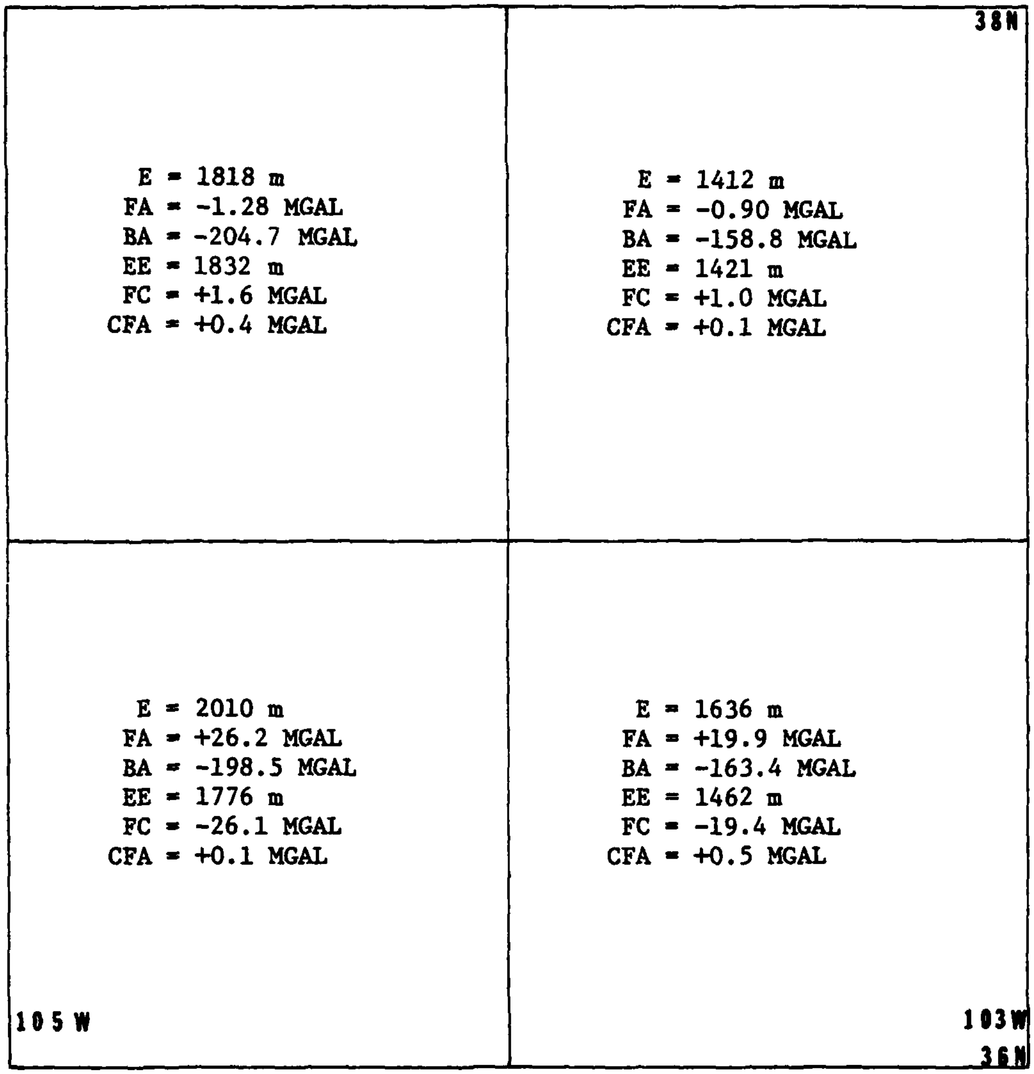

Figure 6. Graphic representation of the algebraic averages of the NOAA gravity and elevation data divided into one degree latitude and longitude blocks. E = elevation; FA = free air anomaly; BA = Bouguer anomaly; FC = Faye correction; EE = equivalent elevation; CFA = corrected free air anomaly (FA + FC).

measurement, of the near surface rock (the positive mass) is larger than the gravitational effect of the negative mass at the compensation level simply because the near surface rock is nearer the measured station. This means that a positive free air anomaly is in part caused by depth to compensation and does not necessarily indicate crustal loading. It is possible that the total observed free air anomaly can be explained in terms of the depth of isostatic compensation. Therefore, if the free air anomaly is to be used in an estimation of isostatic adjustment, a correction must be applied.

The correction applied to the observed free air anomaly for the effect of depth to compensation is generally called the Faye correction, after the man who first discussed the effect in the Nineteenth Century. One method of calculating the Faye correction uses the Bouguer anomaly to determine the elevation of the surface of a slab which is in isostatic balance (Woollard, 1962). This is done by assuming, if isostatic adjustment is complete, the Bouguer anomaly is related to the surface elevation of the crustal load causing the adjustment. The elevation of this surface slab is thought of as the equivalent elevation (h') derived from the Bouguer anomaly ($h' = BA/2\pi\gamma\rho$; where γ is the gravitational constant and ρ is the assumed density). The equivalent elevation is subtracted from the station elevation (h) and the difference (Δh) defines the slab thickness used in the Faye correction (F.C.): $F.C. = 2\pi\gamma\rho\Delta h$. The Faye correction is subtracted from the free air anomaly to produce a corrected free air anomaly value, which is actually the isostatic anomaly since this computation has removed the effect of depth of compensation upon

the free air anomaly. As a result of applying the Faye correction to the free air anomalies in the study area (figure 6) the corrected free air anomalies clearly suggest regional isostatic equilibrium.

Although regional isostatic equilibrium is established, the locally positive average free air anomalies of the southern two blocks (figure 6) are indications of a lack of local compensation. The Quaternary volcanic rock covering most of the southern two blocks of the study area is missing in the northern portion of the study area and is assumed to be the cause of the large positive free air anomaly in the southern two blocks. If this is so, the free air anomaly can be used to estimate the rock thickness. If a density of 2.67 g/cc is assumed for the volcanic rock, and the formula for the gravitational effect of a slab is solved, a thickness of 180 m is indicated for the Quaternary volcanic rocks. As a confirmation of the rock thickness calculated from gravity data, a water well at Capulin National Monument penetrated 196 m of volcanic rock. The real thickness is probably somewhat irregular, and the value computed from the gravity data appears to be a good estimate.

Comparison of the free air map and topographic map (figure 7) shows that positive topographic features are also areas of positive free air gravity anomalies throughout the Basin and Great Plains. This relationship is to be expected (Woollard, 1959), and the larger topographic features are associated with larger local positive free air anomalies.

The area of the Capulin free air gravity map (figure 8) is covered by volcanic rocks of three sequences - Raton, Clayton, and Capulin. The average free air anomaly over the map is about +55 mgal, with a large

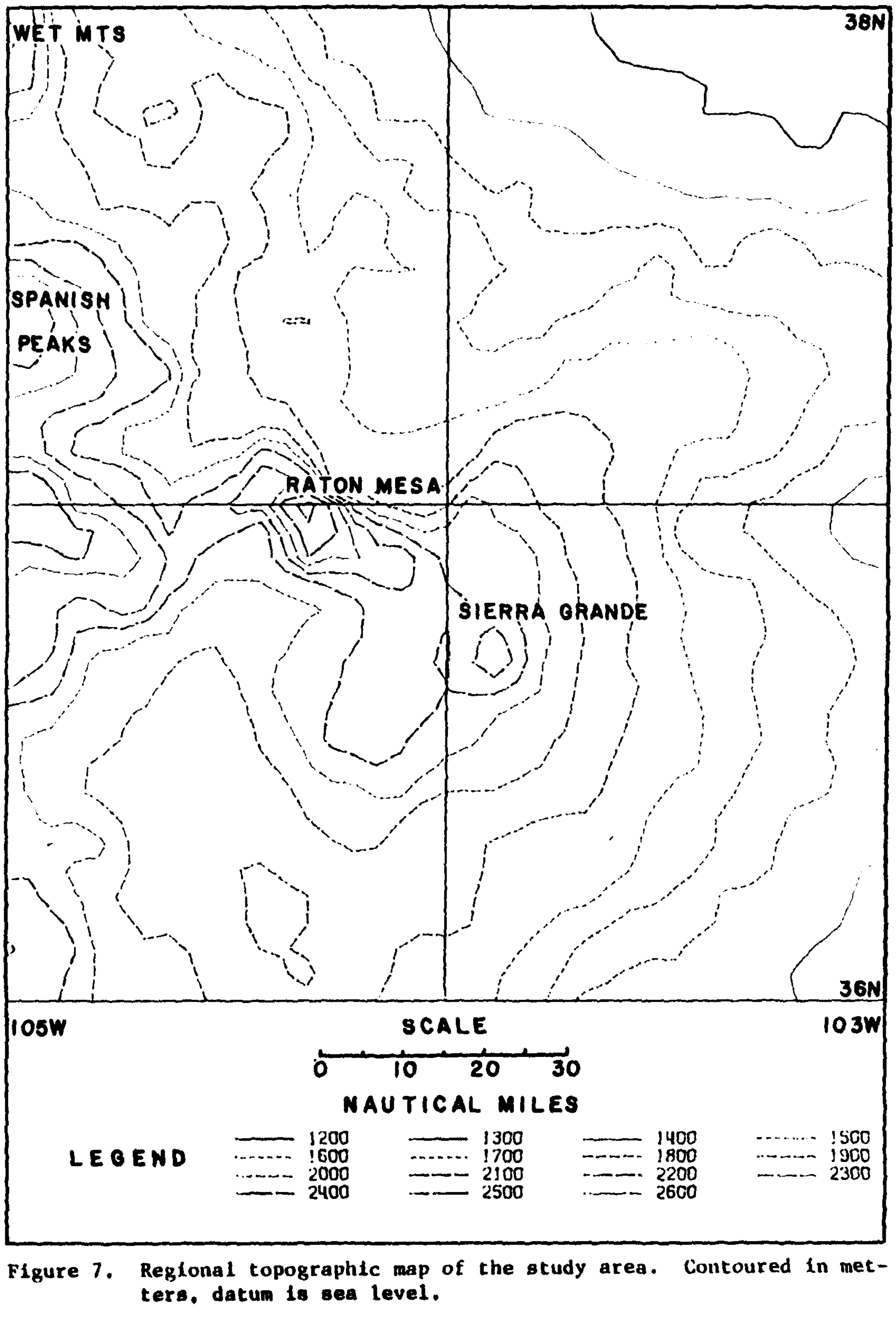

Figure 7. Regional topographic map of the study area. Contoured in meters, datum is sea level.

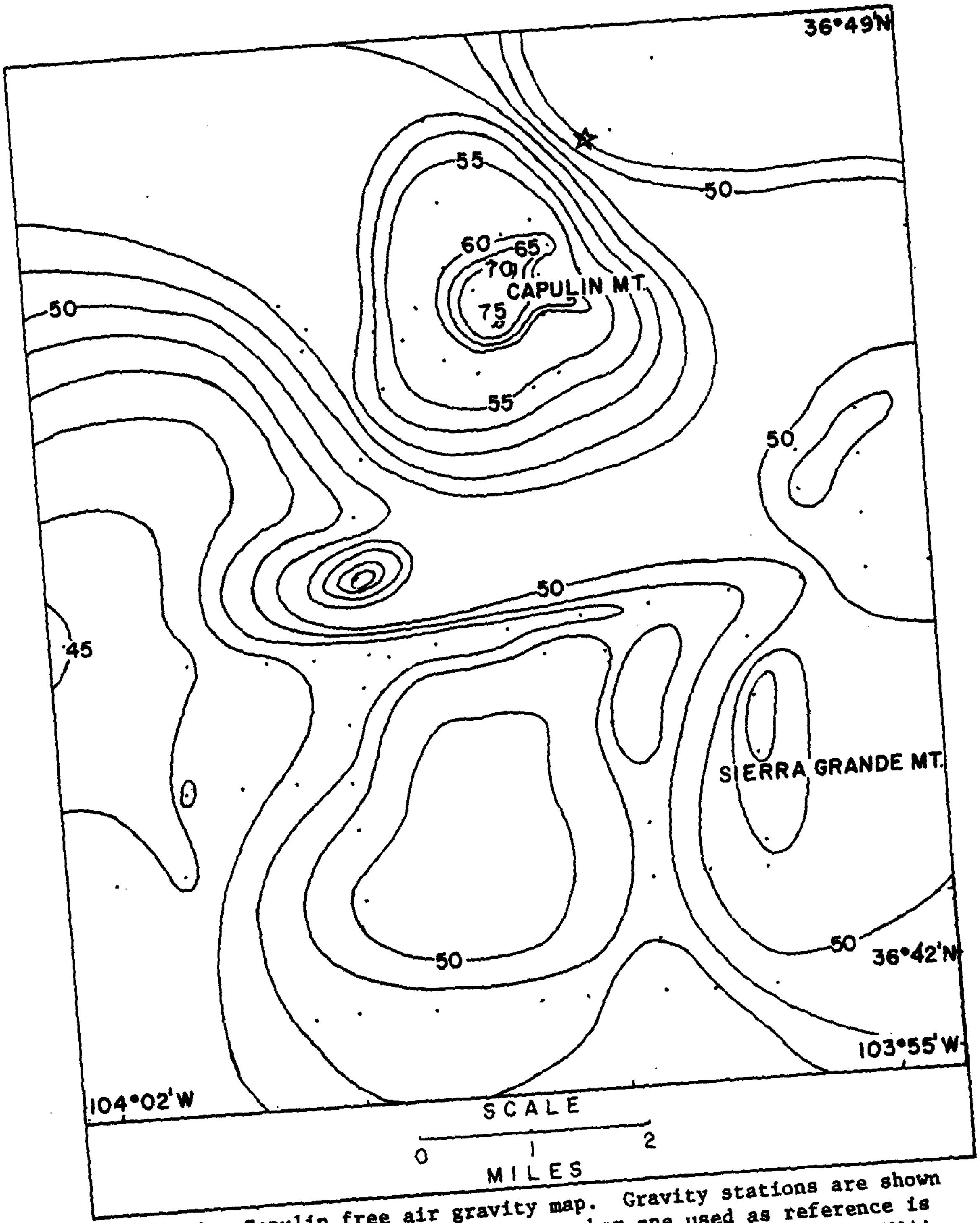

Figure 8. Capulin free air gravity map. Gravity stations are shown by dots (·), and station number one used as reference is designated by a star. Station number one is also a NOAA gravity station, therefore, correlating the Capulin gravity data to the NOAA gravity data.

free air anomaly of +70 mgal associated with Capulin Mountain. This large free air anomaly at the mountain station (+70 mgal) is +15 mgal different than the regional free air value immediately around the mountain (+55 mgal). The 335 m cone comprising the mountain has approximately the same volume as a right cylinder 112 m high with the same radius of 500 m. The gravitational effect of such a cylinder, assuming a density of 2.67 g/cc, would be 12.4 mgal if the top of the cylinder is located at mountain peak elevation. This calculated value is not precisely equal to the 15 mgal anomaly observed associated with Capulin Mountain, but the method of calculation is only approximate. Agreement is close enough to allow the assumption that the gravitational effect of Capulin Mountain itself is 15 mgal.

Bouguer Gravity Data

The plot of average elevation against average Bouguer anomalies (from figure 6) indicates an inverse relationship between elevation and the Bouguer data (figure 9). The Bouguer anomaly is actually the negative gravity effect of the root increment below the compensation level. As the terrain elevation increases, the root increment below the compensation level also increases in thickness to maintain isostatic equilibrium. An increase in the thickness of the root below compensation level results in a more negative Bouguer anomaly. The Bouguer gravity maps (in hand drawn form - figure 10, and computer plotted form - figure 11) indicate this relationship between rising topography (figure 7) and a decreasing Bouguer equipotential surface. The slab assumed in making the Bouguer correction results in the computation of a Bouguer anomaly that is excessively negative in areas which are distinguished

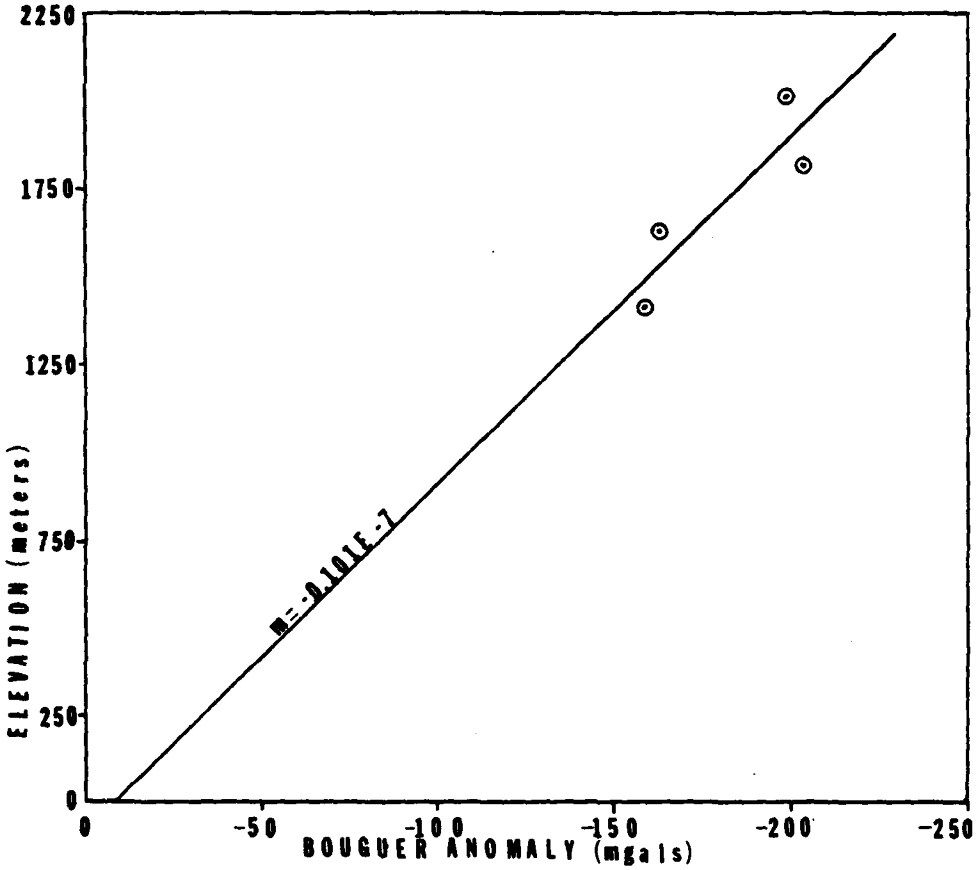

Figure 9. Plot of the averaged NOAA elevation data vs, the averaged NOAA Bouguer gravity data. The slope of the line, m, shows the inverse relationship of elevation and Bouguer gravity values.

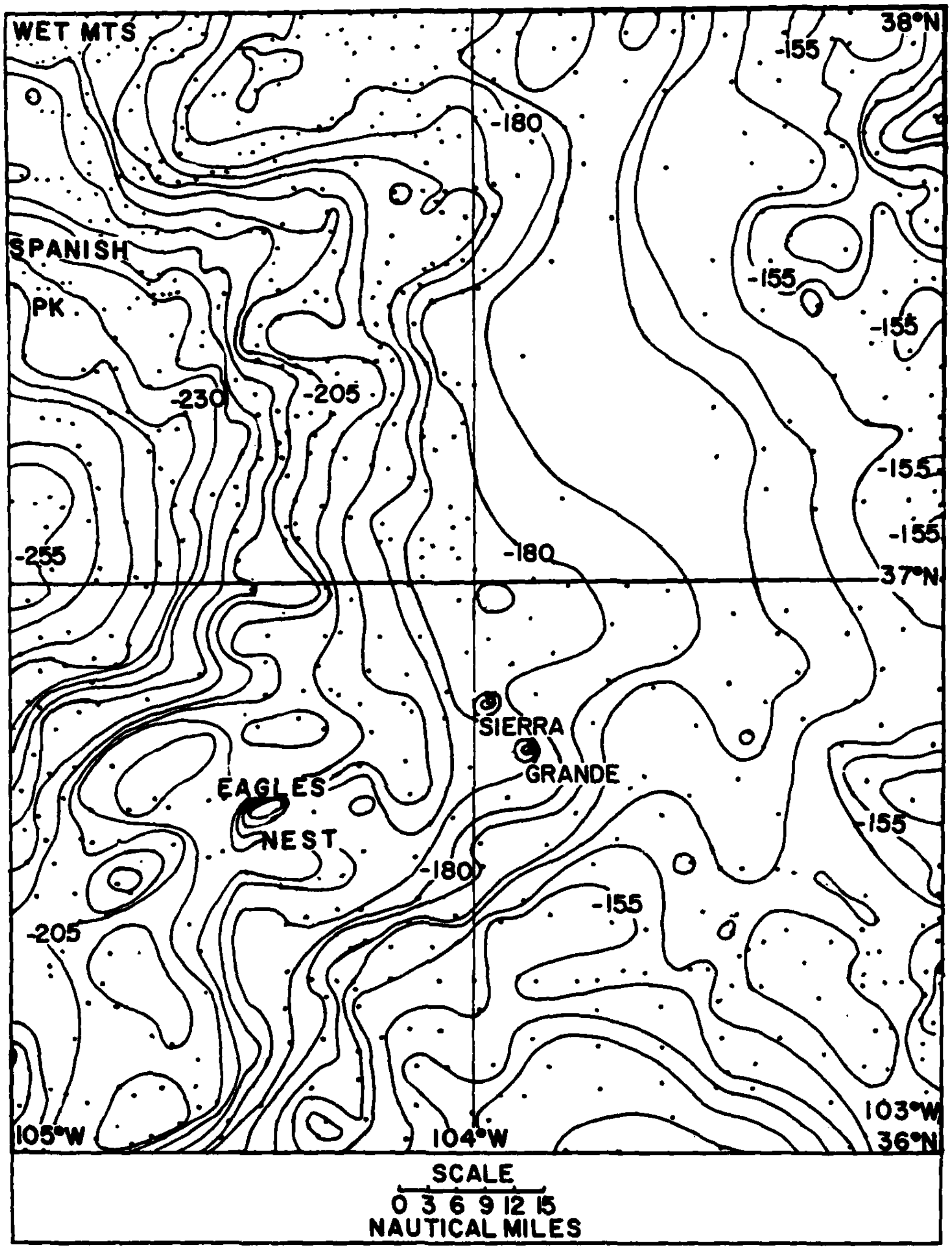

Figure 10. Regional Bouguer gravity map using NOAA gravity data. The dots represent the gravity stations. Datum is sea level, and a density of 2.67 g/cc was used in calculating the Bouguer correction.

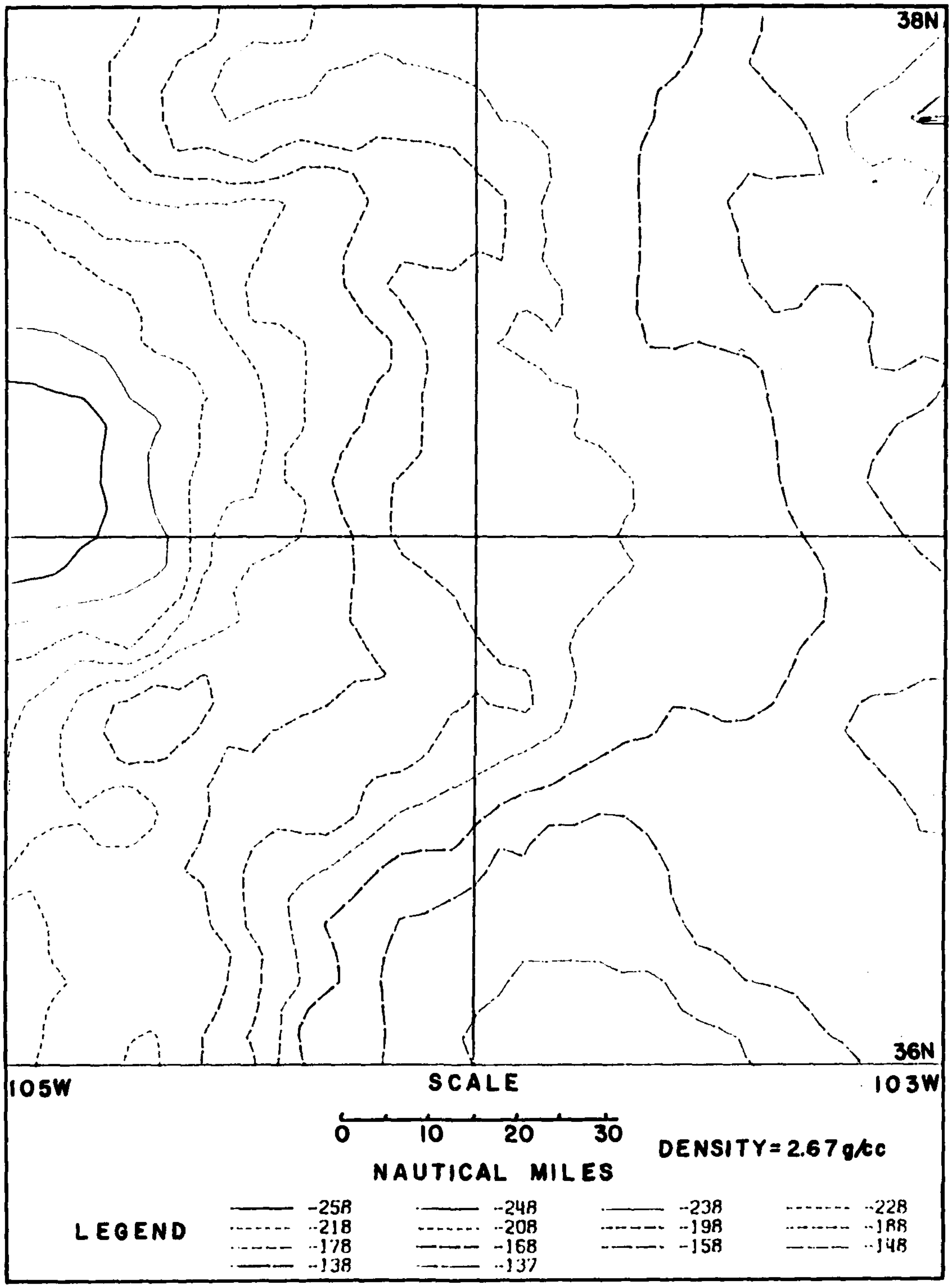

Figure 11. Regional Bouguer anomaly map of the study area. Gravity stations are the same as in figure 10. Contour interval is 10 mgal, datum is sea level.

by topographically isolated terrain, such as mountains. Sierra Grande Mountain is an example of this effect; however, Spanish Peaks and the Wet Mountains regions have sufficient areal extent to allow the slab assumption in the Bouguer calculation.

Eagles Nest Mountain has associated with it both a positive free air anomaly and positive relief with respect to the surrounding Bouguer surface on the Bouguer anomaly map. The positive free air anomaly is expected due to the near surface mass effect of the mountain. The presence of positive relief on the Bouguer equipotential gravity surface may indicate a near surface high density body, which would cause the Bouguer correction to be too small, or it may indicate the extension below datum of the igneous material forming the mountain. In either case, it appears that the density of the rocks forming Eagles Nest Mountain is greater than 2.67 g/cc.

The free air anomalies corrected for the Faye effect in the study area have already been shown to indicate isostatic adjustment, and the computation of isostatic anomalies directly from Bouguer anomalies can be used to add validity to this conclusion. The computation of the isostatic anomalies done here is based upon the Airy isostatic model with the density contrasts and formulas suggested by Woollard (1969). The slab thickness of the mass below the compensation level is determined by assuming that part of the negative Bouguer anomaly is caused by the presence of a slab of crustal material displacing heavier mantle material. Woollard (1969) determined that a crustal density of 2.92 g/cc is representative of the crustal rock at the compensation level (M-discontinuity)

and a density of 2.67 g/cc is representative of the upper crustal rock. The gravitational effect of the elevated surface is equal to the simple Bouguer correction computed using a density of 2.67. However, the effect of the surface slab upon a measured value on the surface is exaggerated as compared to the effect of the compensating root slab upon the same measurement as previously discussed. Therefore, if the region is in isostatic balance, the observed simple Bouguer anomaly is equal to the Bouguer gravity effect computed for the surface slab with average elevation in the area, minus the exaggeration effect of slab position. Previously, it was shown that this exaggeration effect is approximately equal to the observed free air anomaly. The isostatic anomalies for each one degree block in the study area have been calculated in this manner, and the values are shown in table 1.

These isostatic anomalies show the study area to be in near isostatic equilibrium, as was suggested in the free air anomaly discussion. Qureshy (1962) studied the Bouguer data for all of Colorado and concluded that the eastern portion of the state, including the northern part of this report's study area, is in isostatic equilibrium. The slight positive bias in the results may be explained by either crustal thickening or increased crustal density (Woollard, 1969).

Table 1 includes calculations of crustal thickness using Shurbet's (1966) density model and formulas. The crust thins from west to east, and continues to thin east of the study area. Stewart and Pakiser (1962) calculated a seismic refraction profile using the Gnome explosion. Their computed thickness is very close to the crustal thicknesses

Table 1. Theoretical and actual gravity anomalies in the study area. All values averaged over one degree block.

Area $1^o x 1^o$ N-W	Elevation h (meters) (1)	Theoretical gravity due to the positive mass g_p mgal (2)	Obs. BA p=2.67 g/cc mgal (1)	Obs. FAA mgal (1)	Isostatic anomaly FA-BA-gp	Compensation "root" H km (3)	Crustal thickness T km (4)
36-103	1636	182.8	-163.4	+19.9	+0.5	9.07	43.71
36-104	2010	224.6	-198.5	+26.2	+0.1	11.02	46.03
37-103	1412	157.8	-158.8	-0.9	+0.1	8.82	43.23
37-104	1818	203.1	-204.7	-1.2	+0.4	11.37	46.19

(1) from figure 6

(2) $g_p = 2\pi\gamma\rho h$, where $\rho = 2.67$g/cc, and h = average terrain elevation

(3) from Shurbet (1966) $H = BA/2\pi\gamma\rho = BA/18.01$, where H is the thickness of the compensation root; $\rho = 2.67$ g/cc

(4) from Shurbet (1966) $T = 33 + H + h$, where T is crustal thickness, H is root thickness, and h is terrain elevation

calculated using gravity data in this report.

In addition to the NOAA Bouguer gravity data, a separate Capulin Bouguer gravity map (figure 12) was prepared from data collected by the author. The Bouguer anomaly associated with Capulin Mountain is about -200 mgal, which is approximately 20 mgal more negative than the adjacent area. Since the mountain is a feature with little area, the slab assumed in the Bouguer correction has exaggerated the Bouguer anomaly. Because the mountain itself is 335 m high, a total of 37.4 mgal was subtracted from the measured value as a part of the total Bouguer correction for the height of the mountain. The actual gravitational effect of the mountain has previously been shown to be about 15 mgal. Therefore, the Bouguer correction applied to the mountain station was exaggerated by 22.4 mgal. Correction for this exaggeration shows the area beneath the mountain to be only slightly more negative than the surrounding area, and no additional mass deficiency exists beneath the mountain as compared to the surrounding area.

Since the study area, including the Capulin area, has been shown to be in isostatic balance, the Bouguer equipotential surface is expected to reflect variations in crustal thickness as well as local changes in crustal density. Therefore, the Bouguer anomalies can be used to calculate sedimentary thickness in the Basin. Calculations of this kind were carried out to produce a basement relief or structure map.

Raton Basin Basement Structure Map

In previous studies (Griggs, 1948; Baltz, 1965), subsurface structure in the Basin has been deduced from surface rocks and well log

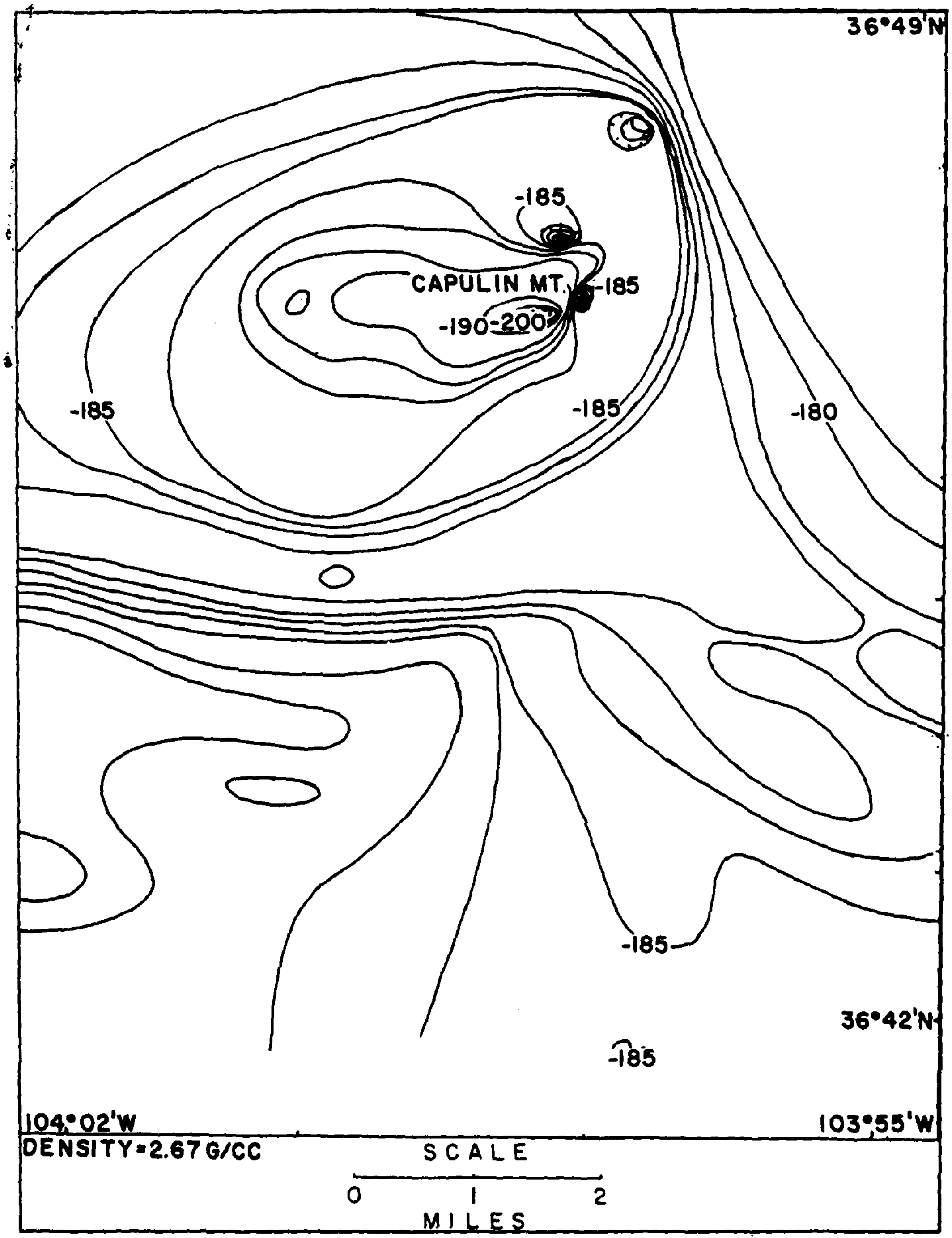

Figure 12. Capulin Bouguer gravity map. Data stations are the same as shown in Figure 8. Density used for the Bouguer corrections is 2.67 g/cc.

data. A basement relief map based on structural data cannot be drawn because geologic mapping in the Basin is incomplete. However, Bouguer gravity data were used in this study to deduce crustal thicknesses and to determine basement structure (or relief). The basement surface computed is defined as the boundary between the less dense sedimentary rocks above and denser crystalline rocks below. Intrusive rocks that penetrate the strata are also classified as basement rocks because their presence causes effective thinning of the sedimentary column in the computation.

The best method for determining basement relief is based upon the realization that the Bouguer anomaly is actually the negative gravity effect of the slab or root which has displaced the heavier material of the sub-compensation level. In this study, it is assumed that the negative effect is locally affected by less dense sedimentary rocks displacing heavier basement rocks; therefore, the variation in the Bouguer gravity values can be interpreted in terms of variation in the thickness of the sedimentary rocks.

As a first step in constructing a basement relief map for the Basin it was necessary to ascertain the regional trend of the Bouguer gravity map. A second order polynomial surface was empirically determined to best represent the Bouguer gravity surface as discussed in Chapter II. Variation between this regional trend and the observed local Bouguer gravity values is assumed to be caused by differences in thickness and density of the sedimentary rocks.

The areal extent of the various lithologic units is shown in plate

1; Clark (1966) gives representative densities for the rock types present. Representative densities for the columnar sections (figure 3) for the Las Vegas and Raton Basins, respectively, were found to be 2.27 g/cc based on the densities reported by Clark (1966). The density contrast between the representative density for the Basin and the density used in the Bouguer correction (2.67 g/cc) is -0.4 g/cc. Estimations of lateral variations in the density contrast throughout the Basin were based on the following criteria: 1) sedimentary rock thinning near the Apishipa, Cimarron, and Sierra Grande Arches; 2) presence of volcanic rock in the southern portion of the Basin; 3) higher density intrusive rocks near Spanish Peaks and Wet Mountains regions; and 4) an average sedimentary rock density of 1.8 g/cc (producing a -0.87 g/cc density contrast) for the Great Plains (east of the Apishipa Arch - Sierra Grande Arch axes) as determined by Shurbet (1966). A representative calculation from the Bouguer gravity map (figure 10) along 37^{o}N, 104^{o}-105^{o}W is included (figure 13).

At 37^{o}N, 104.5^{o}W (figure 13), the Bouguer anomaly value, determined from the Bouguer gravity map, is -216 mgal. The regional Bouguer trend value (-210 mgal) was computed from a second order polynomial surface described in Chapter II. The residual gravity value (Δg) at 37^{o}N, 104.5^{o}W is the difference between the Bouguer gravity value and regional trend value at that point (-210 + 216 mgal = +6 mgal). The density contrast value ($\Delta\rho$) at 37^{o}N, 104.5^{o}W, determined from the density contrast model, is -0.58 g/cc. The depth to the basement relief surface is found

Figure 13. Basement structure profile derived from NOAA Bouguer gravity data along 37^{o}N, 104^{o}-105^{o}W.

A. The regional Bouguer dip is determined by a smooth curve through the Bouguer anomaly equipotential surface.

B. The difference of the regional Bouguer dip from the Bouguer anomaly equipotential surface in A is known as the residual gravity (Δg).

C. The density contrast model ($\Delta\rho$) is constructed from the known densities of the stratigraphic units in the Basin and subtracting those densities from the 2.67 g/cc density used in the Bouguer correction. Since the sediment density is 1.8 g/cc and it is assumed that the sediments are displaced crustal rock (ρ = 2.67 g/cc), the gravity effect of this displacement is negative.

D. The depth to the basement structure surface (h) is calculated by using Δg from B and $\Delta\rho$ from C above in the gravity mass effect formula: $h = \Delta g / 2\pi\Delta\rho\gamma$.

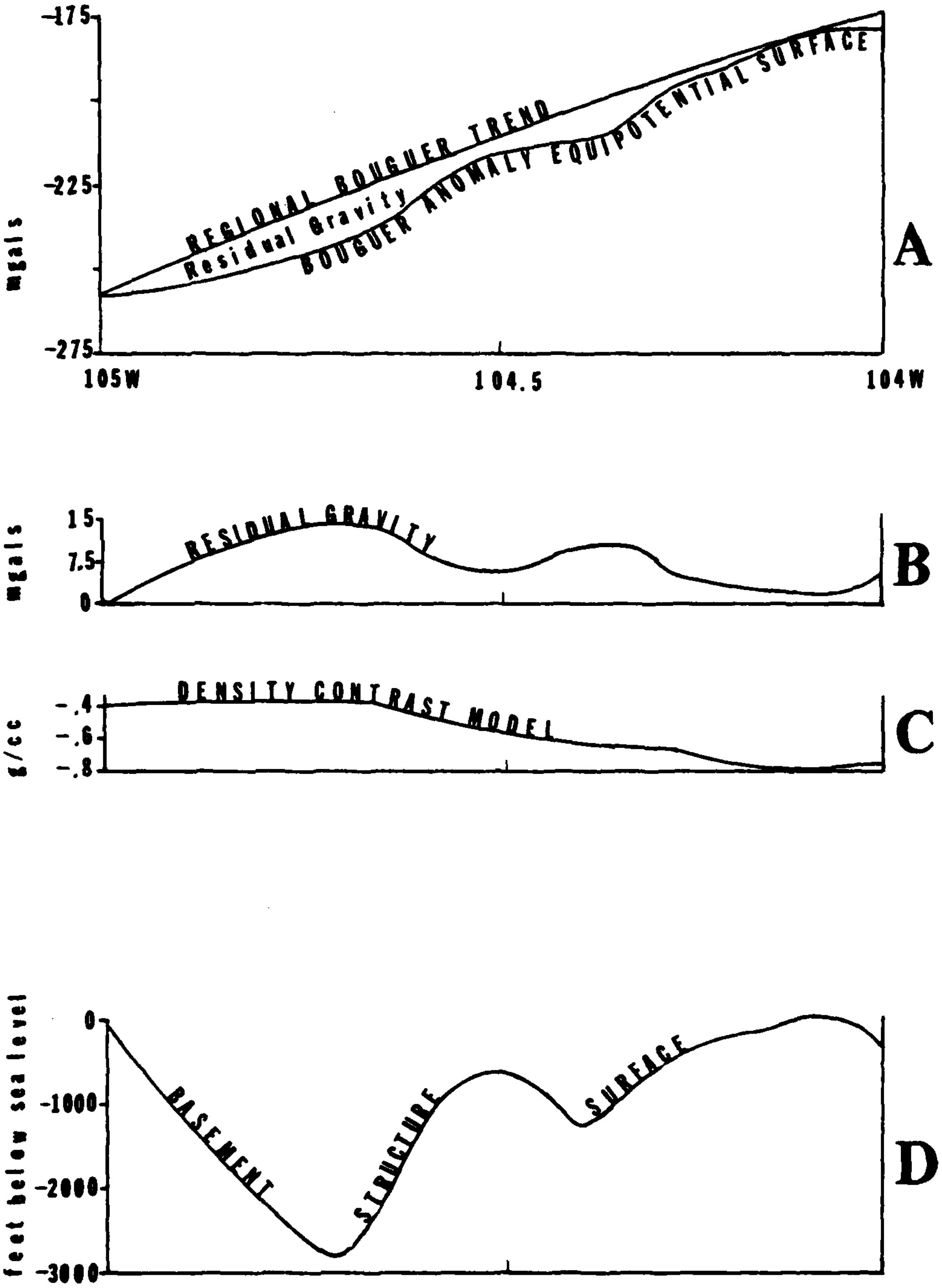
-175
-225
-275
mgals
REGIONAL BOUGUER TREND
Residual Gravity
BOUGUER ANOMALY EQUIPOTENTIAL SURFACE
A
105W
104.5
104W
15
7.5
0
mgals
RESIDUAL GRAVITY
B
-.4
-.6
-.8
g/cc
DENSITY CONTRAST MODEL
C
0
-1000
-2000
-3000
feet below sea level
BASEMENT STRUCTURE SURFACE
D

by solving the gravitational effect formula for depth (h), using the Δg and $\Delta\rho$ values above: $h = \Delta g/2\pi\gamma\Delta\rho = -810$ feet (below sea level). This type of calculation was repeated for each of the 2,400 density contrasts in the Basin, and the resulting depths to basement structure were then contoured by the computer techniques described in Chapter II. The accuracy of the depths to the basement structure surface was independently verified using well log data (Baltz, 1965) and a measured section from the Raton Basin (McGehee, 1955).

In order to describe the correlation between the geology on plate 1 and the basement structure on plate 2, the same topographic names are used to refer to features on both maps. This practice is justified because the features named on the basement structure map all have assocated topographic features. In the area of the Wet Mountains and Spanish Peaks, the basement structure map shows that basement rock is exposed; that is, there are no sedimentary rocks present. The structurally high Apishipa Arch area on the basement relief map extends southeast of the Wet Mountains. The basement rises at about 1.5° to approximately 1,500 feet of vertical relief over a ten mile distance. The Apishipa Arch area is outlined by positive relief for approximately 50 miles on the basement structure map. The basement structure map shows the Apishipa Arch as the eastern boundary to the Basin.

The Delcarbon and La Veta syncline areas are shown on the basement structure map as depressions. The Delcarbon depression is above sea level and the La Veta depression is below sea level; both depressions

deepen to the south. The axis of the La Veta depression is the deepest depression on the basement structure map and defines the Raton Basin axis.

A positive relief feature on the basement relief map between the La Veta and Delcarbon depressions is also associated with intrusive rocks on the geologic structure map (plate 1). The shallow depth to known oil bearing formations of Cretaceous age (Baltz, 1965) make this anticline a favorable site for petroleum exploration. However, the heat from the intrusive activity may have destroyed any oil present, in a manner similar to the destruction of coal beds found elsewhere in the Basin and described in Chapter I.

The Cimarron Arch is an area of positive basement relief and clearly separates the Raton and Las Vegas Basins. It is asymmetric in shape, steeper on the north slope (4.5°) than the south slope (2.9°), and has approximately 3,500 feet of vertical relief. The Cimarron Arch area extends about fifty miles, from the west edge of the basement structure map to the Sierra Grande Arch area. The marked relief of this basement feature suggests the Arch has effectively prevented intertonguing of Las Vegas and Raton Basin's sedimentary rocks. As the Basins were downwarped and isostatic adjustment occurred to compensate for the accumulating sediments, the Cimarron Arch remained a positive structural feature. Although not a significant topographic or gravity feature today, the Arch was important in the development of the Basin.

The Sierra Grande Arch area is roughly defined by moderate relief on the basement structure map for approximately twenty miles east of

the Las Vegas Basin. Total positive relief increases about 1,000 feet over a twelve mile distance, producing a gentle 0.8^{o} slope. The whole eastern sector of the basement structure map is a low relief positive area, rising slowly to the Apishipa and Sierra Grande Arch areas.

A previously unmapped and unnamed basement trough, which is in near alignment with a left lateral fault south of Spanish Peaks (plate 1), trends northeast from Raton Basin toward Apishipa Arch. The trough deepens southeast, towards the Raton Basin, and may be fault controlled. As a structurally low feature, the unnamed trough may contain significantly more sediments than areas surrounding it. The margins of the unnamed trough may prove favorable for future petroleum exploration. Presence of this trough is confirmed on the Raton Basin magnetic map.

Raton Basin Magnetic Map

The Raton Basin vertical magnetic data is tabulated and included in Appendix C. The magnetic data is shown in both hand drawn (figure 14) and computer plotted formats (plate 3). The computer plotted magnetic map is drawn at the same scale as the basement structure map for comparison. Zeitz *et al.*, (1969) showed that the Colorado sedimentary rocks in the Basin are essentially nonmagnetic, the metamorphic and volcanic rocks are weakly to moderately magnetic, and the Precambrian quartz monzonite rocks are moderately to strongly magnetic. The Raton Basin magnetic maps actually represent the surface of the basement rocks in the Basin. Magnetic anomalies may also be associated with lateral changes in rock types, but there is no geologic evidence for basement

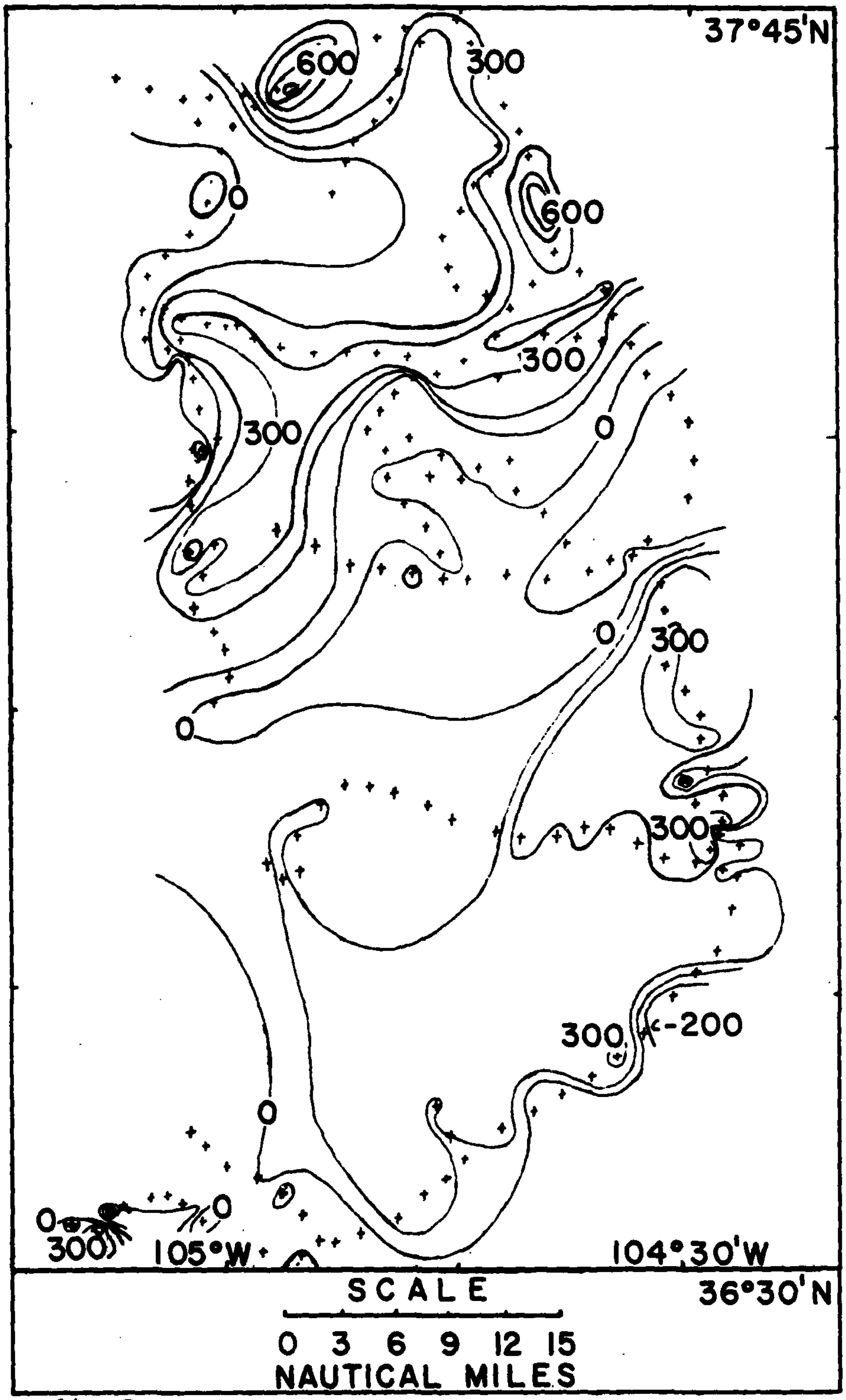

Figure 14. Raton Basin magnetic map. The crosses represent magnetic stations. Station number one is used as reference and is shown circled in the lower left corner of the map.

rock type changes in the Basin with the exception of those areas of known intrusive rocks.

Metasedimentary rocks are exposed near the Cimarron Arch and these rocks are near station number one, which was the magnetic survey datum. Magnetic measurements in the area of the metasedimentary rocks gave no indication that these rocks have higher magnetic susceptibilities than the sedimentary rocks in the Basin. Therefore, it is reasonable to assume that the rocks in New Mexico have the same magnetic susceptibilities that Zeitz et al., (1969) reported for Colorado rock types. Some lack of detail in the magnetic map in the southern portion of Raton Basin is the result of poor road access. All magnetic measurements were made along roads.

Structural depressions (plate 1) are associated with negative magnetic anomalies (plate 3) in the Basin. The La Veta and Delcarbon synclines both have distinct low magnetic anomalies associated with them; the unnamed trough detected on the basement structure map also has a distinct low magnetic anomaly associated with it. The magnetic anomaly associated with the unnamed trough makes it appear to deepen to the northeast, opposite the direction determined on the basement structure map. However, this apparent deepening probably reflects only the computer response to the lack of magnetic stations in the eastern part of the survey area.

Positive magnetic anomalies are associated with positive structural features. For example, the unnamed anticline between the La Veta and Delcarbon synclines has a significant positive magnetic anomaly

associated with it. The Cretaceous age sediments with known oil shows are only thinly buried near this anticline.

Capulin vertical magnetic data were also studied as an addition to the Raton Basin magnetic data. The Capulin data are tabulated and included in Appendix B with the Capulin gravity data. Unlike the sediment filled Raton Basin, the Capulin area is covered by volcanic rocks, which have significantly higher magnetic susceptibilities than the sedimentary rocks beneath. Some of the magnetic anomalies in the Cauplin area (figure 15) are associated with topographic features. For example, there is a magnetic anomaly associated with Capulin Mountain. However, a positive magnetic anomaly on the east slope of the mountain is not associated with a topographic feature. Free air gravity anomalies also mark this area, and this anomaly relationship may be an indication of lateral vents or dikes.

Variation in the magnetic properties of different volcanic rock types (Dobrin, 1976) would be helpful in identifying magnetic anomaly patterns in volcanic regions. Indeed, the largest positive magnetic anomaly is near Sierra Grande Mountain; smaller but equally distinctive positive magnetic anomalies are near Capulin Mountain. The unusually high magnetic susceptibility of the Sierra Grande sequence (indicated by its magnetic anomaly) may be diagnostic of these volcanic rocks and aid in determining their areal extent.

Capulin Local Seismic Study

In addition to gravity and magnetic measurements, an effort was made to determine natural seismicity in the Capulin area. It was

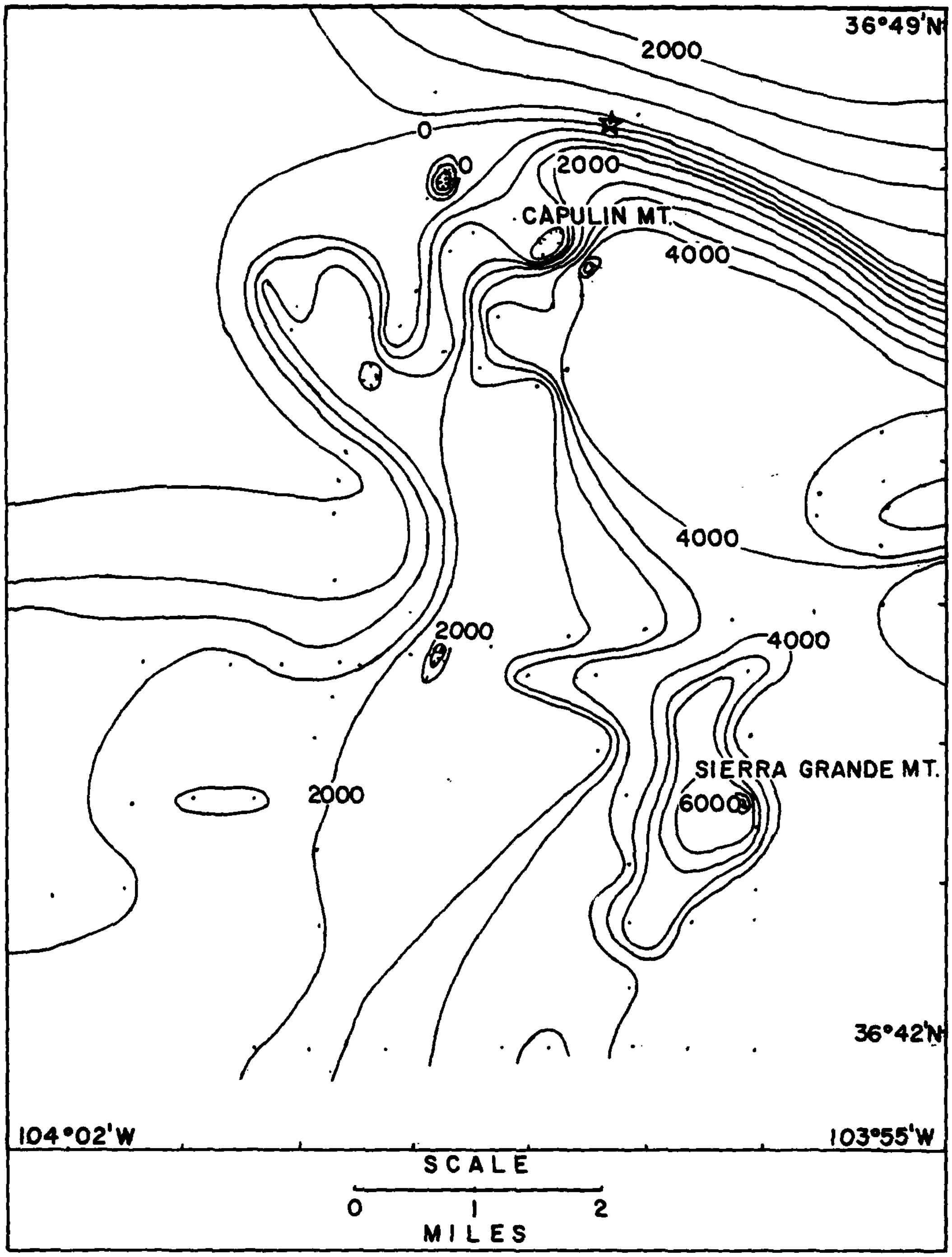

Figure 15. Capulin magnetic map. The dots represent magnetic stations. Station number one is used as reference and is represented by a star.

thought that some tectonic activity may be in progress. The results of the seismic survey in the Capulin area and all known seismic activity during the Twentieth Century are included in table 2. The epicenters of the earthquakes in table 2 are also shown on a map of northeastern New Mexico (figure 16).

A bar graph (figure 17) indicates the distribution of seismic activity in northeast New Mexico from 1900 to 1980. The lack of any significant recorded seismic activity during the first half of this century is due largely to the lack of recording equipment or populace to observe any shocks. Since 1962 the number of recorded events have increased due to the installation of permanent seismograph networks.

In the last five years seismic activity in New Mexico has declined (Sanford, 1981), yet this study suggests that the Capulin area has rather high seismic activity. The events recorded during this study were local in origin and small in magnitude, and were not recorded elsewhere

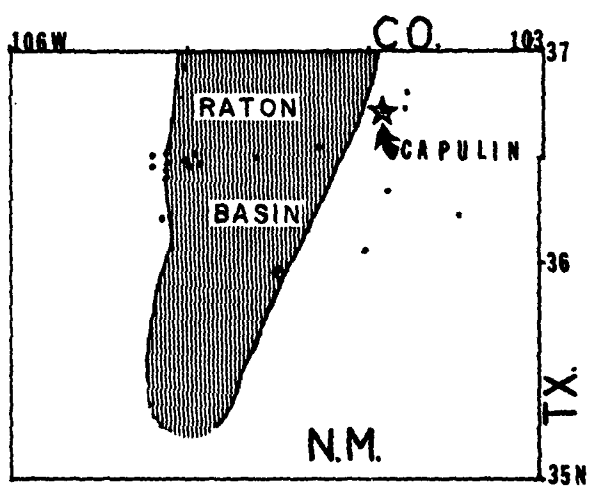

Figure 16. Geographic location of seismic events strong enough to be felt by local population in northeast New Mexico from 1900 to 1980.

Table 2. Recorded Earthquake Activity in the Study area of New Mexico 1900-1981.

SOURCE	DATE YR-MO-DAY	TIME GMT	LAT °N	LONG °W	INTENSITY modified Mercali or local magnitude
1	06-04-19	2100	-	-	V
1	06-04-20	1300	-	-	VI
2	24-08-13	0423	36.0	104.5	V
2	52-08-13	2042	36.5	105.0	V
2	63-06-06	0806	36.6	104.4	2.7
2	66-09-24	0734	36.4	105.1	2.7
2	66-09-24	0827	36.4	105.1	2.4
2	66-09-25	1011	36.3	105.1	2.8
2	66-09-25	1223	36.5	105.1	2.8
2	72-02-20	2310	36.4	104.9	1.5
2	72-02-20	2323	36.4	104.9	2.2
2	75-05-16	0138	36.9	105.0	1.5
2	75-05-16	0726	36.5	104.7	1.9
2	75-06-21	0542	36.1	104.0	2.0
3	79-09-19	0539	36.4	103.7	1.8
3	80-09-12	2138	36.5	105.1	2.3
4	81-07-24	1613			
4	81-07-24	1815			
4	81-08-27	0220			
4	81-08-27	0238			
4	81-07-27	1554			
4	81-07-27	1738			
4	81-07-30	1824			
4	81-08-25	2034			
4	81-08-27	2041			
4	81-09-01	2124			
4	81-09-01	2254			
4	81-09-09	1724			
4	81-09-16	0336			

Source Data:

1. Anonymous, The Raton Range (April 21, 1906) shock felt at Folsom, NM
2. Sanford *et al.*, (1981)
3. Sanford (1981)
4. Capulin data (this report) epicenters assumed at or near Capulin, NM. No intensities were calculated, but the sensitivity of the equipment would indicate the relative intensities to be much smaller than previously recorded in the area.

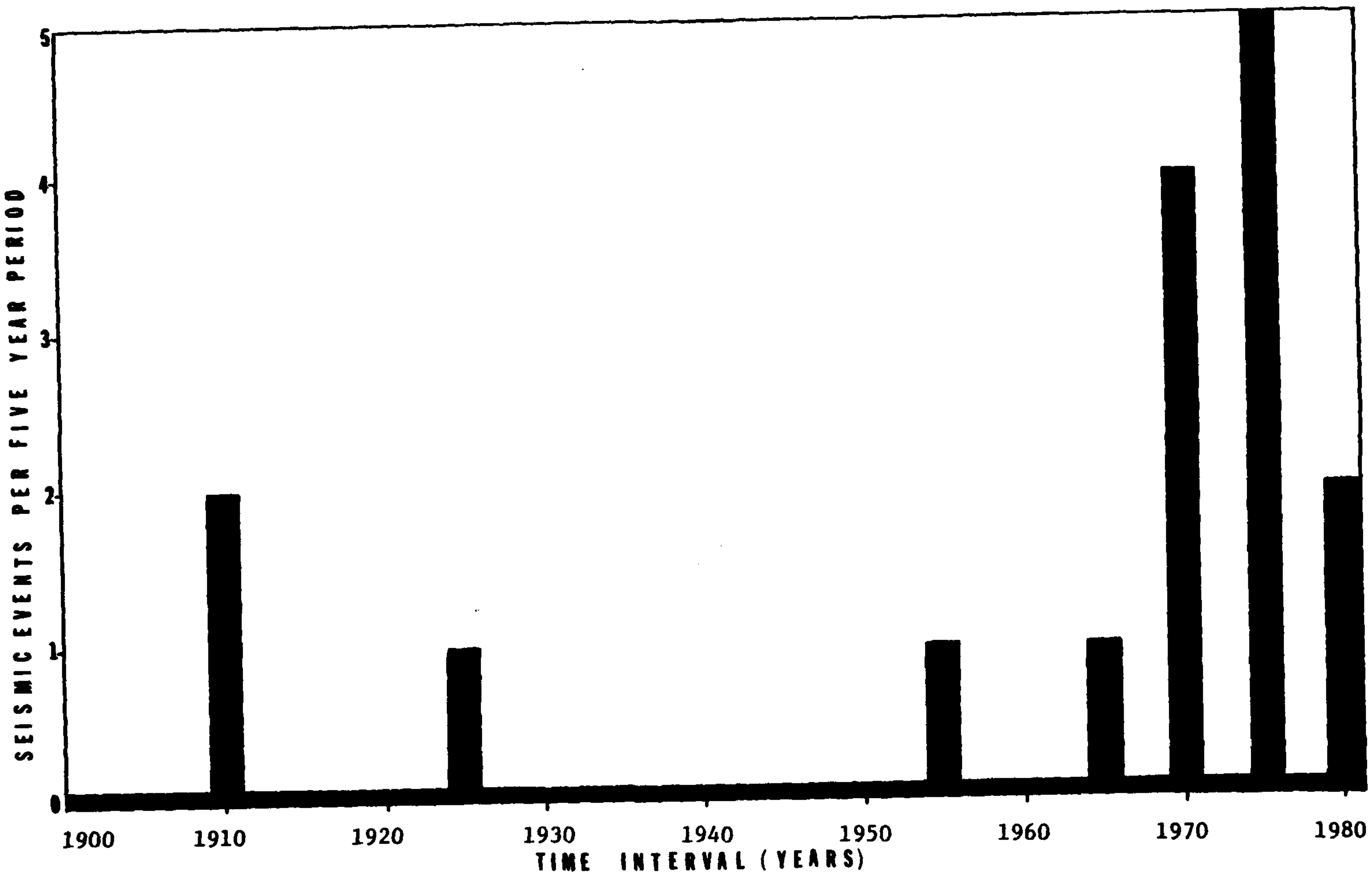

Figure 17. Bar graph representation of the frequency of seismic events in Table 2 in five year increments. Time interval is 1900 to 1980.

in the state (J.J. Wolff, personal communication, 1981). Some of the events recorded may have been local mining blasts or sonic booms, although sonic booms are usually easily distinguished (figure 18).

The presence of seismicity near Capulin suggests this area to be either affected by dormant vulcanism, or by tectonic adjustment along faults in the area. Sanford et al., (1981) suggest that seismic activity in northeast New Mexico may be due to an eastern extension of the Jemez Lineament in western New Mexico. Continued monitoring of the Capulin seismicity would be necessary to determine the source and extent of the local seismic activity.

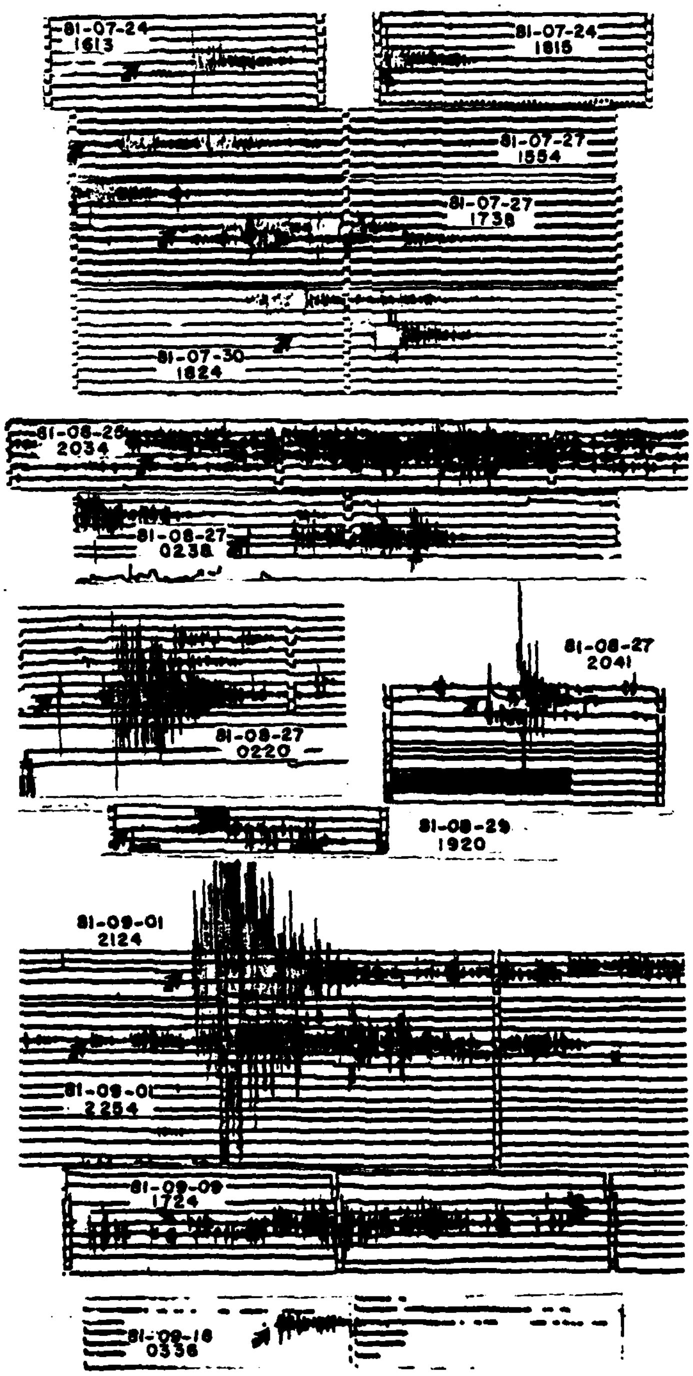

Figure 18. Seismograms from the Capulin seismic survey. The day-time groups correspond to Table 2.

CHAPTER IV

CONCLUSIONS

The geophysical measurements and the interpretation reported in this thesis meet the objectives set out in Chapter I. Furthermore, the interpretation of the data of these geophysical surveys lead to the following results:

1. The free air and Bouguer gravity data both indicate the study area is in near perfect isostatic adjustment. Correlation between this report and studies in adjacent areas indicate the Colorado - northeast New Mexico - west Texas region is in isostatic balance.

2. A large free air gravity anomaly in the southern portion of the study area is the result of local crustal loading by Quaternary volcanic activity. The thickness of the volcanic rock is estimated to 180 m based on the gravitational effect represented in the free air anomaly.

3. The basement relief map constructed from Bouguer gravity data has a high correlation with known geologic structures.

4. The Raton magnetic map generally represents the same basement surface as that constructed from Bouguer gravity data.

5. The Capulin area and adjacent High Plains are seismically active. Further investigation of the local seismicity is important.

6. The basement structure map and Raton magnetic map indicate areas of potential benefit in future petroleum exploration. The high heat flow in the Basin may have economic importance. If the heat flow is found to be a result of dormant vulcanism, seismic studies, as in the Capulin area, may be helpful in determining the extent of the thermal field.

References Cited

Bachman, G.O.; C.H. Dane, 1962, Preliminary Geologic Map of the northeastern part of New Mexico, USGS Misc. Geologic Investigations, Map I-358.

Baldwin, B.; W.R. Muehlberger, 1959, Geologic Studies of Union County, N.M., N.M. Bureau of Mines and Mineral Resources (NMBMMR), Bull. 63, Socorro, NM.

Baltz, E.H., 1965, Stratigraphy and History of Raton Basin and Notes on San Luis Basin, Colorado-New Mexico, AAPG, Bull., V. 49, No. 11, p. 2041-2075.

Brill, K.G., 1952, Stratigraphy in the Permo-Pennsylvanian zeugogeosyncline of Colorado and northern New Mexico, GSA, Bull., V. 63, No. 8, p. 809-880.

Clark, S.P., 1966, Handbook of Physical Constants, GSA Memoir 97, p.467-481.

Compton, R.R., 1962, Manual of Field Geology, John Wiley & Sons, Inc., NY, NY, p. 338.

Davis, J., 1973, Statistics and Data Analysis in Geology, John Wiley & Sons, Inc., NY, NY.

Dobrin, M.B., 1976, Introduction to Geophysical Prospecting, 3rd Edition, McGraw-Hill Books, San Francisco, CA.

Edwards, C.C.; M. Reiter; C. Shearer; W. Young; 1978, Terrestial heat flow and crustal radioactivity in northeastern New Mexico and southeastern Colorado, GSA, Bull., V. 89, p. 1134-1350.

Griggs, R.C., 1948, Geology and Ground Water Resources of eastern Colfax County, New Mexico, MNBMMR, Socorro, NM.

Hamilton, W.; L.C. Pakiser, 1965, Geology and Crustal cross section of the United States along the 37th Parallel, USGS Misc. Geologic Investigations, Map I-448.

Johnson, R.B., 1969, Geologic Map of the Trinidad Quadrangle South Central Colorado, USGS Misc. Geologic Investigations, Map I-558.

Jones, L.M.; R.C. Walker; J.C. Stormer, 1974, Isotope composition of Sr and the origin of volcanic rocks of the Raton - Clayton District, northeast New Mexico, GSA, Bull., V. 85, p. 33-36.

Jurice, C.A.; L.C. Gerhard, 1969, Colorado Raton Basin: mineral resources and geologic section, Mountain Geologist, V. 6, No. 3, p. 81-84.

McGehee, J.R., 1955, Colorado Measured Section, Rocky Mountain Assoc. of Geologists, Denver, Colorado.

Qureshy, M.N., 1962, Gravimetric - isostatic studies in Colorado, JGR, V. 67, No. 7, p. 2459-2467.

Reiter, M.; A.J. Mansure; C. Shearer, 1979, Geothermal characteristics of the Rio Grande rift within the southern Rocky Mountain complex, in, Rio Grande rift: Tectonics and Magmatism (R.E. Riecker, ed.), AGU, Washington, D.C., p. 253-267.

Reinhart, P.S., 1981, SAS/Graph User's Guide, 1981 Edition, SAS Institute, Inc., Cary, NC.

Sanford, A.R., 1981, Earthquakes in New Mexico, 1978-1980, (unpublished manuscript).

_____ K.H. Olsen; L.H. Jaksha, 1981, Earthquakes in New Mexico, 1849-1977, NMBMMR, Circular 171.

Shurbet, D.H., 1966, Gravity field and isostatic equilibrium of the Llano Estacado of Texas and New Mexico, GSA, Bull., V. 77, p. 213-222.

Smith, R.B., 1970, Regional gravity survey of western and central Montana, AAPG, Bull., V. 67, No. 2, p. 2459-2467.

Stewart, S.W.; L.C. Pakiser, 1962, Crustal structure in eastern New Mexico interpreted from the Gnome Exposion, SSA, Bull., V. 52, p. 1017-1030.

Stormer, J.C., 1972, Ages and nature of volcanic activity on the high plains of New Mexico and Colorado, GSA, Bull., V. 83, p. 2443-2448.

Suppe, J.; C. Powel; R. Berry, 1975, Regional topography, seismicity, Quaternary volcanism, and the present-day tectonics of the western United States, Am. J. of Science, V. 275-A, p. 379-436.

Wanek, A.A., 1963, Geology and fuel resources of the southwestern part of the Raton Coal Field, Colfax County, New Mexico, USGS Coal Investigations, Map C-45.

Wanek, A.A.; C.B. Read; G.O. Robinson; W.H. Hayes; M. McCallum, 1964, Geologic Map and Sections of Philmont Ranch Region, New Mexico, USGS Misc. Geologic Investigations, Map I-425.

Wollard, G.P., 1959, Crustal structure from gravity and seismic measurements, JGR, V. 64, No. 10, p. 1521-1544.

_____ 1962, The relation of gravity anomalies to surface elevation, crustal structure and geology, U. Wisc. Geophysics Polar Res. Center, Report 62-9.

_____ 1969, Regional variation in Gravity, in, The Earth's Crust and Upper Mantle (P.J. Hart, ed.), AGU Monograph 13, Washington D.C., p. 320-341.

Zeitz, I.; P.C. Bateman; M.D. Crittenden; A. Giscom; E.R. King; R.J. Roberts; G.R. Lorentzen, 1969, Aeromagnetic investigation of crustal structure for a strip across the western United States, GSA, Bull., V. 80, No. 9, p. 1703-1714.

APPENDIX A

NOAA GRAVITY AND ELEVATION DATA

Explanation of Table Headings

Lat	Northern latitude of station in degrees.
Long	Western longitude of station in degrees.
Elev	Station elevation in meters above sea level.
FAA	Free air anomaly, calculated from a datum of sea level. The free air correction (FAC) is 0.3085 mgal/m and is applied to the observed gravity reading (OGR): FAA = OGR + FAC.
BA	Bouguer anomaly, calculated using a datum of sea level, station elevation, and a density of 2.67 g/cc. The Bouguer correction (BC) is $2\pi\gamma\rho h$, or 0.0837 mgal/m, and is applied to the FAA: BA = FAA - BC.

LAT	LONG	ELEV	FAA	BA
37.500	104.247	1728.800	-0.100	-193.500
37.275	104.377	1743.400	-13.500	-208.300
37.327	104.275	1732.200	-10.300	-204.100
37.043	104.038	1765.400	15.100	-182.300
37.117	104.247	1745.000	2.600	-192.500
37.038	104.080	2016.400	-9.000	-234.000
37.400	104.628	1958.300	-7.900	-227.100
37.405	104.627	1918.400	-7.200	-221.900
37.415	104.640	1931.200	-6.800	-222.900
37.000	104.500	1900.000	-0.400	-200.000
37.284	104.045	2077.200	-3.200	-235.700
37.289	104.825	2230.100	4.800	-245.000
37.001	104.703	2116.200	-3.700	-240.500
37.011	104.758	2289.000	9.300	-240.200
37.016	104.802	2289.700	7.700	-248.300
37.017	104.747	2218.000	3.500	-244.300
37.029	104.729	2152.500	-2.200	-243.000
37.029	104.902	2373.200	13.000	-254.000
37.034	104.902	2201.600	-2.100	-248.400
37.034	104.934	2331.400	23.100	-253.900
37.037	104.083	2357.400	-7.000	-237.000
37.037	104.507	2114.700	19.500	-217.000
37.153	104.542	1852.000	-18.400	-225.600
37.156	104.992	2301.200	-1.400	-258.800
37.159	104.637	1985.000	-13.300	-233.200
37.160	104.807	2079.300	-13.900	-246.000
37.162	104.954	2246.700	-6.100	-257.500
37.169	104.503	1836.100	-19.600	-224.100
37.182	104.807	2199.700	-2.700	-248.800
37.186	104.505	1824.500	-22.000	-225.700
37.207	104.083	2033.300	-6.600	-239.700
37.217	104.833	2243.000	1.000	-249.300
37.240	104.702	2131.200	-2.200	-240.600
37.252	104.854	2328.700	11.500	-248.600
37.187	104.857	2017.500	-10.700	-236.400
37.209	104.510	1894.000	-15.700	-227.300
37.276	104.087	2136.900	9.000	-235.000
37.257	104.702	2265.000	18.000	-235.200
37.134	104.574	1867.900	-15.500	-226.800
37.142	104.887	2154.300	-14.900	-256.000
37.152	104.512	1921.800	-8.700	-223.700
37.152	104.915	2192.700	-13.800	-256.200
37.129	104.303	2047.300	-18.700	-247.800
37.129	104.846	2087.300	-18.300	-252.400
37.122	104.708	1972.700	-19.700	-240.400
37.124	104.648	1938.200	-15.800	-232.700
37.128	104.684	1946.800	-16.500	-236.400
37.129	104.597	1888.500	-16.400	-227.800
37.121	104.729	1979.400	-21.100	-242.600
37.110	104.526	1958.000	-2.400	-221.000
37.075	104.637	1980.300	-9.800	-231.400
37.075	104.803	2115.000	-11.800	-248.500
37.077	104.519	2016.900	6.400	-219.100
37.098	104.617	1941.300	-9.100	-225.400
37.100	104.790	2058.300	-17.100	-247.400
37.051	104.812	2150.700	-3.700	-249.500
37.051	104.870	2301.200	3.300	-254.000
37.170	104.511	1829.100	-17.600	-222.000
37.295	104.530	1864.800	-16.300	-224.600
37.400	104.830	1946.500	-3.100	-220.000
37.155	104.914	2192.700	-10.400	-255.400
37.127	104.337	2087.300	-17.500	-250.500
37.122	104.756	2021.100	-16.900	-242.800
37.122	104.647	1949.500	-13.800	-230.700
37.142	104.557	1868.200	-15.900	-224.700
37.132	104.512	1955.800	-0.600	-219.200
37.044	104.506	2109.200	20.400	-215.300
37.170	104.511	1829.100	-19.900	-224.600

LAT	LONG	ELEV	FAA	BA
37.295	104.530	1864.700	-18.500	-227.200
37.400	104.650	1940.400	-5.300	-223.100
37.135	104.610	1901.000	-15.400	-228.100
37.130	104.532	2072.000	-18.400	-250.200
37.173	104.512	1825.800	-20.700	-225.000
37.167	104.508	1820.100	-21.400	-225.000
37.337	104.503	1900.400	-14.400	-227.300
37.415	104.967	2642.000	65.800	-234.700
37.405	104.624	1921.300	-8.400	-223.400
37.447	104.652	1952.200	-4.300	-227.300
37.426	104.587	1887.900	-9.500	-220.700
37.425	104.979	2561.500	+7.600	-238.800
37.442	104.763	2137.000	9.300	-229.700
37.472	104.352	2186.000	13.900	-230.500
37.473	104.828	2159.300	13.000	-228.400
37.485	104.800	2132.700	10.600	-227.800
37.486	104.882	2175.100	12.300	-230.600
37.485	104.752	2103.100	0.400	-228.700
37.482	104.552	1881.500	-4.300	-214.300
37.456	104.535	1933.300	-3.300	-220.100
37.500	104.712	1969.600	-5.700	-226.100
37.468	104.676	1966.800	-6.800	-226.900
37.362	104.679	1984.900	-3.800	-225.900
37.355	104.805	2205.800	8.200	-238.400
37.386	104.838	2367.400	33.000	-231.700
37.369	104.767	2161.800	10.400	-231.300
37.296	104.852	2301.200	9.400	-247.900
37.302	104.552	1962.900	-15.500	-226.500
37.294	104.935	2516.100	32.800	-248.500
37.292	104.898	2395.400	19.000	-243.900
37.357	104.704	2027.500	-1.400	-228.100
37.307	104.557	1372.400	-9.400	-219.000
37.367	104.501	1539.500	-11.700	-217.500
37.015	104.119	1853.200	22.800	-184.400
37.035	104.016	1799.200	18.700	-182.400
37.042	104.045	1765.700	15.200	-182.200
37.043	104.119	1834.300	21.300	-183.700
37.155	104.385	1353.100	0.400	-207.300
37.162	104.106	1665.800	0.800	-187.600
37.172	104.377	1816.000	-3.300	-206.500
37.184	104.143	1633.700	-9.400	-192.200
37.221	104.275	1719.400	-6.500	-198.900
37.2[illegible]	104.416	1831.200	-9.500	-214.400
37.223	104.455	1735.100	-20.100	-219.700
37.231	104.354	1787.000	-5.700	-205.700
37.234	104.307	1721.800	-9.500	-202.100
37.235	104.297	1764.200	-8.100	-205.500
37.236	104.387	1649.900	1.700	-162.700
37.238	104.490	1809.300	-15.700	-225.900
37.245	104.425	1765.700	-17.900	-215.500
37.250	104.045	1642.600	1.800	-181.800
37.250	104.118	1726.100	5.400	-187.600
37.205	104.227	1571.200	-9.300	-196.300
37.144	104.187	1662.400	-8.000	-194.000
37.187	104.400	1325.100	-5.500	-209.800
37.278	104.174	1660.900	-3.500	-194.300
37.278	104.210	1691.600	-7.200	-196.300
37.279	104.037	1637.100	0.700	-162.300
37.279	104.247	1723.900	-5.700	-198.600
37.252	104.340	1756.000	-8.000	-204.500
37.261	104.400	1749.600	-16.100	-211.900
37.257	104.151	1714.200	-0.100	-191.800
37.137	104.058	1708.100	7.700	-183.200
37.148	104.332	1777.300	-2.100	-200.900
37.125	104.027	1707.800	9.600	-181.300
37.127	104.269	1766.200	2.200	-194.500
37.113	104.247	1733.700	0.900	-192.900
37.075	104.117	1754.100	12.300	-133.300

LAT	LONG	ELEV	FAA	BA
37.076	104.185	1745.600	7.100	-186.000
37.079	104.142	1763.100	12.700	-185.000
37.108	104.385	2013.500	20.000	-205.100
37.109	104.202	1717.300	3.000	-169.000
37.087	104.050	1748.600	13.500	-161.300
37.092	104.432	2219.900	36.000	-210.200
37.057	104.058	1772.700	15.600	-182.500
37.063	104.406	2429.900	60.700	-211.000
37.071	104.371	2171.400	34.900	-207.900
37.065	104.094	1764.500	13.800	-183.400
37.062	104.202	1822.700	11.800	-192.000
37.413	104.247	1686.800	-13.300	-202.100
37.412	104.115	1647.400	0.600	-183.500
37.021	104.491	2180.000	29.200	-215.300
37.295	104.302	1714.300	-14.400	-206.300
37.452	104.200	1691.300	1.200	-187.000
37.425	104.404	1781.900	-5.600	-203.000
37.412	104.226	1679.400	-9.200	-197.100
37.454	104.210	1662.500	-2.000	-190.200
37.454	104.245	1693.000	-7.700	-197.700
37.454	104.291	1713.300	-8.200	-199.900
37.401	104.234	1690.100	0.900	-185.000
37.462	104.429	1789.500	0.700	-199.300
37.479	104.164	1712.400	5.100	-185.300
37.480	104.425	1815.100	-0.200	-203.200
37.435	104.365	1727.600	-7.400	-201.200
37.481	104.294	1718.200	-8.600	-201.100
37.455	104.175	1668.300	1.900	-186.300
37.455	104.404	1773.300	-6.200	-204.600
37.456	104.134	1703.500	6.800	-183.600
37.498	104.092	1736.100	11.300	-182.800
37.498	104.225	1719.400	2.300	-189.400
37.494	104.320	1688.600	-12.700	-201.700
37.498	104.401	1748.000	-5.100	-200.700
37.381	104.173	1655.800	-13.900	-198.900
37.375	104.104	1694.400	2.100	-187.300
37.381	104.136	1633.700	-11.700	-194.500
37.381	104.209	1630.400	-13.000	-201.000
37.381	104.317	1858.700	4.000	-203.700
37.382	104.239	1701.700	-11.200	-201.000
37.396	104.464	1788.600	-9.600	-209.700
37.297	104.340	1754.000	-13.400	-207.500
37.307	104.319	1739.200	-11.800	-206.400
37.292	104.467	1801.400	-18.500	-220.100
37.358	104.252	1716.600	-11.200	-203.200
37.365	104.354	1812.300	-4.600	-207.400
37.367	104.465	1796.800	-14.000	-215.100
37.368	104.067	1677.000	6.300	-179.100
37.366	104.392	1801.700	-8.300	-210.500
37.367	104.420	1790.100	-11.400	-211.700
37.360	104.239	1767.500	-4.700	-202.500
37.336	104.172	1649.600	-14.900	-199.500
37.337	104.467	1787.300	-16.400	-216.400
37.337	104.228	1691.900	-14.200	-203.500
37.346	104.012	1563.000	-1.900	-176.700
37.352	104.042	1627.300	3.500	-178.400
37.310	104.287	1745.600	-9.700	-205.000
37.333	104.057	1505.700	-2.300	-182.000
37.335	104.273	1735.600	-10.100	-204.300
37.291	104.429	1772.400	-17.000	-215.300
37.283	104.374	1743.300	-14.100	-209.300
37.963	104.380	1888.500	8.100	-203.000
37.990	104.595	1704.700	-2.800	-193.500
37.990	104.717	1728.300	-3.200	-198.600
37.997	104.615	1754.400	-7.900	-204.200
37.915	104.610	1671.500	-0.300	-187.300
37.933	104.703	1745.900	4.300	-190.900
37.335	104.327	1671.500	-3.200	-199.000

LAT	LONG	ELEV	FAA	BA
37.905	104.933	2128.700	36.200	-201.600
37.823	104.748	1728.500	1.500	-191.700
37.847	104.545	1822.700	27.500	-176.200
37.543	104.718	1959.600	1.800	-217.300
37.772	104.610	1762.400	14.700	-182.400
37.772	104.852	1850.700	0.300	-206.600
37.789	104.607	1785.200	17.500	-182.100
37.791	104.829	1818.100	-2.300	-205.700
37.792	104.753	1761.400	2.700	-194.200
37.835	104.607	1772.400	18.300	-179.800
37.846	104.531	1831.500	29.800	-174.900
37.846	104.945	2171.100	26.900	-215.800
37.852	104.827	1808.100	1.300	-200.800
37.835	104.827	1811.400	-3.400	-203.200
37.820	104.826	1930.600	1.400	-203.200
37.821	104.862	1884.900	3.700	-207.000
37.821	104.897	1952.200	6.100	-212.100
37.825	104.925	2036.800	15.900	-214.000
37.827	104.741	1727.600	0.0	-193.400
37.864	104.712	1725.700	2.300	-191.100
37.864	104.337	1323.300	1.400	-202.500
37.876	104.369	1737.200	15.600	-180.000
37.888	104.854	1853.800	0.700	-206.600
37.893	104.667	1709.300	3.600	-187.400
37.893	104.827	1867.300	8.600	-200.300
37.903	104.854	1351.400	3.400	-203.600
37.910	104.790	1356.300	9.500	-193.100
37.912	104.827	1810.500	3.400	-199.000
37.920	104.624	1702.000	2.000	-168.300
37.921	104.929	2071.100	30.000	-201.600
37.922	104.764	1801.700	5.600	-195.800
37.922	104.898	1932.900	15.000	-203.400
37.926	104.832	1901.600	9.200	-203.400
37.933	104.365	1570.600	6.400	-202.700
37.934	104.852	1825.500	3.000	-201.500
37.930	104.637	1755.800	4.500	-191.600
37.936	104.675	1763.500	2.900	-194.500
37.935	104.712	1767.500	1.600	-196.300
37.936	104.750	1763.300	-1.100	-193.300
37.937	104.946	2144.600	39.300	-200.300
37.994	104.760	1660.600	-15.800	-201.600
37.997	104.523	1605.700	-5.200	-184.900
37.993	104.552	1632.300	-5.100	-187.000
37.993	104.578	1667.600	-4.300	-190.900
37.972	104.562	1684.300	1.400	-130.900
37.973	104.591	1736.100	1.300	-193.100
37.976	104.777	1701.400	-11.600	-202.200
37.941	104.968	2241.800	46.700	-205.900
37.942	104.613	1707.500	3.400	-190.500
37.942	104.987	2348.500	55.600	-226.000
37.953	104.538	1716.000	2.600	-139.300
37.901	104.794	1767.500	-5.200	-203.000
37.943	104.856	1781.600	-2.800	-202.200
37.575	104.892	1972.700	-3.100	-223.300
37.582	104.853	1948.000	-3.300	-221.200
37.607	104.766	1919.300	1.900	-212.700
37.610	104.577	1891.000	1.100	-210.300
37.597	104.623	1917.200	-4.300	-219.100
37.606	104.687	1896.500	0.500	-211.500
37.596	104.774	1924.300	-0.500	-215.800
37.571	104.590	1960.800	4.700	-214.500
37.566	104.922	2009.900	-3.500	-228.400
37.565	104.740	1934.300	-2.100	-213.400
37.529	104.643	1841.600	-4.800	-221.500
37.542	104.573	1942.300	1.900	-215.300
37.542	104.647	1902.300	-5.700	-219.000
37.542	104.952	2047.600	-5.700	-232.600
37.542	104.536	1965.400	5.200	-214.500

LAT	LONG	ELEV	FAA	BA
37.523	104.856	2074.200	4.500	-227.400
37.521	104.372	2119.300	9.000	-227.400
37.521	104.099	1952.900	-3.000	-232.100
37.522	104.977	2032.400	-2.800	-235.900
37.611	104.672	1866.600	-1.500	-210.300
37.618	104.642	1851.200	-3.500	-210.400
37.618	104.608	1880.000	-0.400	-210.000
37.617	104.794	1894.000	-3.600	-215.600
37.622	104.782	1984.300	-2.500	-213.300
37.627	104.731	1873.000	-0.800	-210.300
37.635	104.815	1908.400	0.0	-213.500
37.632	104.786	1912.600	1.200	-212.300
37.627	104.554	1890.700	3.300	-208.100
37.644	104.705	1830.000	-2.100	-205.700
37.614	104.523	1373.500	-0.300	-210.400
37.648	104.823	1910.000	1.300	-212.700
37.652	104.744	1867.200	0.200	-208.000
37.656	104.510	1814.800	-0.900	-205.000
37.667	104.842	1912.000	2.100	-211.700
37.550	104.704	1825.400	5.700	-203.300
37.600	104.552	1334.600	6.300	-203.900
37.607	104.673	1802.300	1.100	-200.400
37.672	104.800	1857.800	-2.900	-210.000
37.563	104.920	2010.100	-2.000	-228.300
37.653	104.793	1856.800	-2.900	-210.700
37.823	104.743	1727.900	1.700	-191.400
37.735	104.750	1764.700	4.000	-192.700
37.715	104.955	1959.300	11.000	-203.100
37.717	104.743	1828.600	6.100	-198.300
37.945	104.667	1749.900	1.200	-194.300
37.947	104.707	1702.000	-10.300	-200.700
37.525	104.781	1882.400	-0.300	-210.700
37.710	104.319	1872.700	4.700	-204.000
37.847	104.833	1809.000	4.000	-197.000
37.710	104.816	1872.000	2.100	-207.300
37.647	104.835	1808.900	2.000	-200.200
37.523	104.692	1952.800	-3.000	-221.300
37.625	104.781	1882.400	-2.700	-213.300
37.620	104.733	1833.400	-2.700	-213.400
37.755	104.833	1818.400	-6.200	-204.700
37.521	104.635	1917.200	-8.800	-223.300
37.521	104.621	1929.400	-7.100	-223.000
37.516	104.647	1915.100	-9.200	-223.500
37.513	104.907	2181.300	12.200	-231.700
37.512	104.939	2123.200	3.300	-234.100
37.509	104.636	1929.100	-8.000	-224.300
37.508	104.975	2137.300	2.000	-236.900
37.506	104.535	1942.500	5.500	-213.700
37.505	104.622	1908.700	10.400	-224.000
37.505	104.647	1944.000	-7.200	-224.800
37.505	104.662	1987.000	-2.400	-224.000
37.505	104.632	1916.300	10.100	-224.500
37.504	104.684	1961.100	-5.600	-225.000
37.675	104.855	1913.200	2.100	-211.800
37.679	104.652	1776.700	1.000	-196.800
37.587	104.552	1913.500	17.100	-196.300
37.687	104.857	1938.500	4.900	-211.300
37.637	104.687	1802.900	4.500	-197.000
37.589	104.763	1829.400	-1.800	-206.400
37.695	104.627	1795.900	6.200	-194.400
37.595	104.809	1865.700	-0.600	-209.200
37.696	104.835	1838.200	5.200	-211.700
37.702	104.716	1797.100	1.700	-197.200
37.705	104.677	1773.000	4.200	-194.000
37.706	104.878	1928.200	3.400	-212.200
37.708	104.585	1798.900	10.200	-193.900
37.712	104.937	1943.400	6.300	-211.000
37.713	104.904	1926.500	2.300	-212.600

LAT	LONG	ELEV	FAA	BA
37.717	104.552	1829.100	15.400	-189.000
37.717	104.525	1819.000	17.400	-186.000
37.725	104.737	1831.300	0.100	-198.000
37.731	104.649	1798.900	5.800	-194.300
37.731	104.826	1851.400	-0.900	-208.000
37.736	104.562	1806.900	12.200	-189.000
37.748	104.617	1752.000	10.700	-185.100
37.748	104.642	1810.500	15.100	-187.500
37.750	104.629	1720.000	7.900	-184.500
37.755	104.692	1781.900	8.400	-190.000
37.801	104.632	1886.100	25.800	-185.100
37.775	104.130	1459.400	-23.100	-186.500
37.766	104.362	1507.500	-18.400	-187.100
37.767	104.175	1550.800	-15.400	-188.900
37.818	104.200	1576.400	-9.000	-185.400
37.803	104.275	1632.200	2.100	-180.400
37.943	104.437	1635.600	6.400	-176.400
37.948	104.225	1459.100	-13.800	-177.100
37.950	104.318	1545.300	-4.300	-177.200
37.953	104.317	1373.700	-21.900	-175.300
37.965	104.110	1392.300	-22.700	-178.500
37.992	104.368	1518.500	-5.600	-175.500
37.993	104.267	1446.600	-14.000	-175.900
37.966	104.066	1406.000	-16.000	-176.000
37.918	104.253	1483.500	-12.000	-178.000
37.902	104.493	1697.400	12.800	-176.900
37.903	104.400	1646.300	15.400	-173.700
37.855	104.436	1685.200	14.200	-174.100
37.822	104.058	1423.400	-25.700	-185.000
37.842	104.566	1784.000	24.500	-174.800
37.848	104.250	1562.700	-5.700	-186.500
37.866	104.115	1457.400	-19.300	-186.100
37.637	104.025	1543.200	-17.900	-190.600
37.645	104.005	1564.400	-15.600	-192.900
37.547	104.110	1651.100	-7.200	-191.900
37.558	104.070	1634.500	-10.700	-195.600
37.600	104.187	1777.300	0.200	-196.400
37.993	104.433	1593.500	-3.400	-181.800
37.994	104.223	1441.400	-15.100	-176.400
37.994	104.297	1460.700	-13.000	-177.200
37.965	104.297	1496.000	-10.000	-177.500
37.967	104.127	1432.900	-16.300	-176.000
37.977	104.256	1453.300	-13.900	-176.500
37.986	104.172	1442.600	-15.100	-176.500
37.937	104.132	1435.300	-17.500	-178.100
37.937	104.178	1423.900	-17.500	-177.400
37.950	104.386	1550.200	-5.500	-179.000
37.934	104.041	1406.500	-17.900	-175.500
37.948	104.415	1689.500	9.400	-179.500
37.960	104.167	1486.300	-12.900	-179.300
37.801	104.431	1730.000	16.900	-170.300
37.804	104.267	1516.400	-7.000	-175.700
37.575	104.300	1650.000	-18.100	-202.900
37.577	104.425	1805.900	-3.600	-205.700
37.610	104.454	1814.200	-8.800	-211.800
37.585	104.137	1767.000	4.400	-193.200
37.594	104.043	1560.000	-19.300	-194.400
37.546	104.104	1660.200	-5.700	-191.500
37.554	104.087	1546.500	-7.400	-191.700
37.557	104.190	1758.100	3.500	-193.000
37.566	104.052	1606.000	-11.400	-191.200
37.560	104.031	1692.500	-1.100	-193.400
37.560	104.443	1343.900	-2.400	-209.300
37.539	104.436	1370.000	2.300	-206.300
37.542	104.292	1668.000	-12.800	-199.500
37.527	104.210	1723.300	2.700	-190.600
37.522	104.133	1668.900	1.100	-187.700
37.612	104.023	1553.100	-17.400	-191.600

LAT	LONG	ELEV	FAA	BA
37.615	104.378	1763.900	-7.100	-204.500
37.615	104.313	1675.200	-17.300	-204.700
37.622	104.194	1697.700	-5.900	-195.900
37.615	104.472	1820.300	-4.600	-213.300
37.640	104.018	1542.000	-13.500	-191.100
37.644	104.322	1557.000	-19.100	-204.500
37.614	104.423	1749.000	-16.900	-212.500
37.613	104.339	1700.800	-15.300	-215.700
37.612	104.195	1699.600	-5.300	-195.500
37.651	104.072	1553.600	-17.900	-191.500
37.675	104.169	1592.300	-17.300	-195.500
37.673	104.077	1586.800	-12.600	-190.500
37.673	104.107	1630.400	-10.500	-192.900
37.660	104.157	1622.800	-13.800	-195.400
37.672	104.002	1564.300	-19.100	-187.500
37.659	104.140	1619.100	-13.500	-194.700
37.725	104.250	1644.100	-5.800	-192.600
37.517	104.000	1763.200	5.100	-185.500
37.512	104.429	1785.600	-6.100	-206.000
37.509	104.534	1711.100	4.500	-180.700
37.508	104.343	1730.700	-8.800	-202.400
37.502	104.158	1712.100	6.200	-185.200
37.677	104.367	1713.000	-9.400	-201.100
37.677	104.329	1682.300	-15.600	-199.100
37.667	104.393	1777.000	0.100	-198.000
37.696	104.082	1572.700	-2.900	-190.100
37.700	104.422	1341.300	10.400	-195.300
37.728	104.432	1833.500	13.900	-189.400
37.729	104.100	1558.700	-14.300	-188.700
37.740	104.496	1809.300	15.200	-184.100
37.746	104.478	1852.000	23.600	-183.200
37.793	104.226	1617.900	-3.000	-184.100
37.796	104.500	1331.300	28.100	-176.700
37.802	104.009	1434.500	-23.100	-185.300
37.803	104.303	1670.300	6.300	-180.400
37.807	104.127	1432.700	-21.500	-184.000
37.817	104.271	1604.500	-0.100	-179.500
37.775	104.344	1486.200	-23.800	-187.100
37.777	104.337	1827.600	23.800	-180.500
37.750	104.077	1520.000	-17.500	-187.700
37.751	104.445	1887.000	27.800	-183.100
37.755	104.112	1463.600	-24.300	-186.000
37.765	104.500	1840.700	25.600	-180.200
37.772	104.405	1851.700	25.100	-181.900
37.784	104.137	1463.000	-22.300	-186.000
37.792	104.332	1753.200	17.500	-173.500
37.849	104.497	1811.400	29.300	-173.200
37.850	104.199	1566.500	-12.700	-181.500
37.850	104.464	1779.100	23.600	-175.100
37.830	104.142	1487.400	-15.700	-182.100
37.319	104.497	1323.200	29.000	-175.400
37.328	104.241	1364.500	-4.500	-179.500
37.865	104.146	1464.600	-14.900	-178.800
37.872	104.114	1439.900	-17.200	-178.500
37.885	104.077	1424.000	-17.900	-177.200
37.889	104.400	1753.800	16.500	-179.200
37.390	104.040	1410.000	-16.300	-174.100
37.903	104.113	1438.200	-13.400	-176.500
37.910	104.005	1394.500	-16.500	-172.500
37.910	104.252	1483.500	-11.900	-177.900
37.923	104.132	1421.300	-13.100	-177.200
37.925	104.041	1407.000	-15.900	-173.400
37.925	104.077	1426.300	-15.500	-175.200
37.931	104.258	1499.900	-10.500	-173.100
36.000	104.010	1719.800	44.100	-148.300
36.072	104.406	1824.900	24.600	-179.500
36.160	104.465	1804.700	6.600	-193.100
36.305	104.080	1551.900	49.100	-158.100

LAT	LONG	ELEV	FAA	BA
36.307	104.295	1857.600	39.500	-159.400
36.320	104.402	1817.100	21.000	-182.200
36.407	104.402	1842.000	24.400	-181.500
36.437	104.408	1799.500	7.800	-193.500
36.023	104.154	1821.900	40.000	-157.700
36.046	104.235	1850.700	42.200	-164.700
36.067	104.028	1751.500	46.600	-149.000
36.055	104.322	1768.300	40.500	-157.200
36.074	104.133	1800.500	49.300	-151.400
36.177	104.397	1771.300	13.900	-184.300
36.142	104.064	1779.900	49.300	-149.700
36.247	104.412	1771.000	15.400	-182.600
36.191	104.330	1758.300	21.900	-174.600
36.490	104.355	1918.400	17.500	-197.200
36.435	104.285	2033.000	36.600	-190.700
36.416	104.300	1875.100	23.400	-180.200
36.436	104.295	1919.300	26.900	-187.700
36.370	104.332	1865.700	30.000	-178.900
36.305	104.068	1808.500	46.400	-155.700
36.335	104.261	1877.300	42.700	-167.100
36.306	104.356	1816.300	23.400	-174.600
36.250	104.253	1820.900	43.400	-160.100
36.277	104.321	1844.300	37.400	-165.800
36.357	104.259	1862.600	49.400	-170.000
36.114	104.354	1795.300	33.700	-167.000
36.031	104.072	1746.500	43.000	-152.300
36.126	104.261	1895.300	46.600	-165.500
36.370	104.244	1937.100	51.000	-171.100
36.407	104.152	1950.200	30.400	-167.000
36.423	104.055	1905.300	41.300	-171.700
36.437	104.242	2015.700	42.400	-182.900
36.450	104.127	2300.300	75.900	-161.400
36.152	104.133	1861.200	62.300	-145.700
36.198	104.205	1379.300	50.900	-159.200
36.303	104.167	1944.000	53.200	-164.200
36.364	104.098	1905.200	50.600	-162.400
36.227	104.152	1857.100	55.400	-155.400
36.276	104.259	1855.200	45.500	-162.200
36.307	104.098	1368.500	50.400	-156.500
36.305	104.193	1923.000	54.500	-161.100
36.216	104.072	1373.300	56.400	-153.000
36.172	104.256	1866.500	54.000	-166.000
36.307	104.025	1808.700	43.900	-158.300
36.308	104.250	1677.300	40.200	-169.600
36.912	104.444	2046.700	24.400	-204.300
36.995	104.432	2373.000	50.200	-215.000
36.892	104.437	2017.200	21.100	-204.300
36.811	104.446	1937.000	9.600	-206.700
36.748	104.462	1888.400	5.100	-205.900
36.540	104.553	1937.500	18.900	-197.300
36.655	104.443	1981.600	20.700	-200.900
36.557	104.325	2042.000	30.100	-193.400
36.703	104.387	1936.200	4.900	-208.300
36.365	104.457	1970.000	13.000	-205.300
36.912	104.444	2046.700	22.000	-206.300
36.755	104.492	1926.300	9.800	-205.500
36.840	104.228	2072.300	36.600	-195.000
36.338	104.145	2193.300	52.500	-192.700
36.877	104.026	2068.700	47.100	-186.400
36.902	104.115	2349.600	72.500	-190.200
36.653	104.328	2052.400	31.700	-197.800
36.525	104.143	2260.000	53.000	-195.000
36.995	104.325	2634.400	84.600	-210.000
36.990	104.154	1951.000	32.100	-136.000
36.915	104.205	2434.300	80.500	-194.000
36.962	104.260	2476.500	76.400	-190.500
36.969	104.039	1935.600	52.400	-184.000
36.910	104.327	2515.400	93.300	-202.100

LAT	LONG	ELEV	FAA	BA
30.511	104.008	2118.400	50.700	-180.000
30.531	104.033	2113.300	51.500	-184.300
30.633	104.232	2159.300	53.400	-184.200
30.592	104.342	2021.500	37.000	-188.400
30.752	104.066	2080.000	39.700	-193.000
30.735	104.318	2050.000	23.900	-200.000
30.735	104.218	2065.400	33.100	-200.100
30.520	104.150	2147.300	43.900	-195.200
30.609	104.027	2108.300	46.800	-188.900
30.502	104.247	2034.300	44.100	-185.000
30.733	104.251	2000.000	25.300	-193.300
30.770	104.145	2156.500	42.200	-190.700
30.310	104.500	1931.300	13.300	-202.000
30.810	104.304	2285.200	61.400	-194.100
30.602	104.297	1978.400	21.800	-199.400
30.930	104.433	2023.600	[illegible]	-207.600
30.813	104.305	1988.600	22.700	-197.000
30.730	104.130	2117.100	37.900	-190.000
30.755	104.488	1921.800	[illegible]	-206.000
30.542	104.305	2254.300	37.400	-190.300
30.519	104.254	2201.000	55.000	-190.100
30.703	104.441	2054.500	21.700	-203.700
30.892	104.443	2034.500	23.100	-204.400
30.629	104.633	1921.500	13.000	-191.100
30.713	104.540	1902.000	10.200	-196.400
30.629	104.537	1845.300	7.200	-197.000
30.534	104.542	1857.500	7.000	-195.100
30.551	104.659	1833.200	-1.300	-203.400
36.598	104.737	1877.200	15.500	-194.500
30.542	104.819	1949.200	16.700	-201.100
30.512	104.915	1958.800	12.500	-206.400
30.533	104.922	1902.700	4.000	-209.500
30.522	104.587	1825.200	5.500	-198.600
30.563	104.735	1924.000	12.000	-202.300
30.620	104.675	1893.700	16.400	-195.900
30.623	104.578	1854.700	8.300	-197.100
30.687	104.792	1950.900	15.900	-199.300
30.727	104.590	1944.900	23.100	-194.400
30.308	104.702	2199.500	27.000	-210.400
30.353	104.597	2149.400	13.900	-221.500
30.397	104.755	2429.400	53.000	-233.300
30.560	104.935	2000.200	4.000	-214.300
30.549	104.988	2080.600	12.700	-219.900
30.539	104.790	1938.300	14.200	-202.500
30.536	104.840	1950.400	11.500	-200.600
30.695	104.790	1900.000	19.700	-200.100
30.590	104.871	2121.100	26.000	-211.000
30.714	104.962	2318.000	37.900	-221.400
30.758	104.904	2236.300	31.900	-218.200
30.650	104.921	2229.900	31.100	-218.300
30.702	104.857	2114.700	19.100	-217.300
30.333	104.837	2223.100	16.900	-232.300
30.510	104.909	1955.000	10.200	-203.400
30.521	104.985	2022.700	6.400	-217.700
30.654	104.795	2186.000	14.700	-229.700
30.532	104.754	2222.300	5.500	-239.900
30.608	104.775	2256.400	9.600	-242.700
30.807	104.557	2351.400	19.300	-241.400
30.887	104.625	2485.300	37.100	-240.300
30.869	104.982	2279.900	9.300	-245.600
30.539	104.369	2136.300	30.600	-208.000
30.979	104.937	2329.300	27.000	-255.300
30.934	104.971	2585.200	33.200	-250.000
30.913	104.935	2564.000	15.000	-249.300
30.921	104.376	2533.500	30.200	-247.100
30.922	104.764	2471.000	34.000	-242.300
30.825	104.909	2179.000	11.000	-232.000
30.759	104.942	2312.500	[illegible]	-229.000

LAT	LONG	ELEV	FAA	BA
36.405	104.820	2156.500	19.700	-221.400
36.607	104.971	2352.500	27.300	-235.000
36.629	104.688	1921.400	21.300	-193.500
36.512	104.774	1900.400	-3.400	-213.500
36.625	104.756	1907.100	19.100	-194.100
36.625	104.823	1987.300	23.400	-198.300
36.514	104.943	2146.900	26.400	-213.700
36.654	104.987	2325.000	38.800	-221.100
36.567	104.851	1970.200	15.300	-205.000
36.537	104.538	1799.200	3.400	-197.700
36.655	104.538	1807.200	7.300	-201.500
36.511	104.927	1969.500	10.100	-210.100
36.514	104.946	1991.600	9.900	-212.700
36.518	104.964	2008.000	9.200	-215.300
36.523	104.997	2039.400	6.400	-221.600
36.667	104.926	2164.200	33.000	-210.400
36.117	104.560	1916.000	12.600	-201.600
36.117	104.650	1905.000	7.000	-205.400
36.117	104.668	1902.900	7.400	-205.300
36.119	104.923	2191.200	35.800	-209.200
36.114	104.981	2254.000	31.200	-220.900
36.115	104.512	1619.700	6.700	-190.600
36.113	104.771	2021.400	25.500	-202.500
36.362	104.593	1735.200	4.800	-194.300
36.007	104.700	1889.500	1.100	-210.200
36.195	104.660	1623.900	4.400	-199.200
36.088	104.685	1909.300	4.000	-209.400
36.095	104.737	1704.300	4.700	-208.300
36.113	104.890	2150.300	35.500	-205.000
36.106	104.591	1903.400	12.300	-200.700
36.177	104.995	2169.900	19.400	-223.300
36.205	104.855	1955.600	12.100	-206.400
36.235	104.595	1838.000	4.900	-200.700
36.235	104.580	1545.400	5.500	-200.400
36.313	104.805	2228.000	51.700	-197.000
36.323	104.920	2016.100	15.900	-208.000
36.363	104.717	1829.500	5.400	-199.200
36.405	104.617	1839.200	4.500	-201.200
36.415	104.858	1913.900	7.500	-206.000
36.477	104.757	1374.500	-7.500	-217.300
36.024	104.537	1387.300	23.500	-187.500
36.026	104.695	1080.600	1.400	-208.900
36.397	104.937	2050.700	22.100	-207.200
36.408	104.866	1923.000	5.300	-209.500
36.460	104.950	2018.100	10.100	-209.300
36.330	104.923	1990.300	14.600	-207.400
36.355	104.897	1940.100	12.800	-204.100
36.294	104.927	2071.700	20.300	-211.300
36.117	104.686	1913.500	8.200	-205.700
36.117	104.596	1894.500	7.500	-204.300
36.455	104.843	1902.300	8.000	-204.100
36.436	104.792	1582.300	6.200	-210.200
36.480	104.776	1873.900	-6.100	-215.700
36.355	104.697	2260.600	46.700	-206.700
36.262	104.837	1915.100	13.400	-200.700
36.261	104.765	1384.900	10.700	-200.100
36.348	104.792	1888.500	15.500	-195.600
36.035	104.650	1947.100	12.400	-207.200
36.079	104.730	1932.400	3.900	-207.100
36.071	104.993	2190.000	25.700	-219.100
36.068	104.592	1917.200	10.800	-203.500
36.056	104.527	1870.600	17.300	-191.800
36.044	104.632	1928.500	9.000	-206.300
36.050	104.791	2001.400	17.600	-206.300
36.020	104.816	1995.300	13.000	-205.200
36.022	104.762	1963.300	11.300	-208.200
36.013	104.545	1901.300	23.900	-188.600
36.015	104.650	1928.500	8.500	-207.100

LAT	LONG	ELEV	FAA	BA
30.018	104.614	1944.000	13.400	-203.900
30.025	104.994	2148.800	27.600	-212.600
30.023	104.741	1953.200	9.900	-208.500
30.027	104.900	2155.200	37.400	-205.600
30.034	104.868	2090.600	32.000	-201.700
30.040	104.939	2135.000	30.900	-207.600
30.310	103.185	1479.600	-1.100	-166.500
30.145	103.183	1416.700	-11.100	-169.700
30.008	103.203	1407.000	5.900	-151.500
30.470	103.488	1720.900	27.500	-164.600
30.477	103.250	1385.900	12.000	-165.300
30.494	103.362	1651.700	20.000	-164.700
30.290	103.463	1608.400	15.300	-164.500
30.240	103.400	1600.300	15.400	-165.100
30.275	103.275	1514.900	1.300	-166.100
30.138	103.475	1561.200	14.600	-154.700
30.197	103.489	1585.000	18.400	-158.700
30.202	103.364	1481.600	5.200	-160.400
30.159	103.417	1521.600	11.700	-156.400
30.173	103.275	1405.600	1.000	-162.500
30.181	103.344	1407.000	4.200	-159.800
30.348	103.453	1611.800	17.900	-162.200
30.330	103.253	1536.300	6.100	-165.700
30.395	103.345	1375.300	3.300	-167.300
30.006	103.488	1483.600	20.800	-139.100
30.110	103.428	1462.100	11.300	-152.100
30.138	103.498	1474.000	10.700	-148.000
30.055	103.383	1500.500	21.700	-145.000
30.302	103.433	1637.100	15.100	-167.900
30.373	103.400	1584.400	7.700	-169.400
30.332	103.029	1414.000	-1.300	-159.400
30.317	103.041	1408.600	-1.100	-156.500
30.273	103.041	1398.500	-4.700	-161.000
30.234	103.041	1383.900	-4.900	-159.200
30.165	103.040	1374.300	-3.700	-157.200
30.137	103.041	1361.200	-2.000	-156.400
30.100	103.040	1367.200	-9.300	-162.100
30.381	103.027	1433.400	4.200	-156.000
30.443	103.023	1439.000	3.400	-155.400
30.498	103.035	1425.900	2.600	-157.000
30.455	103.020	1426.800	1.000	-157.800
30.430	103.177	1533.500	7.100	-164.300
30.422	103.152	1507.100	3.600	-164.600
30.419	103.020	1434.700	-0.200	-160.700
30.400	103.068	1459.100	2.300	-160.700
30.397	103.180	1465.000	2.400	-165.600
30.377	103.048	1429.100	0.0	-159.400
30.350	103.175	1478.000	0.300	-164.900
30.350	103.125	1459.400	1.300	-161.900
30.350	103.070	1437.700	2.200	-158.500
30.310	103.180	1478.100	0.100	-165.100
30.310	103.013	1399.000	-7.500	-164.000
30.290	103.132	1440.600	-1.500	-163.400
30.290	103.073	1413.400	-5.200	-163.400
30.280	103.180	1477.200	0.0	-165.300
30.274	103.040	1400.000	-7.600	-164.400
30.230	103.038	1362.300	-7.200	-161.900
30.217	103.125	1433.900	-7.500	-165.000
30.216	103.082	1412.100	-7.800	-165.300
30.133	103.038	1384.400	-4.300	-159.200
30.179	103.132	1405.100	-6.800	-164.100
30.140	103.037	1367.500	-8.500	-161.600
30.082	103.037	1361.200	12.000	-164.900
30.423	103.450	1646.400	21.600	-162.400
30.333	103.310	1525.700	1.900	-168.000
30.263	103.495	1641.700	23.500	-166.000
30.240	103.096	1421.400	-4.400	-163.500
30.143	103.127	1396.100	10.500	-166.900

LAT	LONG	ELEV	FAA	BA
36.087	103.132	1387.000	-7.800	-163.100
36.395	103.465	1584.000	24.100	-16[illegible]
36.452	103.185	1539.200	8.000	-164.000
36.410	103.115	1481.400	3.000	-162.000
36.351	103.149	1463.300	3.200	-163.400
36.217	103.150	1441.000	-7.700	-169.000
36.013	103.132	1375.900	-7.700	-161.600
36.079	103.237	1396.600	0.100	-156.000
36.442	103.150	1515.500	5.600	-163.800
36.452	103.187	1541.700	5.000	-160.500
36.148	103.843	1759.000	52.300	-144.400
36.155	103.976	1384.900	57.500	-155.200
36.003	103.824	1656.900	45.300	-139.900
36.117	103.615	1555.600	27.500	-144.300
36.316	103.694	1799.800	44.400	-156.000
36.305	103.794	1751.400	37.700	-158.100
36.252	103.757	1730.700	42.100	-151.300
36.406	103.727	1350.100	55.300	-151.300
36.394	103.649	1793.800	45.200	-155.400
36.321	103.511	1762.300	39.900	-159.400
36.320	103.652	1775.200	42.000	-156.500
36.424	103.840	1895.200	59.700	-152.100
36.412	103.954	1867.500	54.000	-153.000
36.423	103.523	1726.900	29.900	-163.200
36.451	103.900	1914.100	53.300	-160.700
36.257	103.999	1911.100	58.000	-155.700
36.262	103.614	1716.300	38.000	-155.800
36.203	103.882	1729.900	40.500	-146.600
36.175	103.606	1629.200	33.100	-149.000
36.139	103.757	1713.500	49.000	-142.500
36.049	103.593	1462.600	23.800	-139.700
36.051	103.982	1695.400	47.400	-142.100
36.000	103.706	1414.300	21.400	-136.700
36.101	103.900	1713.300	47.300	-144.200
36.112	103.739	1639.300	41.000	-142.200
36.303	103.975	1770.900	40.200	-153.500
36.303	103.747	1743.300	36.100	-158.900
36.323	103.550	1588.900	25.700	-160.100
36.055	103.648	1827.000	25.000	-179.200
36.537	103.684	1590.100	43.100	-168.200
36.627	103.522	1773.900	33.200	-165.100
36.625	103.937	2063.000	47.300	-182.300
36.590	103.610	1816.300	41.300	-161.600
36.590	103.793	1757.100	45.600	-173.000
36.543	103.993	2061.500	56.500	-174.000
36.552	103.703	1980.100	46.700	-163.500
36.510	103.757	1884.500	53.700	-157.000
36.542	103.850	1932.300	45.200	-170.900
36.502	103.545	1756.200	30.400	-166.100
36.998	103.682	1817.800	26.000	-177.200
36.739	103.996	2094.000	45.800	-188.500
36.746	103.755	1930.300	43.300	-172.500
36.705	103.876	2656.900	95.500	-201.700
36.672	103.792	1952.000	42.800	-175.500
36.751	103.538	1770.100	29.000	-168.400
36.797	103.801	1870.900	23.200	-181.000
36.992	103.597	1782.300	23.000	-176.200
36.900	103.975	2073.500	48.000	-183.000
36.933	103.707	1849.900	26.500	-180.300
36.947	103.375	1953.000	39.400	-130.000
36.878	103.580	1813.000	25.000	-177.000
36.844	103.921	1952.700	36.700	-181.700
36.863	103.837	2144.200	57.900	-181.800
36.803	103.664	2030.900	48.000	-179.100
36.815	103.623	1847.600	37.300	-169.300
36.337	103.722	1924.400	37.900	-177.300
36.650	103.752	1943.400	43.900	-173.300
36.742	103.992	2081.200	43.600	-189.000

LAT	LONG	ELEV	FAA	BA
36.593	103.613	1814.500	39.700	-163.100
36.756	103.329	2022.100	42.300	-177.800
36.805	103.958	2101.700	49.000	-186.000
36.979	103.955	2294.200	66.100	-188.400
36.507	103.995	1994.000	46.300	-175.000
36.700	103.023	1428.000	7.000	-152.600
36.949	103.000	1345.400	-3.000	-155.600
36.855	103.145	1409.300	-7.400	-163.100
36.844	103.327	1632.300	10.600	-171.900
36.913	103.227	1457.000	-6.300	-167.300
36.913	103.365	1488.200	-5.300	-171.800
36.712	103.234	1552.500	14.300	-159.200
36.714	103.034	1474.400	6.500	-153.300
36.735	103.414	1586.700	2.200	-175.100
36.533	103.360	1653.600	19.100	-165.700
36.567	103.444	1723.300	26.300	-166.400
36.757	103.307	1628.600	16.400	-165.600
36.735	103.395	1682.000	15.600	-172.400
36.833	103.017	1431.900	-1.600	-161.300
36.795	103.197	1600.800	12.600	-166.400
36.948	103.408	1537.000	-2.100	-174.100
36.917	103.090	1364.200	-8.100	-160.700
36.969	103.195	1404.500	-7.700	-164.300
36.972	103.345	1481.100	-3.000	-168.700
36.750	103.138	1325.600	7.900	-162.700
36.562	103.279	1540.800	13.000	-162.200
36.534	103.127	1477.600	6.500	-158.300
36.656	103.324	1625.700	18.500	-163.200
36.656	103.469	1741.100	25.900	-167.700
36.656	103.181	1555.300	20.000	-151.700
36.612	103.072	1489.000	18.500	-147.900
36.517	103.487	1741.900	23.300	-166.200
36.828	103.473	1716.200	19.900	-172.000
37.852	103.306	1258.200	-14.500	-155.300
37.777	103.250	1282.900	-9.400	-152.900
37.792	103.347	1314.000	-13.000	-160.800
37.996	103.133	1217.400	-20.000	-156.200
37.851	103.096	1265.300	-8.000	-150.200
37.830	103.200	1264.000	-12.400	-153.900
37.775	103.168	1275.000	2.700	-139.900
37.677	103.093	1325.300	-2.300	-150.600
37.996	103.203	1225.900	-21.900	-159.100
37.946	103.133	1217.400	-19.900	-156.200
37.996	103.037	1216.300	-13.300	-149.400
37.939	103.055	1236.600	-13.200	-151.600
37.939	103.200	1292.400	-13.500	-158.100
37.881	103.090	1265.500	-8.500	-150.100
37.830	103.200	1264.000	-12.300	-153.700
37.823	103.142	1280.500	0.0	-143.100
37.778	103.166	1275.000	2.700	-139.500
37.746	103.148	1287.500	-0.100	-144.000
37.748	103.080	1336.700	3.200	-143.400
37.696	103.120	1313.400	-3.800	-150.800
37.691	103.042	1355.400	1.500	-150.000
37.677	103.093	1325.300	-2.400	-150.600
37.634	103.040	1377.700	6.700	-147.300
37.611	103.025	1414.300	9.800	-146.300
37.536	103.002	1449.300	6.000	-156.000
37.529	103.065	1465.900	8.800	-157.300
37.553	103.067	1460.900	7.500	-155.700
37.782	103.137	1289.600	6.400	-137.700
37.805	103.025	1290.800	14.100	-130.100
37.848	103.225	1274.000	-10.600	-153.100
37.853	103.367	1275.500	-0.400	-143.000
37.758	103.267	1314.900	-10.600	-157.800
37.703	103.069	1352.400	2.200	-149.000
37.988	103.398	1258.800	-15.400	-156.200
37.995	103.233	1203.700	-21.300	-156.300

LAT	LONG	ELEV	FAA	BA
37.502	103.243	1561.800	19.700	-154.900
37.022	103.016	1423.700	9.600	-149.300
37.025	103.008	1375.000	8.000	-145.600
37.642	103.397	1363.700	-0.500	-153.000
37.643	103.087	1342.300	0.500	-149.500
37.503	103.005	1448.400	4.000	-157.300
37.510	103.125	1474.300	11.600	-153.200
37.512	103.333	1550.700	22.100	-154.000
37.533	103.027	1463.600	7.100	-156.400
37.643	103.147	1375.900	-2.800	-155.700
37.638	103.028	1339.000	3.000	-149.100
37.635	103.350	1361.800	-8.500	-160.900
37.558	103.070	1422.500	3.000	-150.000
37.555	103.367	1426.200	5.200	-154.200
37.557	103.497	1496.300	0.100	-167.100
37.365	103.383	1568.000	20.400	-157.200
37.146	103.093	1524.300	13.600	-156.900
37.470	103.076	1510.300	13.000	-153.200
37.365	103.083	1588.000	20.400	-157.100
37.278	103.012	1558.700	16.100	-158.100
37.191	103.067	1527.000	16.100	-154.600
37.190	103.012	1550.700	15.600	-154.500
37.146	103.083	1524.300	13.500	-156.800
37.093	103.017	1411.500	3.700	-154.000
37.408	103.067	1550.600	19.000	-154.400
37.265	103.075	1592.800	18.600	-159.300
37.118	103.077	1434.600	2.500	-157.500
37.278	103.342	1721.500	29.400	-163.000
37.337	103.033	1559.400	15.100	-159.200
37.337	103.142	1581.900	21.100	-155.800
37.370	103.083	1589.800	19.000	-158.700
37.380	103.030	1536.600	14.800	-157.000
37.382	103.242	1615.100	18.700	-161.800
37.475	103.402	1459.100	5.400	-157.200
37.475	103.373	1522.200	13.200	-156.900
37.475	103.155	1309.700	9.300	-159.400
37.425	103.167	1505.400	10.300	-158.000
37.472	103.282	1577.000	16.300	-160.000
37.252	103.000	1533.100	15.200	-156.200
37.255	103.290	1668.000	22.000	-165.900
37.235	103.400	1738.300	24.300	-170.000
37.250	103.037	1552.300	14.300	-158.700
37.278	103.083	1593.800	13.100	-160.000
37.278	103.153	1642.000	23.300	-160.300
37.160	103.033	1488.900	10.100	-156.300
37.233	103.085	1565.000	17.500	-159.700
37.235	103.188	1667.200	19.000	-160.000
37.100	103.397	1730.700	23.500	-169.900
37.222	103.498	1786.100	26.700	-173.000
37.142	103.162	1506.100	16.900	-158.100
37.142	103.083	1475.200	5.700	-159.200
37.130	103.003	1400.700	7.600	-156.400
37.133	103.283	1633.700	17.400	-165.200
37.075	103.033	1389.000	-1.000	-156.400
37.003	103.000	1359.400	-3.500	-155.000
37.310	103.302	1718.500	13.400	-173.700
37.398	103.908	1548.400	-0.900	-174.100
37.470	103.525	1690.200	27.900	-161.700
37.143	103.820	1759.900	20.300	-170.400
37.012	103.375	1919.600	33.600	-181.000
37.985	103.533	1239.000	-30.400	-169.100
37.690	103.958	1463.300	-20.000	-183.800
37.985	103.545	1237.900	-31.100	-169.700
37.030	103.710	1437.100	-6.500	-167.500
37.633	103.830	1552.000	-3.200	-173.800
37.543	103.937	1610.500	-7.900	-188.100
37.043	103.965	1524.600	-17.500	-189.900
37.553	103.832	1500.000	-7.100	-175.000

Copy available to DTIC does not permit fully legible reproduction

LAT	LONG	ELEV	FAA	BA
37.730	103.590	1356.700	-10.000	-161.800
37.730	103.765	1460.900	-9.300	-172.700
37.735	103.883	1414.600	-23.000	-181.300
37.708	103.908	1431.300	-22.100	-182.200
37.880	103.763	1333.500	-23.500	-172.700
37.927	103.950	1385.000	-15.700	-176.600
37.935	103.337	1357.000	-15.700	-167.000
37.805	103.902	1373.400	-13.100	-165.800
37.863	103.687	1332.600	-22.900	-172.000
37.805	103.965	1414.300	-13.100	-171.300
37.947	103.785	1311.900	-22.200	-169.000
37.952	103.908	1351.300	-18.000	-169.800
37.953	103.675	1306.100	-30.900	-177.100
37.950	103.578	1255.000	-27.900	-171.700
37.990	103.837	1344.800	-18.200	-168.700
37.816	103.767	1349.300	-23.000	-174.000
37.823	103.985	1402.700	-23.900	-180.000
37.827	103.913	1378.000	-22.000	-177.000
37.853	103.597	1341.400	-14.200	-164.300
37.795	103.802	1378.300	-20.800	-175.000
37.995	103.617	1264.300	-33.700	-175.200
37.995	103.725	1310.900	-26.200	-172.900
37.998	103.950	1369.200	-21.400	-174.600
37.600	103.233	1413.700	3.300	-144.700
37.732	103.293	1333.500	-13.000	-162.200
37.733	103.142	1293.000	-2.300	-146.800
37.750	103.165	1256.300	1.800	-141.900
37.733	103.013	1270.300	2.300	-140.300
37.692	103.117	1316.100	-3.500	-150.000
37.697	103.243	1324.700	-13.400	-158.600
37.730	103.415	1296.000	-15.700	-160.300
37.867	103.450	1335.900	-10.600	-160.000
37.870	103.350	1265.200	-14.900	-156.400
37.872	103.025	1250.500	-2.700	-140.300
37.875	103.170	1248.500	-11.700	-151.400
37.883	103.000	1245.100	-1.000	-140.300
37.867	103.130	1245.400	-10.000	-149.300
37.867	103.233	1266.400	-12.000	-153.700
37.953	103.130	1226.900	-19.500	-156.800
37.933	103.463	1287.500	-15.500	-160.500
37.955	103.022	1206.700	-12.300	-147.800
37.955	103.345	1257.600	-14.600	-155.400
37.940	103.243	1246.900	-16.100	-155.700
37.775	103.363	1301.200	11.000	-134.400
37.775	103.433	1285.600	-17.500	-161.300
37.777	103.137	1305.500	7.800	-138.100

APPENDIX B

CAPULIN GRAVITY AND MAGNETIC DATA

Explanation of Table Headings

Station	Numerical listing of gravity and magnetic station identification. Stations with apostrophe (') are additional magnetic stations.
Lat	Northern latitude of station in degrees.
Long	Western longitude of station in degrees.
Free Air An.	Free air anomaly (FAA) calculated from a datum of sea level. The free air correction (FAC) is 0.3085 mgal/m and is applied to the observed gravity reading (OGR): FAA = OGR + FAC.
Bouguer An.	Bouguer anomaly calculated using a datum of sea level, station elevation, and a density of 2.67 g/cc. The Bouguer correction (BC) is $2\pi\gamma\rho h$, or 0.0837 mgal/m and is applied to the FAA: BA = FAA - BC.
Rel. Mag.	Relative vertical magnetic reading in gammas. Datum is station one.

Station	Lat	Long	Free Air An.	Bouguer An.	Rel. Mag.
1	36.805	103.956	49.0	-186.2	0
2	36.806	103.951	48.8	-183.1	695
2'	36.804	103.960			1710
3	36.800	103.965	57.89	-184.5	1395
3'	36.796	103.963			2070
4	36.792	103.963	64.0	-179.5	925
4'	36.790	103.965			850
5	36.794	103.961	59.25	-185.8	1340
5'	36.792	103.966			1790
6	36.790	103.978	60.0	-187.1	1950
7	36.796	103.982	58.5	-186.6	275
7'	36.798	103.979			-1200
8	36.809	103.980	53.0	-183.5	750
9	36.785	103.983	57.85	-189.3	75
10	36.782	103.969	57.06	-188.7	145
11	36.776	103.973	54.4	-187.9	600
12	36.767	103.969	50.6	-186.7	275
12'	36.755	103.978			-150
13	36.759	103.979	49.3	-186.6	200
14	36.752	103.978	54.8	-181.1	450
15	36.743	103.978	47.63	-186.3	1125
16	36.743	103.992	47.8	-186.2	1500
17	36.744	103.984	47.7	-186.2	2425
17'	36.735	103.979			1250
18	36.744	103.973	47.9	-186.1	2125
19	36.746	103.962	47.5	-184.5	2350
20	36.746	103.951	49.05	-182.6	2775
21	36.748	103.938	49.1	-181.6	3625
22	36.748	103.927	50.05	-181.2	3525
23	36.749	103.917	49.9	-181.3	3500
24	36.779	103.979	58.45	-189.4	1375
25	36.784	103.964	59.3	-204.2	3500
26	36.783	103.971	74.6	-195.0	3800
27	36.756	103.917	49.85	-180.2	4650
28	36.759	103.927	48.7	-180.6	4600
28'	36.762	103.926			4525
29	36.764	103.927	49.1	-180.5	4500
30	36.764	103.917	49.5	-179.7	4750
30'	36.761	103.917			5000
31	36.769	103.917	48.1	-179.3	4700
32	36.742	103.936	49.9	-184.2	4920
33	36.734	103.936	52.5	-182.5	3750
34	36.727	103.935	52.3	-183.2	6050
35	36.723	103.935	51.6	-184.5	5500
36	36.716	103.935	51.3	-185.5	3650
37	36.713	103.935	50.85	-185.7	3860
38	36.713	103.944	50.3	-184.7	3950
39	36.713	103.950	48.8	-185.0	46[illegible]

Station	Lat	Long	Free Air An.	Bouguer An.	Rel. Mag.
40	36.705	103.953	48.0	-185.4	3300
41	36.698	103.952	47.75	-185.0	3600
42	36.698	103.945	47.8	-185.4	4000
43	36.698	103.934	49.3	-185.1	3600
44	36.741	103.968	49.1	-184.5	3450
45	36.741	103.958	48.9	-183.3	3600
46	36.732	103.958	48.0	-184.5	2450
47	36.727	103.953	48.0	-184.4	3750
48	36.719	103.953	48.4	-184.7	3500
49	36.689	103.965	48.4	-185.3	2850
50	36.689	103.972	48.6	-185.6	3200
51	36.689	103.988	48.2	-186.4	2700
52	36.689	104.023	48.1	-187.7	2000
53	36.689	103.999	48.3	-186.5	2350
54	36.712	103.998	52.1	-186.3	1750
55	36.721	103.998	49.3	-187.7	2000
56	36.727	103.999	48.5	-186.9	1650
57	36.734	103.998	47.9	-188.6	1900
58	36.739	103.996	47.8	-187.3	1900
60	36.743	104.003	47.3	-186.1	1375
61	36.743	104.011	45.9	-186.9	1700
62	36.743	104.021	45.85	-187.7	1275
63	36.746	104.042	44.85	-188.3	1375
64	36.727	104.007	47.7	-186.7	1225
65	36.726	104.016	46.3	-187.5	1400
66	36.726	104.025	47.7	-187.5	1725
67	36.708	104.025	45.7	-188.9	1425
68	36.708	104.036	46.8	-189.8	1325
69	36.787	104.005	52.2	-188.2	1775
70	36.784	104.000	52.55	-187.6	1375
71	36.781	104.001	51.4	-188.1	1500
72	36.828	103.990	53.9	-189.8	1725
73	36.789	103.958	54.4	-187.2	5075
74	36.777	103.962	54.4	-186.0	4000
75	36.777	103.974	57.9	-188.3	2675
76	36.792	103.966	54.4	-185.7	2125
77	36.786	103.960	68.1	-180.6	3900
78	36.789	103.964	58.1	-188.8	2975
79	36.815	103.945	49.5	-178.4	2250

APPENDIX C

RATON BASIN MAGNETIC DATA

Explanation of Table Headings

Lat	Northern latitude of station in degrees.
Long	Western longitude of station in degrees.
MAG	Relative vertical magnetic reading in gammas. Station one is datum.

LAT	LONG	MAG	LAT	LONG	MAG
36.340	105.170	53.850	36.340	105.140	552.000
36.300	105.130	-153.720	36.350	105.110	-117.400
36.570	105.030	-5.250	36.570	105.070	-17.090
36.530	105.050	-114.400	36.540	105.020	24.900
36.520	105.010	-7.520	36.520	104.990	-138.220
36.520	104.930	-24.250	36.520	104.920	-119.500
36.330	104.240	125.400	36.350	104.240	142.070
36.320	104.450	108.250	35.760	104.470	173.500
35.700	104.490	-1.610	36.750	104.510	-174.020
36.720	104.530	-201.040	36.710	104.540	-41.010
36.690	104.570	201.610	36.670	104.600	177.030
36.600	104.630	-53.320	35.640	104.500	-7.600
35.630	104.730	105.580	35.600	104.740	57.540
36.620	104.750	11.510	36.540	104.770	132.000
36.550	104.730	79.280	36.560	104.750	114.100
36.550	104.750	150.230	36.540	104.810	155.320
36.550	104.850	-29.150	36.530	104.880	-54.150
36.520	104.890	-90.700	36.550	104.920	-50.920
36.570	104.940	-120.420	36.550	104.970	[illegible]
36.590	104.970	-63.260	36.610	105.020	[illegible]
36.530	105.040	-72.480	36.360	104.400	72.240
36.650	104.490	299.200	36.670	104.520	212.250
36.630	104.550	175.190	36.490	104.580	135.100
36.690	104.610	210.170	36.680	104.640	158.520
36.690	104.730	212.350	36.340	104.710	45.000
36.930	104.730	71.470	36.910	104.700	56.720
36.930	104.320	75.130	36.930	104.340	59.320
36.930	104.300	55.210	36.920	104.900	110.000
36.830	104.930	33.410	36.800	104.920	91.700
36.790	104.940	113.570	36.800	104.900	13.540
36.830	104.460	551.750	46.59	104.460	79.950
36.900	104.400	530.570	36.920	104.470	259.730
36.920	104.530	-80.130	36.950	104.400	233.000
36.930	104.470	99.700	36.900	104.470	312.100
36.990	104.490	224.100	37.030	104.500	234.000
37.030	104.520	330.000	37.070	104.520	345.420
37.110	104.530	209.410	37.130	104.530	214.220
37.100	104.540	-171.090	37.150	104.600	-45.910
37.140	104.590	-125.780	37.120	104.650	-133.510
37.130	104.730	-73.350	37.130	104.740	-69.400
37.120	104.770	-62.340	37.150	104.800	-111.300
37.150	104.830	-17.330	37.150	104.870	81.750
37.150	104.900	151.910	37.170	104.950	353.470
37.150	105.040	274.760	37.150	105.020	424.000
37.190	105.050	135.770	37.210	104.690	94.000
37.230	104.730	13.220	37.22	104.730	40.210
37.210	104.750	-32.840	37.240	104.770	-36.420
37.250	104.810	32.070	37.220	104.790	36.490
37.200	104.530	-150.460	37.230	104.520	-147.730
37.270	104.500	-170.080	37.290	104.520	-150.500
37.310	104.550	-56.720	37.330	104.570	74.800
37.360	104.590	177.220	37.360	104.600	443.200
37.400	104.550	386.240	37.420	104.630	437.750
37.300	104.670	321.320	37.370	104.700	380.950
37.290	104.720	439.370	37.320	104.730	361.150
37.310	104.730	322.230	37.320	104.810	332.240
37.320	104.840	303.250	37.320	104.870	305.320
37.310	104.920	216.260	37.330	104.930	279.020
37.330	104.980	344.070	37.330	105.000	337.540
37.290	105.010	375.470	37.400	105.050	302.150
37.350	105.050	527.060	37.330	105.050	242.830
37.320	105.070	172.280	37.320	105.040	71.090
37.310	104.710	292.040	37.320	104.690	302.060
37.340	104.670	511.180	37.330	104.630	265.000
37.330	104.600	235.640	37.440	104.660	667.550
37.470	104.670	627.020	37.470	104.730	454.920
37.520	104.730	350.590	37.540	104.710	382.750
37.570	104.750	352.180	37.590	104.740	250.340

LAT	LONG	MAG	LAT	LONG	MAG
37.520	104.770	247.110	37.010	104.830	327.310
37.500	104.830	330.030	37.330	104.800	435.310
37.570	104.920	669.190	37.500	104.940	715.370
37.550	104.960	620.370	37.130	105.020	351.820
37.090	105.040	206.530	37.070	105.020	160.810
37.000	105.000	147.210	37.050	105.000	46.400
37.020	105.010	-37.070	37.210	105.030	-23.410
37.240	105.040	-33.020	37.240	105.020	-213.720
37.270	105.040	42.700	37.290	105.050	23.300
37.320	105.070	-39.710	37.300	105.100	19.470
37.300	105.100	57.790	37.410	105.000	55.810
37.420	105.050	-30.320	37.430	105.020	-104.200
37.480	105.020	-133.910	37.500	105.020	-23.050
37.520	105.010	40.370	37.540	104.9[illegible]0	222.150
37.540	104.990	134.500	37.540	105.030	55.590
37.540	105.070	82.280	37.550	105.100	50.240
37.560	105.130	55.160	37.520	105.050	66.770
37.590	104.830	135.490	37.570	104.850	299.630
37.540	104.830	222.930	37.520	104.850	259.810
37.510	104.370	199.590	37.490	104.8[illegible]0	50.400
37.460	104.900	64.340	37.510	104.710	103.020
37.4[illegible]0	104.720	537.540	37.150	104.770	56.300
37.170	104.790	51.900	37.190	104.810	27.420
37.220	104.830	-31.150	37.240	104.840	5.010
37.250	104.850	11.170	37.270	104.540	3.740
37.230	104.330	75.280	37.300	104.800	30.070
37.330	104.730	144.910	37.380	104.760	162.950
37.390	104.770	125.200	37.420	104.780	137.200
37.450	104.760	151.310	37.410	104.740	240.440
37.130	104.810	-102.790	37.100	104.850	-174.550
37.190	104.690	-47.790			

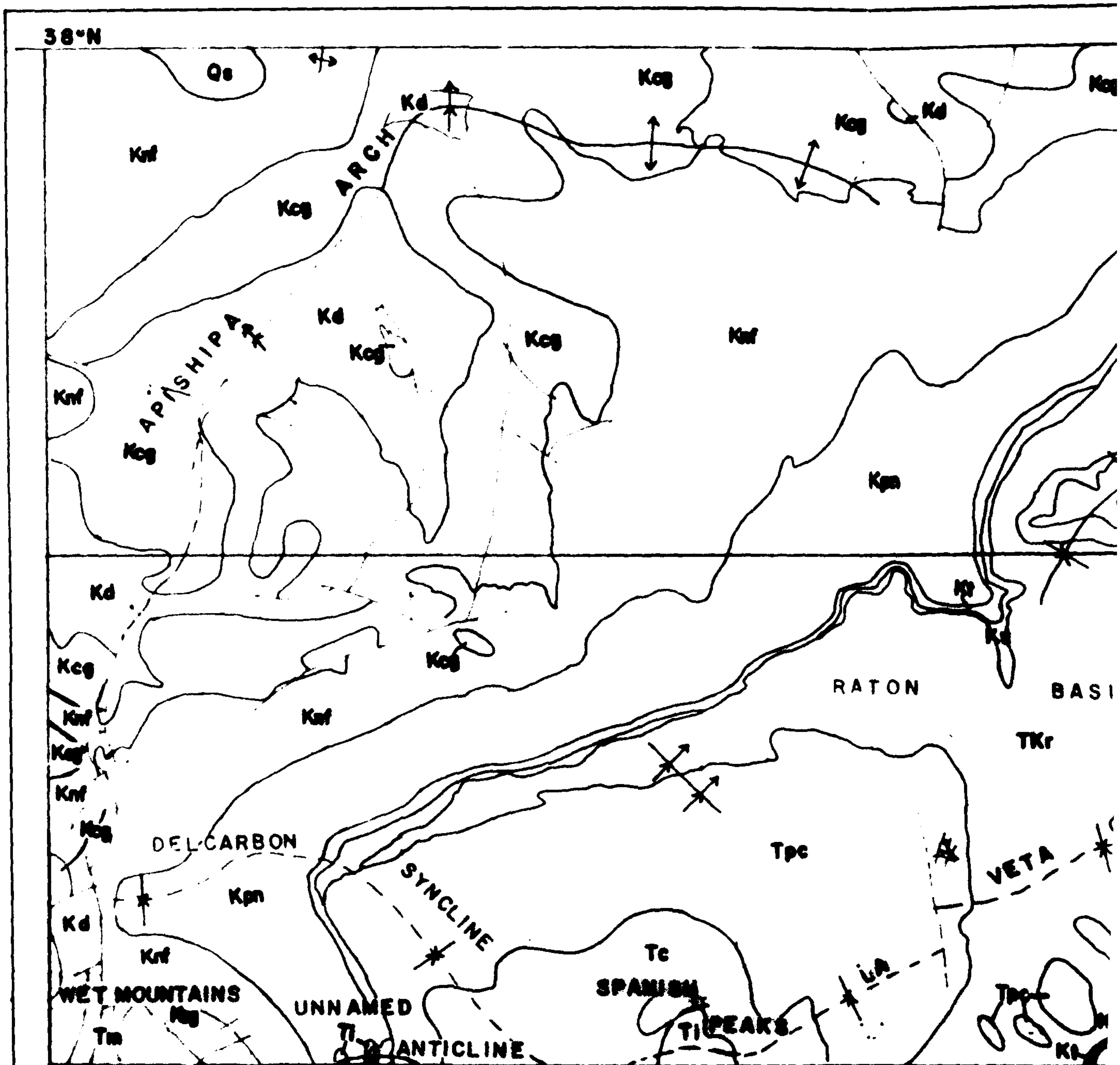
38°N
Qs
Kcg
Kd
Knf
ARCH
APISHIPA
Kcg
Kd
Knf
Kpn
Kt
RATON
BASI
TKr
DEL CARBON
SYNCLINE
Tpc
VETA
Tc
SPANISH
PEAKS
WET MOUNTAINS
UNNAMED
ANTICLINE
Ti
Tm

GEOLO
RATC

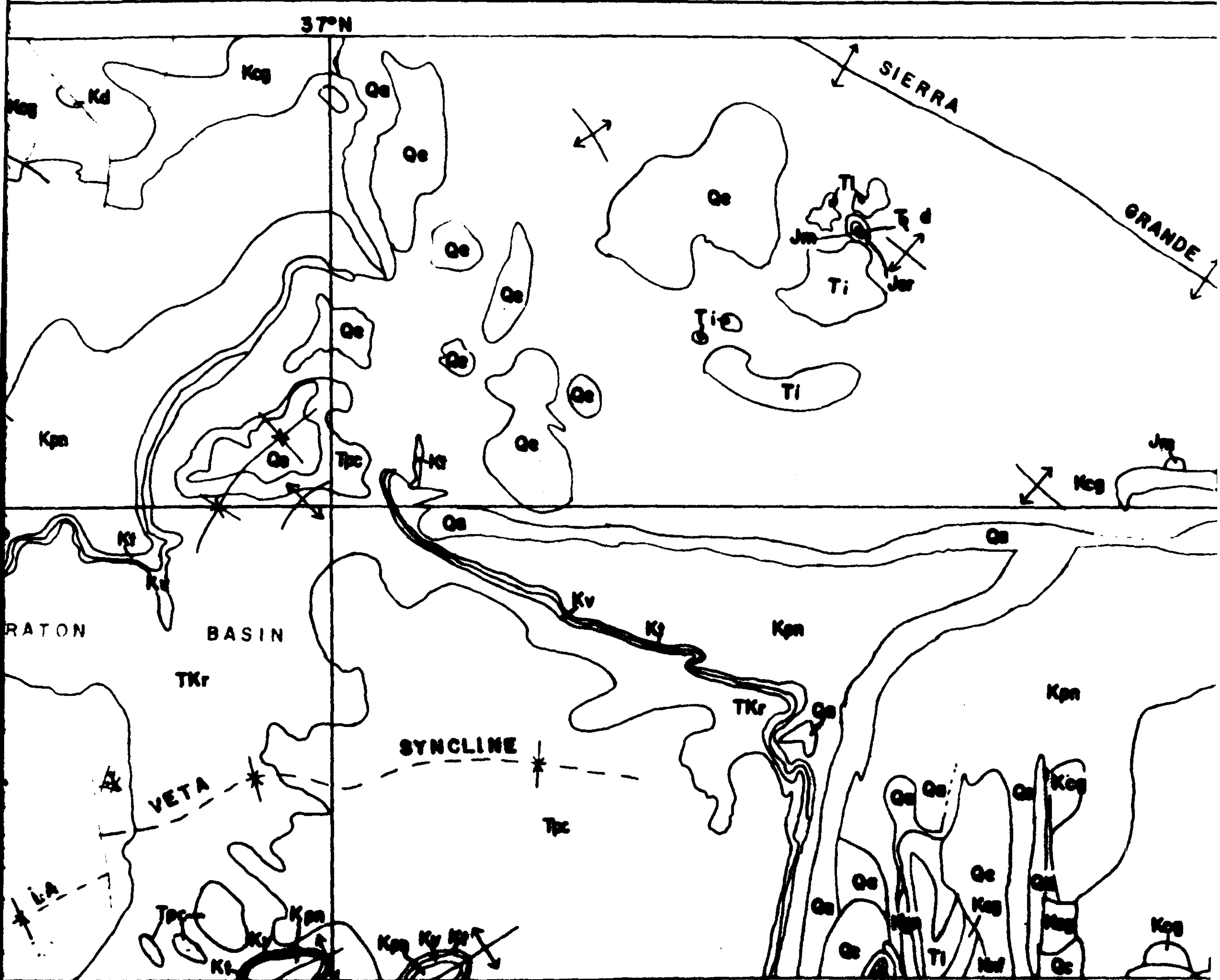

PLATE I
GEOLOGY AND STRUCTURE OF THE RATON BASIN OF N.M. AND COLO.

38°N

104°W

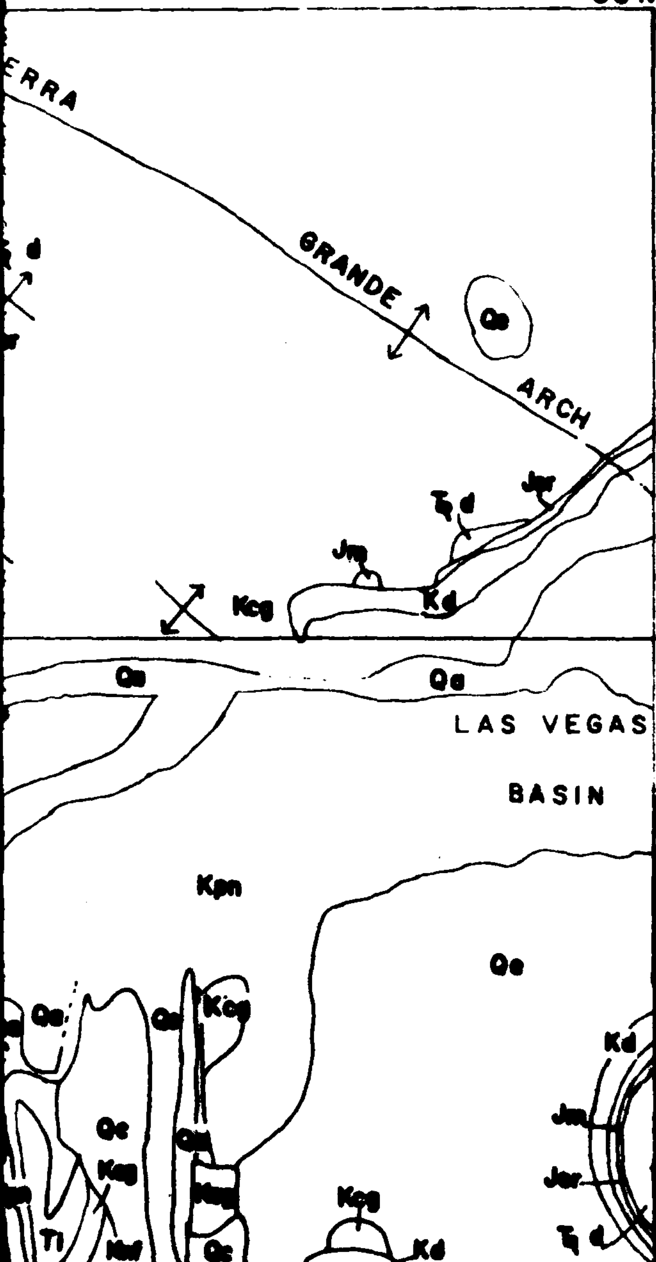

105°W

LEGEND

SYMBOL	FORMATION
Qa	alluvium
Qs	sand
Qc	landslide
Qe	volcanic rock
Tm	metamorphics
Ti	intrusives
Tc	Cuchara
Tpc	Poison Canyon
TKr	Raton
Kv	Vermejo
Kt	Trinadad
Kpn	Pierre
Knf	Niobrara
Kcg	Greenhorn Carlile Graneros
Kd	Dakota
Jm	Morrison Entrada
Jsr	San Rafael
Ꞧd	Dockum Group
PPsc	Sangre de Cristo

FAULT (ball on downthrown side)

SYNCLINE

ANTICLINE

MONOCLINE

CONTACT

SCALE

0 5 10

NAUTICAL MILES

OF THE
COLO.

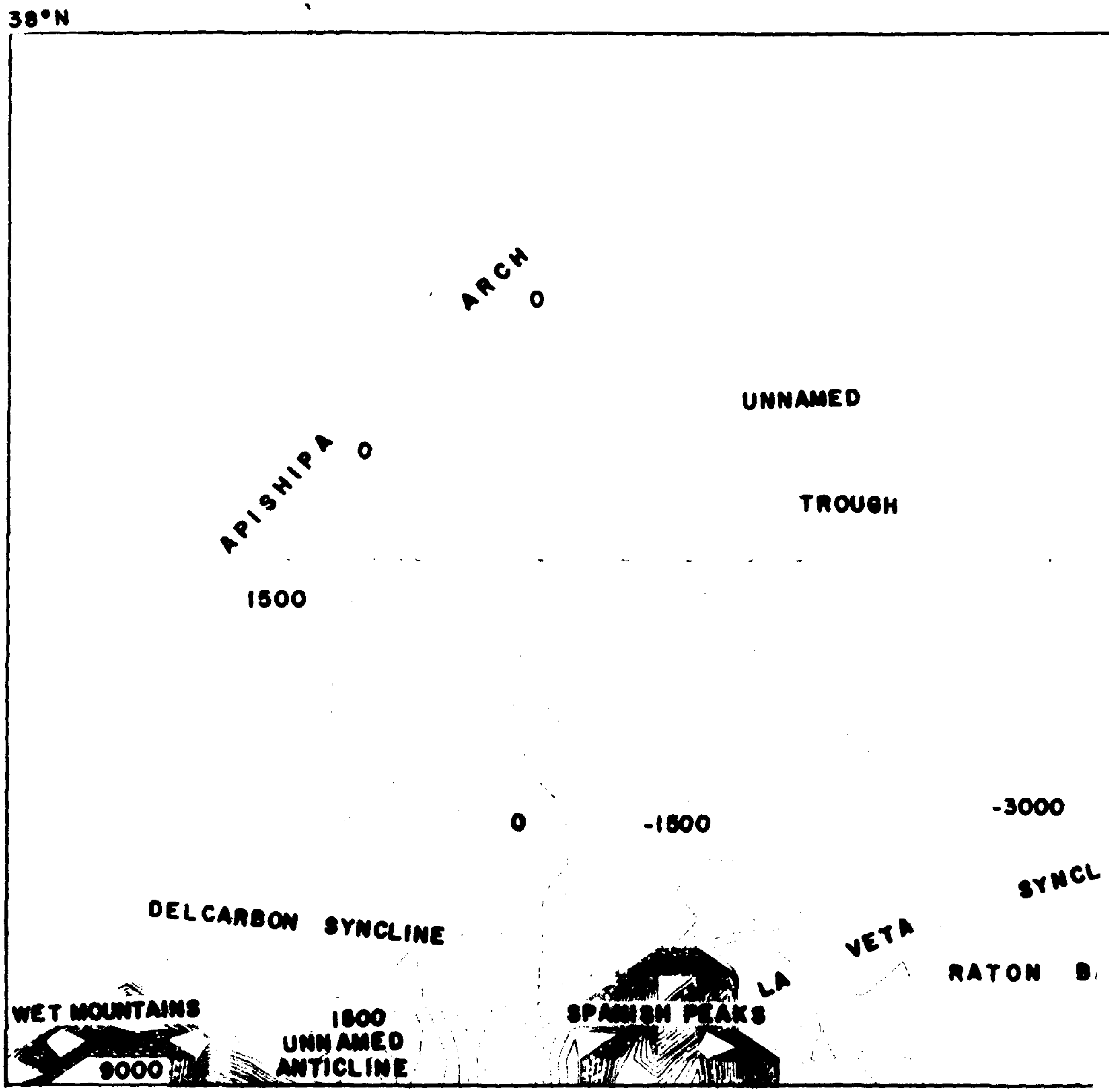
38°N
ARCH
0
UNNAMED
APISHIPA
0
TROUGH
1500
0
-1500
-3000
SYNCL
DELCARBON SYNCLINE
LA VETA
RATON
WET MOUNTAINS
1500
UNNAMED
ANTICLINE
9000
SPANISH PEAKS

BAS
RA

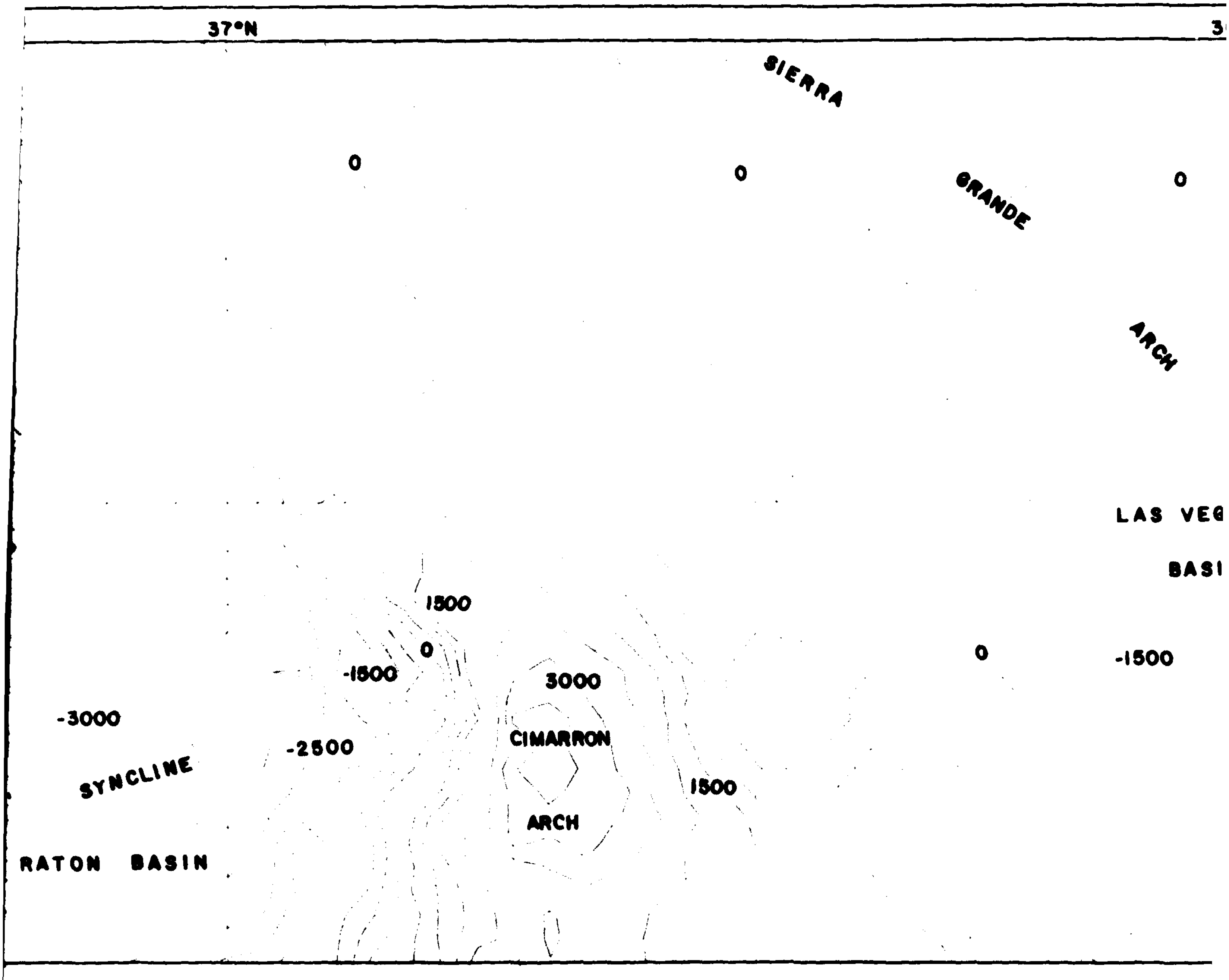

PLATE 2

BASEMENT STRUCTURE MAP FOR THE RATON BASIN OF N.M. AND COLO.

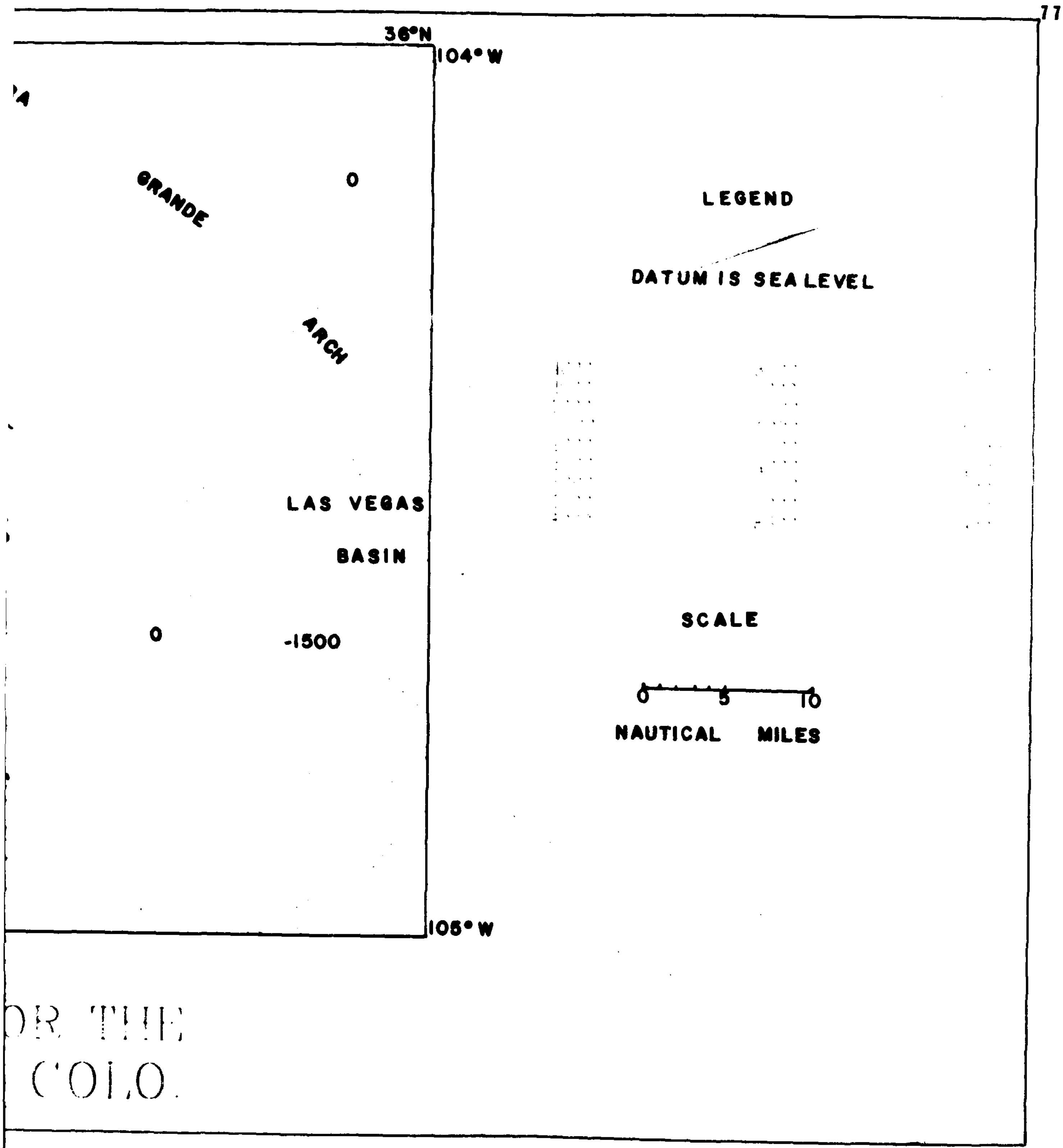
77
36°N
104° W
GRANDE
ARCH
LAS VEGAS
BASIN
0
0
-1500
105° W
LEGEND
DATUM IS SEA LEVEL
SCALE
0 5 10
NAUTICAL MILES
OR THE
COLO.

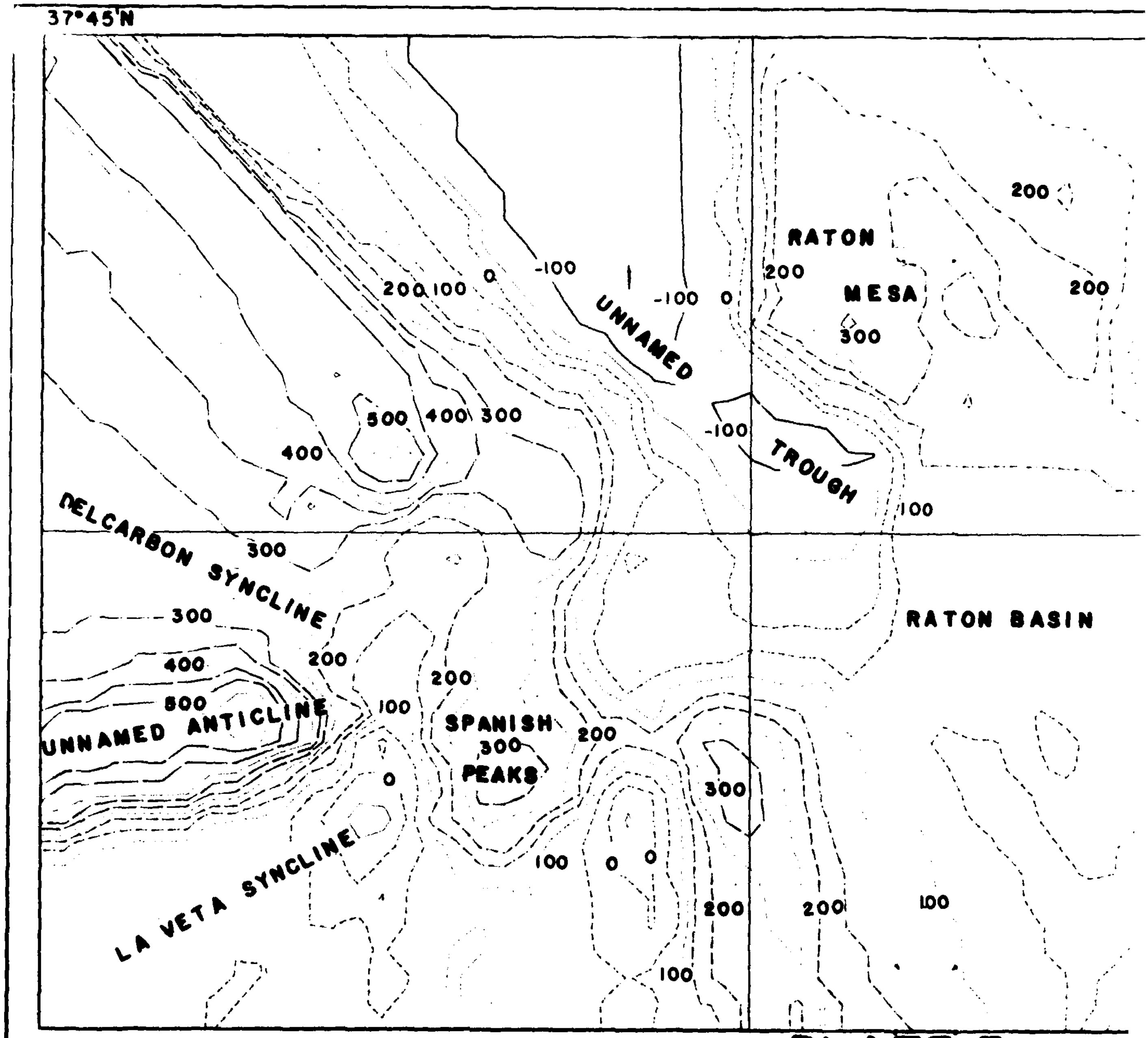

PLATE 3

GROUND MAGNETIC MAP
RATON BASIN OF N.M. A

DATUM IS STATION ONE IN FIGURE

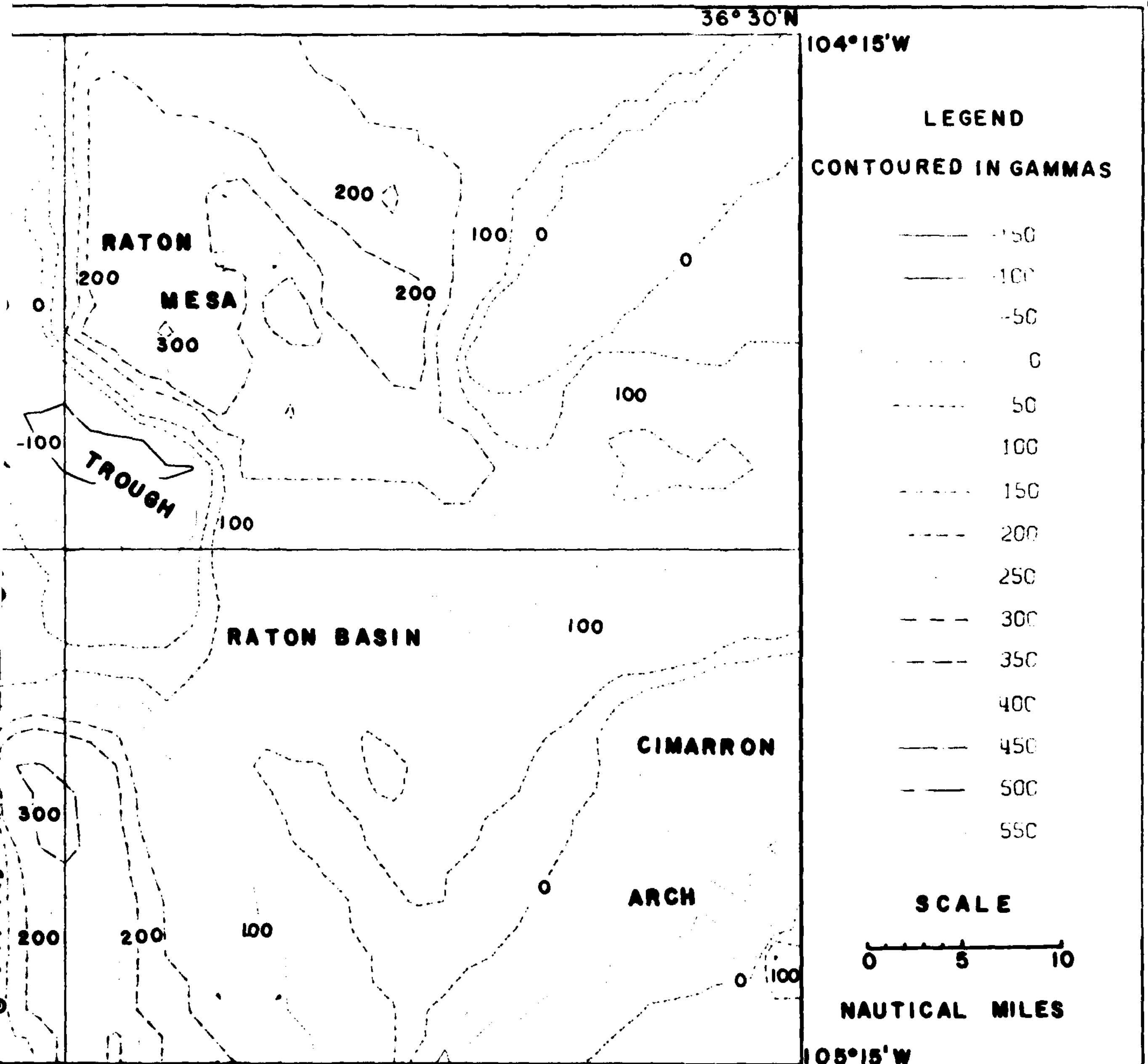

PLATE 3

MAGNETIC MAP FOR THE
SIN OF N.M. AND COLO.

TUM IS STATION ONE IN FIGURE 14

ATE
LMED
8